SULFITE OXIDATION UNDER FLUE GAS DESULFURIZATION CONDITIONS: ENHANCED OXYGEN ABSORPTION CATALYZED BY TRANSITION METALS

BY

Richard Kevin Ulrich, B.S., M.S.

DISSERTATION
Presented to the Faculty of the Graduate School of
The University of Texas at Austin
in Partial Fulfillment
of the Requirements
for the Degree of

DOCTOR OF PHILOSOPHY

THE UNIVERSITY OF TEXAS AT AUSTIN
December 1983

ACKNOWLEDGEMENTS

I would like to express my sincere thanks to everyone that contributed to this project directly or indirectly. Foremost on that list is Dr. Gary Rochelle and all of the members of the FGD group for making the task both worthwhile and enjoyable. Roberto Prada, M.S. 1981, built the apparatus and made the logistics work, saving me untold tedium. Secondly I would like to thank the Chemical Engineering Department, both faculty and staff, for a memorable college experience.

Outside of the scientific aspects was the endless support of my family, Dan, Joy and Sheila Ulrich. The amount of love and interest they showed always made the work worthwhile. They said this day would come and I'm glad they were right.

Special thanks are in order for Julia Busch for her companionship, her advice and and for just being herself. Over the years she has provided a refuge from sulfite oxidation as well as an independent viewpoint of the graduate Chemical Engineering community, which always caused her so much endearing amusement.

Thanks also to all the friends I have met here at the University for the comiseration and relief, especially (in order of appearance) Rick, T.D., John, Mitch & Amy, Tom & Noel. And, of course, best of luck to Pui, Rosa, Yung-Li, Phillip, Dave, Chuck and Rob.

Gratitude is also in order for Dr. D. Himmelblah for making it possible for me to work on this project as a result of his naturally honest, helpful and trustworthy personality. Please be assured, Dave, that I never miss an oppurtunity to relate to others what kind of a person you are.

Financial support was provided to the project and author by the Enviromental Protection Agency.

SULFITE OXIDATION UNDER FLUE GAS DESULFURIZATION CONDITIONS: ENHANCED OXYGEN ABSORPTION CATALYZED BY TRANSITION METALS

Publication No. ___________

Richard Kevin Ulrich, Ph.D.
The University of Texas at Austin, 1983

Supervising Professor: Gary T. Rochelle

The sulfite oxidation reaction was studied by measuring the rate of oxygen absorption across an unbroken interface into 1 liter of unsparged, agitated sulfite (10 mM) and catalyst (0.01 to 100 mM) solution at pH 4-6 and 50^{o}C. At catalyst concentrations enabling enhanced absorption all the incoming oxygen was consumed in a thin interfacial reaction zone and the bulk solution oxygen concentration was zero. Fe, Mn, Co, Cu and Cr ions were potent catalysts under these conditions, Ni was inactive. At 10 mM these catalysts gave pseudo-first order (in oxygen) rate constants of 8.6, 43, 4.7, 95 and 11 s^{-1}, respectively. However, values for Cu and Cr are uncertain because of long transient times. Dry catalyst added in its upper valence state (ferric, cupric, chromic) produced high initial rates that fell in one to six hours to steady state while catalyst added in its lower state (ferrous, manganous, cobaltous) showed no high rates and reached steady-state in less than one minute. Ferric and ferrous eventually resulted in the same rate. The effect of Fe was solubility-limited at a total Fe concentration of about 0.01 mM at pH 5 resulting in an enhancement factor of 2.4 at all higher concentrations. The iron ions cycle, being reduced during initiation and re-oxidized in the reaction zone. Fe was a much stronger catalyst than Mn or Co but its rate was limited by ferric solubility. Thiosulfate (0.05-1 mM) had a stronger inhibiting effect and efficiency on Mn than on Fe. EDTA was an effective inhibitor for Fe at equal or greater concentrations. A generalized free radical mechanism is proposed to model initiation, termination and inhibition of radical chain reactions. Rates for Fe and Co increase with pH from 4 to 5 while those for Mn was unchanged. Strong positive Mn-Fe synergisms were found to cause absorption rates of up to five times those expected.

TABLE OF CONTENTS

Acknowledgments....................iii

Abstract....................v

Table of Contents....................vii

List of Figures....................x

List of Tables....................xiv

Section 1: INTRODUCTION....................1

- 1.1 The Sulfite Oxidation Reaction....................1
- 1.2 Applications of Sulfite Oxidation....................2
  - 1.2.1 Applications to Flue Gas Desulfurization....3
- 1.3 Review of Previous Work on Reaction Mechanisms....6
  - 1.3.1 Experimental Methods....................7
  - 1.3.2 Observed Kinetics....................10
  - 1.3.3 Proposed Mechanisms....................14
- 1.4 Scope of This Work....................18

Section 2: EXPERIMENTAL....................20

- 2.1 Introduction....................20
- 2.2 Method....................21
- 2.3 Apparatus....................24
- 2.4 Procedure....................24

Section 3: OXYGEN ABSORPTION INTO SULFITE/CATALYST SOLUTIONS.....29
3.1 Simultaneous Gas Absorption and Reaction..........29
3.1.1 Physical Models..............................29
3.1.2 Danckwerts Surface Renewal Theory...........35
Section 4: DIFFERENCES BETWEEN BULK AND INTERFACE CONDITIONS.....42
4.1 Introduction.......................................42
4.2 Model of the Interfacial Region...................43
4.2.1 Physical Model...............................43
4.2.2 Mathematical Model...........................46
4.2.3 Transport and Equilibrium Constants.........50
4.3 Results and Discussion............................53
Section 5: KINETICS AND MECHANISMS...............................64
5.1 Mathematical Model of Enhancement due to Free Radical Reactions............................64
5.2 Catalysis by Dissolved Metal Ions.................73
5.2.1 Comparison of Catalysts.....................73
5.2.2 Catalysis by Iron............................81
5.3 Inhibition by Free Radical Scavengers: Thiosulfate..88
5.4 Inhibition by Complexing Agents: EDTA.............98
5.5 The Catalyst Cycle for Iron.......................103

Section 6: DETERMINATION OF MASS TRANSFER CHARACTERISTICS......106
6.1 Introduction......106
6.2 Theory......108
6.3 Results and Discussion......111
Section 7: CATALYTIC SYNERGISM......121
7.1 Introduction......121
7.2 The Synergism Coefficient......122
7.3 Results and Discussion......124
Section 8: RECOMMENDATIONS......135
SUMMARY......138
Introduction......138
Theory......141
Results and Discussion......144
Conclusions......155
Notation......157
Bibliography......163

LIST OF FIGURES

Figure no.	Title	Page
2.1	Experimental apparatus for the pH-stat method	25
2.2	Detailed components of the reactor	26
3.1	Effect of catalyst concentration on gas absorption flux	30
4.1	Depression of interfacial pH due to sulfite oxidation at 10 mM S(4)	58
4.2	Effect of bulk sulfite concentration on the depression of interfacial pH at bulk pH 5	59
4.3	Effect of interfacial sulfite oxidation on the partial pressure of sulfur dioxide above the solution at 10 mM S(4)	63
5.1	Oxygen profile in the interfacial reaction zone	71
5.2	Effect of Mn, Co and Ni catalyst concentration on the enhancement factor at 10 mM S(4) and pH 5	76

Figure no.	Title	Page
5.3	Effect of low Fe concentration on the enhancement factor at 30 mM S(4) and various pH values	77
5.4	Effect of high Fe concentration on the enhancement factor at 10 mM S(4) and pH 4 and 5	78
5.5	Effect of sulfite concentration on the enhancement factor at low and high Fe concentrations and pH 5	85
5.6	Effect of sulfite concentration on the enhancement factor at 30 mM Mn catalyst and pH 5	86
5.7	The absorption rate recovering from inhibition by thiosulfate at 30 mM Mn catalyst, 10 mM S(4) and pH 5	90
5.8	Decrease of enhancement due to the addition of thiosulfate at 30 mM Mn, 10 mM S(4) and pH 5	91
5.9	Determination of the inhibition efficiency of thiosulfate at 30 mM Mn, 10 mM S(4) and pH 5	96

Figure no.	Title	Page
5.10	Decrease in thiosulfate inhibition efficiency as Mn concentration increases at 10 mM S(4) and pH 5	97
5.11	Effect of EDTA additions on the enhancement factor at 0.01 mM Fe, 30 mM S(4) and pH 6	100
5.12	The catalytic cycle for Fe	105
6.1	Effect of agitator speed on the total oxygen absorption rate, Mn and Mn-Fe synergistic catalysts at pH 5	113
6.2	Effect of agitator speed on the total oxygen absorption rate, Fe catalysts at 30 mM S(4) and pH 6	114
6.3	Calculated values of the oxygen mass transfer coefficient and interfacial contact area	116
7.1	Enhancement factors during a Mn scan with 10 mM of a second catalyst present at 10 mM S(4) and pH 5	126
7.2	Synergism coefficients as a function on Mn concentration at 10 mM of a second catalyst at 10 mM S(4) and pH 5	127

Figure no.	Title	Page
7.3	Synergistic enhancement factors for Mn-Fe systems at 10 mM S(4) and pH 5	129
7.4	Synergistic enhancement factors for Mn-Fe systems at 10 mM S(4) and pH 4	130
7.5	Synergism coefficients for Mn-Fe systems at 10 mM S(4) and pH 5	131
7.6	Synergism coefficients for Mn-Fe systems at 10 mM S(4) and pH 4	132
S-1	Effect of Mn, Co, Fe and Ni catalyst concentration on the enhancement factor at 10 mM S(4) and pH 5	145
S-2	Effect of low Fe concentration on the enhancement factor at 30 mM S(4) and various pH values	149
S-3	Decrease of enhancement due to the addition of thiosulfate at 30 mM Mn, 10 mM S(4) and pH 5	151
S-4	Effect of agitator speed on the total oxygen absorption rate, Mn and Mn-Fe synergistic catalysts at pH 5	153

LIST OF TABLES

Table no.	Title	Page
4.1	Liquid phase diffusion and mass transfer coefficients of the dissolved species	52
4.2	Interface conditions as a function of the absorption rate at pH 5, 10 mM S(4) and 400 rpm agitation	54
5.1	Comparison of catalytic activities during enhanced oxygen absorption into 10 mM S(4) and 300 mM S(6) at pH 5, 50°C and 400 rpm agitation	75
S-1	Comparison of catalytic activities during enhanced oxygen absorption into 10 mM S(4) and 300 mM S(6) at pH 5, 50°C and 400 rpm agitation	146

Section 1

INTRODUCTION

1.1 The Sulfite Oxidation Reaction

The oxide of sulfur's +4 valence state exists in aqueous solution as sulfite, SO_3^{-2}, or as bisulfite, HSO_3^-, with a pK_a of 7.20 at 25^oC and infinite dilution (Yui, 1940). Upon oxidation to its +6 form it becomes sulfate, SO_4^{-2}, or bisulfate, HSO_4^-, with a pK_a of 1.98 (Robinson and Stokes, 1965). This reaction may be written in its most basic form as

$$S(4) + 1/2\ O_2 \xrightarrow{\text{catalyst}} S(6) \qquad \text{(Rxn. 1.1)}$$

and is given the generic name "sulfite oxidation" regardless of the protonation state of the reactant and the product. The mechanism of this reaction is so complex that there is currently no generally accepted comprehensive mechanism despite over half a century of research into the area. The principal difficulty in elucidating a mechanism lies in the unique sensitivity of the observed reaction kinetics to experimental conditions; changes in temperature or solution composition often result in changes not only in the rate constants but in reaction orders and even in the mathematical form of the rate expression. Furthermore, sulfite oxidation may be catalyzed or inhibited by trace impurities in the solution. The reaction is generally considered to be a free radical chain with perhaps some non-radical reaction steps and is known to be catalyzed by several types of dissolved transition metal ions. The actual mechanism under any given experimental conditions probably consists of a few reaction steps out of a multitude of known possible steps. The set of important steps probably then changes with changing experimental conditions.

1.2 Applications of Sulfite Oxidation

There are two main engineering applications of sulfite oxidation: the determination of mass transfer characteristics in gas-liquid contactors and the generation of $CaSO_4$ waste products (instead of $CaSO_3$) in flue gas desulfurization (FGD) systems. For mass transfer characterization it is usually necessary that the kinetics of the oxidation reaction be accurately known in order to enable correlation between the observed rate of oxygen absorption into a sulfite/catalyst solution and the mass transfer parameters k_{ox} and a. However, due to the vast complexity and diversity of the reaction the mechanism is not understood well enough to provide the needed kinetic information from first principles so empirical rate forms must be used. Mass transfer characterization via sulfite oxidation has been thoroughly reviewed by Linek and Vacek (1981) and further examples are given by DeWaal and Okeson (1966) and by Westerterp et al. (1963). Applications to FGD systems are discussed in Sec. 1.2.1.

Sulfite oxidation is of scientific interest in the areas of acid precipitation and in free radical oxidations in general. Sulfur dioxide from stack gas, mainly from coal-fired boilers, is absorbed into atmospheric moisture droplets and hydrolyzed to bisulfite. The subsequent oxidation of this suspended bisulfite to sulfate produces sulfuric acid resulting in acid precipitation. The aqueous phase oxidations of sulfite and of various hydrocarbons seem to follow generally parallel reaction mechanisms. Thus, research into sulfite oxidation may serve to elucidate these types of reactions in general for other compounds.

1.2.1 Applications to Flue Gas Desulfurization

In general, an FGD system consists of a scrubber, which absorbs sulfur dioxide into an aqueous solution, and a series of other unit operations designed to extract the resulting sulfur-containing compounds from the solution either as a disposable waste or as a marketable product. The history and synthesis of these processes have been reviewed by Rochelle (1977). The absorbed SO_2 is quickly hydrolyzed to equilibrium amounts of sulfite and bisulfite resulting in a drop in pH across the scrubber. Therefore a source of alkalinity must be continuously added to maintain steady state. In 1978 there were 119 FGD systems either in operation, under construction or being planned in the U.S. The majority of these are designed to accept either lime (CaO) or limestone ($CaCO_3$) as a source of alkalinity and generate either a $CaSO_3$ or $CaSO_4$ waste product, depending on the degree of sulfite oxidation in the system (Borgwardt, 1978). If no oxidation occurs the overall scrubbing stoichiometry with limestone addition is:

$$SO_2(g) + CaCO_3(s) \longrightarrow CaSO_3(s) + CO_2(g) \qquad \text{(Rxn. 1.2)}$$

If oxidation is present the overall stoichiometry becomes:

$$SO_2(g) + CaCO_3(s) + 1/2\ O_2 \longrightarrow CaSO_4(s) + CO_2(g) \qquad \text{(Rxn. 1.3)}$$

The oxidation percentage is defined as the percent $CaSO_4$ (gypsum) in the waste product. Oxidation occurs primarily in the scrubber and in the holding tanks downstream from the scrubber and can approach 100% if residence time is provided in an air-sparged holding tank containing suitable dissolved oxidation catalysts (Hudson, 1980; Gleason, 1977). Therefore the process typically occurring during forced oxidation in a holding tank is the absorption of oxygen from air across a gas-liquid interface and into a sulfite/catalyst solution where the oxidation reaction occurs.

Complete oxidation in an FGD system is sometimes desirable because gypsum is a better waste product than calcium sulfite. Gypsum has a higher settling velocity and crystallizes into larger, blockier particles enabling more complete dewatering and denser compacting. Since the resulting solid waste is completely oxidized it will have no chemical oxygen demand in the landfill. An additional benefit of complete oxidation in a slurry scrubber is reduced scaling because of the high concentration of gypsum seed.

The rate of oxidation is a complex function of the system variables and the sulfite oxidation reaction is not understood well enough to facilitate the prediction of parameter effects accurately enough for system design without resorting to empirical rate correlations. The situation is made more complicated by the fact that changing one parameter in an FGD system can cause changes in other variables, each of which may affect the intrinsic oxidation rate. For example, lowering the pH might raise the concentrations of dissolved oxidation catalysts and total sulfite while decreasing the ratio of sulfite to bisulfite (Rochelle, 1977). The sum of these competing effects on the oxidation kinetics would be, at present, very difficult to predict with any certainty.

1.3 Review of Previous Work on Reaction Mechanisms

Systematic research into the mechanisms of sulfite oxidation began in earnest about 50 years ago (Backstrom, 1927; Reinders and Vles, 1925; Johnstone, 1931). Since that time the growing utility of the reaction in engineering applications and the interest in free radical and inorganic mechanisms in general have prompted many diverse studies of its aspects. An excellent review of past research with emphasis on application to mass transfer characterization has been written by Linek and Vacek (1981). Published accounts follow the classical pattern of studying a problem from a variety of angles to build up a body of literature from which a comprehensive and unified mechanism becomes apparent. A typical article consists of the results of one of several possible types of experiments under certain conditions followed by a reaction mechanism specifically tailored to explain the results. While these mechanisms tend to employ reaction steps from a large common pool of possible steps, there seems to be little overlap in the way they are assembled. Looking at the literature as a whole, one can conclude that the remarkable complexity and sensitivity to conditions of the sulfite oxidation reaction has precluded the synthesis of a comprehensive mechanism to date.

Compared to this project, most previous work on sulfite oxidation was performed at higher total sulfite concentrations, lower catalyst concentrations and higher pH values. Furthermore, most of the literature results were obtained in homogeneous reactors in which there is a significant concentration of oxygen in the bulk solution so the range of reaction rates tend to be lower than those required for studies employing oxygen absorption into an oxygen-free solution. Therefore, there is relatively little literature rate data under FGD conditions. Hudson (1980) performed experiments on calcium and sodium sulfite solutions at pH 4.6 and 300 mM sulfite but the highest catalyst concentration he used was only 0.7 mM Mn and Fe in a homogeneous reactor. One cannot extrapolate his results to higher catalyst concentrations and rates since he reports that the reaction order for Mn is zero when it was found in this work to be one or one-half. Martin et al. (1981) studied Mn-Fe synergism at pH 2-3, Bengtsson (1974) studied Co catalysis at pH 5 and Weisnicht (1978) investigated the oxidation of calcium sulfite slurries at pH 4.3 to 5.5.

1.3.1 Experimental Methods

There are three major experimental avenues associated with sulfite oxidation research: homogeneous reaction, heterogeneous absorption and rapid mixing. Homogeneous reaction involves a bulk phase reaction between dissolved S(4) (total sulfite) and O_2 in the presence of a dissolved catalyst (Fuller and Crist, 1941; Coughanowr and Krause, 1965; Huss et al., 1982). Due to its low solubility, oxygen is either allowed to deplete to stop the reaction (batch mode) or continuously replenished by sparging (CSTR mode). Heterogeneous absorption involves the uptake of O_2 across a gas-liquid interface into a sulfite/catalyst solution under fast reaction conditions so that all the incoming oxygen is consumed in a thin reaction zone at the interface and the bulk phase oxygen concentration is zero (Linek and Mayrhroferova, 1970; Reith and Beek, 1973). Less often, the absorption of sulfur dioxide into an oxygen/catalyst solution is employed (Johnstone and Coughanowr, 1958). A variety of gas-liquid contactors have been used for absorption methods. In the preceding homogeneous or heterogeneous reaction schemes the reaction rate is measured by standard methods such as recording the time dependency of some reactant or product concentration or, for the case of heterogeneous absorption, directly measuring the volume of the gas absorbed. The rapid mixing (or flow thermal) method is carried out by mixing two streams, one containing the S(4) and one the O_2, in a tubular flow reactor and measuring the temperature rise as a function of distance (residence time) down the reactor. The reaction rate is then calculated from the known heat of reaction (Barron and O'Hern, 1966; Srivastava et al., 1968; Mishra and Srivastava, 1975). Either stream may carry the catalyst (Chen and Barron, 1972). Experimental constraints make it difficult to use the same solution in the different reaction schemes (Bengtsson and Bjerle, 1975). For example, faster kinetics are generally required for enhanced oxygen absorption in order to deplete all bulk phase oxygen and to confine the reaction zone to a narrow region at the gas-liquid interface (Sec. 3.1). Such a solution may not be suitable for homogeneous experiments because it would be difficult to sparge oxygen in fast enough to establish a substantial bulk phase concentration and thus obtain homogeneous reaction conditions. In the studies where the same solution has been employed in both homogeneous and heterogeneous experiments, the kinetics for the homogeneous case seem to be the faster (Johnstone and Coughanowr, 1958; Chen and Barron, 1972). This effect is usually attributed to a decrease in the rate of the heterogeneous case due to the residence time of a fluid element at the gas-liquid interfacial reaction zone being shorter than the induction time of the reaction (Schultz and Gaden, 1956; Phillips and Johnson, 1959).

Inhibitor and spectroscopy studies may be used in conjunction with the above reaction schemes to give specific information on free radical oxidation reactions. Inhibitors are chemical compounds that retard free radical reactions by reacting with chain-carrying radicals making them unavailable for further reaction (Backstrom, 1927; Alyea and Backstrom, 1929; Lim et al., 1982). Since only one inhibitor molecule can stop a lengthy reaction chain a large reduction in the oxidation rate can be brought about by small amounts of inhibitor. Kinetic information may be garnered from the degree and time dependency of the depression in the reaction rate caused by the addition of a known amount of inhibitor. The most commonly used inhibitors in sulfite oxidation studies are hydroquinone, ethanol and EDTA. Liquid-phase spectroscopy during reaction is a very powerful family of methods that can give time-dependent information on the concentrations and structures of free radical reaction intermediates (Hayon et al., 1972; Dogliotti and Hayon, 1967; Eriksen, 1974; Zagorski et al., 1971). However, the use of spectroscopy in free radical research requires a large capital expenditure for equipment and specialized experimental expertise to conduct the research and interpret the results.

1.3.2 Observed Kinetics

A large variety of kinetic rate constants, rate expressions and temperature dependencies have been observed for sulfite oxidation. The kinetics of the reaction are so sensitive to reagent impurities and experimental conditions that it is usually impossible to reproduce literature data accurately (Linek and Mayrhoferova, 1970). As a result there are few clear-cut kinetic dependencies from the literature that can be counted on to hold true in any given experiment but some vague trends can be concluded from a thorough review.

Experiments with known free radical scavengers have shown that the reaction is essentially free radical in nature (Altwicker, 1977) so the observed kinetics can be expected to follow the forms common to this class of mechanisms; non-integer rate orders, multi-term expressions, variation of kinetic behavior with conditions and general complexity of reaction phenomena are frequently observed. Backstrom (1927) has shown that the upper limit on the reaction's chain length (at trace concentrations of catalyst and 0.6 M total sulfite) is about 50,000.

As with hydrocarbon free radical oxidation, sulfite oxidation is significantly catalyzed by dissolved transition metals with multiple valence states such as Mn, Fe, Co, Cu and Cr. The intrinsic reaction rate is known to be very low in the absence of catalyst although it has been suspected that reagent impurities, such as iron, may be acting as a trace catalyst in these cases. Huss et al. (1978) have shown that the rate approaches zero when trace impurities are removed by chelation. The upper valence state of a transition metal seems to be more catalytically active; observed initial rates are higher when catalyst is added in its upper state. This is manifested in rapid mixing experiments as higher rates when the catalyst is added with the oxygen-containing stream than when it is contained in the sulfite-containing stream (Chen and Barron, 1972; Altwicker, 1976; Mishra et al., 1976). However, in systems at steady state the ratio of valence states may reach an equilibrium.

The effects of pH on sulfite oxidation rates is not generally agreed upon but lower pH seems to lower the rate more often than raise it (Reinders and Vles, 1925; Turney, 1965). There are several ways that pH could affect the overall rate. Many of the sulfoxy compounds-sulfite, sulfate and several radicals-can exist as protonated species. Some elementary reactions in the proposed overall mechanisms are known to be faster or slower depending on the protonation state (Hayon et al., 1972). It has been claimed that SO_3^{-2} is more quickly oxidized than HSO_3^- (Hudson, 1980; Fuller and Crist, 1941) in attempts to explain pH effects but there is no clear evidence for any difference in rates between the two species. Changes in acidity can affect the complexation of the dissolved transition metal catalysts thereby changing their redox potential (Huss et al., 1982; Bailar et al., 1973) and perhaps changing their catalytic activity. Different steps in the chain reaction may become rate limiting at different pH values due to pH-dependent stabilities of reaction intermediates. For example, the sulfate radical, $SO_4^{\cdot-}$, is unstable above pH 8 and therefore could only be a chain carrier at low pH (Hayon et al., 1972). Finally, if the upper state of the transition metal is the catalytically active species then the pH dependency of the catalytic regeneration step may become important. The oxidation of ferrous to ferric is highly pH-dependent, being between first and second order in OH^- (Tamura et al., 1976; Stumm and Lee, 1961).

The simplest way to model the observed kinetics is with a power series:

$$\text{reaction rate} = k_r[O_2]^m[S(4)]^n[\text{catalyst}]^p \qquad (1.1)$$

The reaction orders for elementary single-step reactions are the integers 0, 1 or 2 depending on the stoichiometry. However, sulfite oxidation is not a single elementary step but rather a set of series and parallel reactions involving a number of intermediates. While the above rate expression is sometimes suitable for empirical data correlation it can rarely be extrapolated very far since its form does not, in general, reflect the actual mechanism. Therefore, the apparent reaction orders m, n and p (which must be allowed to take on positive or negative integer or non-integer values in order to fit the data) and the rate constant varies widely throughout the literature. Additional concentration terms for H^+ (or OH^-) and inhibitors are sometimes added to Eq. 1.1 raised to their own apparent reaction orders.

The most interesting phenomenon associated with sulfite oxidation is catalytic synergism which occurs when two or more catalysts are simultaneously present and the resulting oxidation rate is higher or lower than would be expected from the individual catalytic activities of the single catalysts (Altwicker and Nass, 1983). Synergism is described as positive or negative depending of whether the resulting rate is greater or smaller than the rate expected from the independent parallel reactions. Johnstone (1931) first noticed a positive synergism between Mn and Fe and a negative effect between Mn and Cu. Martin et al. (1981) claim that the Mn-Fe synergism comes about due to the promotion of Fe-catalyzed oxidation by Mn. This conclusion was reached by comparing the reaction orders with respect to sulfite for the reaction catalyzed by Mn, Fe and the combination.

1.3.3 Proposed Mechanisms

No generally accepted comprehensive mechanism for sulfite oxidation has been proposed to date due to the extreme complexity of this reaction. The actual mechanism under any circumstances probably consists of a set of elementary steps out of a large number of possible steps. However, the kinetics of these numerous possible steps and the properties of the reactants and products are largely unknown since they involve unstable free radicals that cannot be isolated for study; they only appear in conjunction with other radicals and reactions during the actual oxidation process.

Since the mechanism is chiefly free radical in nature it would seem best to model it as such. A thorough review of free radical reactions will not be given here since there are many books on the subject (Huyser, 1973; Walling, 1957; Edwards, 1962) but a firm grasp of this area of chemical theory is necessary to understand and develop sulfite oxidation mechanisms. There are three main types of reactions in free radical chemistry: initiation, propagation and termination. An initiation reaction results in the generation of a free radical, perhaps by the oxidation or reduction of a non-radical ion or molecule. The propagation reactions are the cyclic set of reactions that generate the product. A typical propagation reaction involves the transfer of an unpaired electron thus transfering the free radical character from one species to another and resulting in no net generation or consumption of free radicals. The termination step consumes free radicals to stop the propagation cycle usually by the combination of two radicals to form a non-radical.

By far the most successful sulfite oxidation mechanism yet proposed is the Backstrom mechanism (Backstrom, 1934; Barron and O'Hern, 1966; Chen and Barron, 1972; Mishra and Srivastava, 1976). This mechanism seems to work best at sulfite concentrations above about 0.1 M, basic pH values and less than 1 mM catalyst. While limited in performance, the Backstrom mechanism undoubtedly reflects much of what is actually happening under the conditions of its applicability and serves as a good example of free radical oxidation mechanisms. The dots represent the unpaired electron and identifies the species as a free radical. The species are written as unprotonated since the pK_a values of all the intermediates are not known.

Initiation: $Me^U + SO_3^{-2} \longrightarrow Me^L + SO_3^{\dot{-}}$

Propagation:
$$SO_3^{\dot{-}} + O_2 \longrightarrow SO_5^{\dot{-}}$$
$$SO_5^{\dot{-}} + SO_3^{-2} \longrightarrow SO_5^{-2} + SO_3^{\dot{-}}$$
$$SO_5^{-2} + SO_3^{-2} \longrightarrow 2SO_4^{-2}$$

(sum) $2SO_3^{-2} + O_2 \longrightarrow 2SO_4^{-2}$

Termination: $2SO_5^{\dot{-}} \longrightarrow$ inert products

The rigorous solution for the overall rate is a multi-term expression but with the assumption that the chain length is very long (many propagation cycles before termination) and if the first propagation reaction is much faster than the other two the rate expression reduces to the form of Eq. 1.1:

$$\text{rate} = k_r[O_2]^0[SO_3^{-2}]^{3/2}[Me^U]^{1/2}$$

Whenever experiments result in these observed reaction orders it can be said that the Backstrom mechanism is a possible reaction scheme. The Backstrom mechanism is similar to reaction mechanisms known to be operative for some liquid phase free radical oxidations of hydrocarbons (Twigg, 1962; Turney, 1965).

One of the limits to testing this type of candidate mechanism lies in understanding the elementary steps themselves. The characteristics of these electron exchange reactions are intimately linked to the coordination of the reactants and this often restricts the degree of theoretical treatment that may be applied (Taube, 1970; Boozer and Hammond, 1954). The effects of anions and cations that are not consumed in the reaction may be due to the utilization of these ions as ligands. Some ligands seem to function as redox reaction catalysts for some elementary steps such as the accelerating effect of phosphate on ferrous/ferric reactions (Tamura et al., 1976; Bailar et al., 1973). Other anions, such as ammonium, seem to inhibit electron transfer reactions (Mishra and Srivastava, 1975).

1.4 Scope of this Work

The purpose of this project was to study sulfite oxidation under flue gas desulfurization (FGD) conditions. These conditions differ from those usually employed in other studies which tend to be either mass transfer characterization projects at higher S(4) concentrations and pH but lower catalyst levels or acid precipitation studies at trace amounts of S(4) and catalyst and lower pH. The experiments were performed at pH 4 to 6 and 0.01-0.03 M sulfite to simulate the conditions in typical FGD oxidizing units. The reaction occurred under heterogeneous conditions where oxygen was absorbed out of air at 50^0C into an agitated, unsparged sulfite/catalyst solution typically containing 0.1 to 100 mM of Mn, Fe, Co, Cu, Cr or Ni. Under these conditions the reaction kinetics were so fast that all of the incoming oxygen was consumed in a thin reaction zone at the gas-liquid interface and the bulk solution oxygen concentration was maintained near zero. The absorption rate was measured via the pH-stat method (Chan and Rochelle, 1982) since this technique allows solution concentrations to remain constant indefinitely while the absorption rate comes to steady state.

The scope of this project was to determine what factors are important in fixing the reaction rate, and therefore the absorption rate, under FGD conditions and to elucidate some aspects of the reaction mechanism when common FGD catalysts are present. The principal solution effects that were considered included catalyst concentration, S(4) concentration, pH and agitation rate. Catalytic synergism was studied by having two catalysts present simultaneously in the solution. The results of these experiments were correlated to hypothesized reaction steps with equations describing simultaneous reaction and mass transfer under these conditions in order to judge the validity of proposed reaction steps.

Section 2

EXPERIMENTAL

2.1 Introduction

The absorption of oxygen into sulfite/catalyst solutions to study sulfite oxidation kinetics has an advantage over closed-system batch methods because the reaction may proceed at steady state with constant oxygen concentrations. The oxygen absorption method may be used to measure the kinetics heterogeneously or homogeneously. For the heterogeneous case the kinetics must be very fast relative to the mass transfer capabilities of the reactor (via high concentrations of catalyst and/or sulfite) so that all the oxygen is consumed in a thin "reaction zone" at the gas-liquid interface and no oxygen penetrates to the bulk solution. For the homogeneous case the kinetics are much slower than the mass transfer capability so the bulk solution is saturated with oxygen and the reaction proceeds at the same rate at any point in the solution. The oxidation rate, and hence the rate of absorption, for the homogeneous case is then a function of the reaction kinetics only, but for the heterogeneous case the absorption rate is a function of both kinetic and mass transfer effects.

The solutions chosen for this study were intended to be similar to those found in actual FGD operations. The systems that employ oxidation in an air-sparged vessel would be designed to have fast kinetics for the greatest efficiency and would probably operate under heterogeneous conditions. Therefore the solution composition in this study was chosen to result in the use of heterogeneous absorption to measure the reaction rate. In this study, as in most oxidizing FGD systems, gas phase resistance to O_2 absorption is negligible.

2.2 Method

Oxygen was absorbed across an unbroken gas-liquid interface and into an agitated solution containing dissolved sulfite and catalyst. All incoming oxygen was consumed at the interface so the bulk liquid oxygen concentration was always near zero. The conditions for a given experiment were usually variations of one or more default conditions:

$50^{o}C$

pH 5

10 mM S(4) (total sulfite)

10 mM catalyst (Mn, Fe, Co, Cu, Cr or Ni)

300 mM S(6) (total sulfate)

0.184 atm O_2 above the solution (water-saturated air at $50^{o}C$)

400 rpm agitation ($k_{ox}=8.2X10^{-3}$ cm/s)

The ionic strength of this solution is about 0.925 M. Other substances were added for certain experiments, such as thiosulfate for inhibitor studies. These default conditions were chosen to approximate the environment in a typical FGD oxidizer or scrubber but no attempt was made to conform them to any specific FGD process. Since nearly all current and planned FGD systems utilize limestone or lime as a source of alkalinity they would be expected to have Ca^{+2} as the major cation in the solution, but for this study Na^{+} was used as the spectator cation because Na_2SO_3 and Na_2SO_4 are available in much purer form than the corresponding Ca salts (Hudson, 1980). Reagent purity is very important in the study of free-radical oxidations since one inhibitor molecule can break a reaction chain and prevent the oxidation of a large number of molecules. Impurity levels as low as 10^{-7} M can significantly affect the rate of sulfite oxidation under some circumstances (Bengtsson and Bjerle, 1975).

The O_2 absorption rate was measured via the pH-stat method. Since the predominant species at pH 5 are bisulfite (the reactant) and sulfate (the product) a hydrogen ion is liberated during the oxidation reaction:

$$HSO_3^- + 1/2\ O_2 \longrightarrow SO_4^{-2} + H^+ \qquad \text{(Rxn. 2.1)}$$

The above reaction is written for bisulfite oxidation but if the actual species being oxidized is sulfite a proton is still liberated due to the sulfite/bisulfite equilibrium. A probe detects the drop in pH and causes a pH-stat apparatus to dispense a Na_2SO_3 solution into the reactor to maintain the pH setpoint.

$$SO_3^{-2} + H^+ \longrightarrow HSO_3^- \qquad \text{(Rxn. 2.2)}$$

Summing the above two reactions gives the overall sulfite oxidation stoichiometry.

$$SO_3^{-2} + 1/2\ O_2 \longrightarrow SO_4^{-2} \qquad \text{(Rxn. 2.3)}$$

The concentrations of all species in the solution remain constant except for sulfate. Sulfite is added and oxygen is absorbed at the same rate as they are consumed. The sulfate concentration is relatively high at the start of the experiment (0.3 M) so it will rise only a couple of percent over a run lasting for several hours. The pH-stat method is useful only at pH values that are between the pK_a values of sulfate (1.45) and sulfite (6.57).

2.3 Apparatus

Fig. 2.1 is a block diagram of the experimental apparatus which is the same used by Chan and Rochelle (1982) for measurement of limestone dissolution rates.

The reactor (Fig. 2.2) was a plexiglass cylinder 14 cm in diameter (154 cm^2 cross-sectional area) and 15 cm deep with four 1.5 cm baffles. A snap-on lid with access holes provided segregation from outside air. One liter of solution was agitated by a polypropylene propellor with three 1.5 cm square-pitch blades that pulled the solution down in the middle.

2.4 Procedure

The following procedure is for establishing a steady state absorption rate under any given conditions. Several different types of experiments may be performed with minor variations of this procedure. The most common experiment for this work was to vary the con-

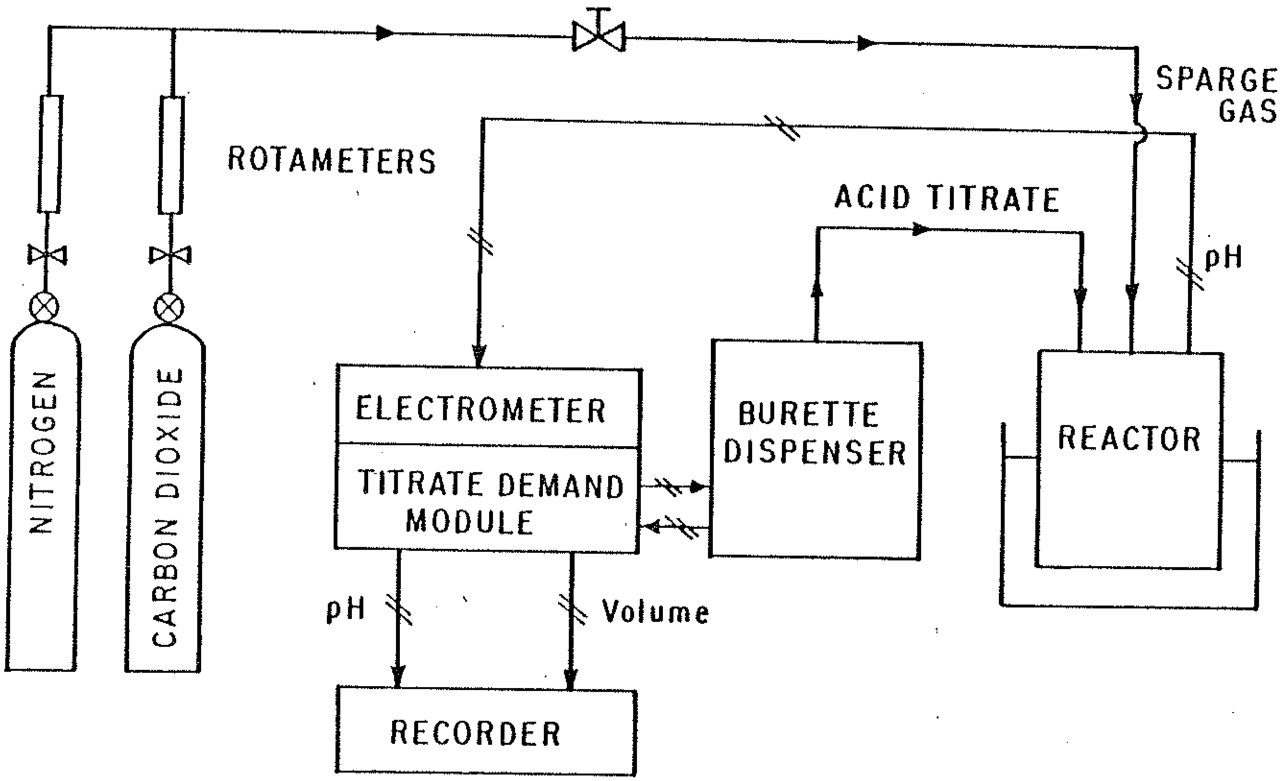
SPARGE GAS
ROTAMETERS
ACID TITRATE
pH
NITROGEN
CARBON DIOXIDE
ELECTROMETER
TITRATE DEMAND MODULE
BURETTE DISPENSER
REACTOR
pH
Volume
RECORDER

Figure 2.1: Experimental apparatus for the pH-stat method

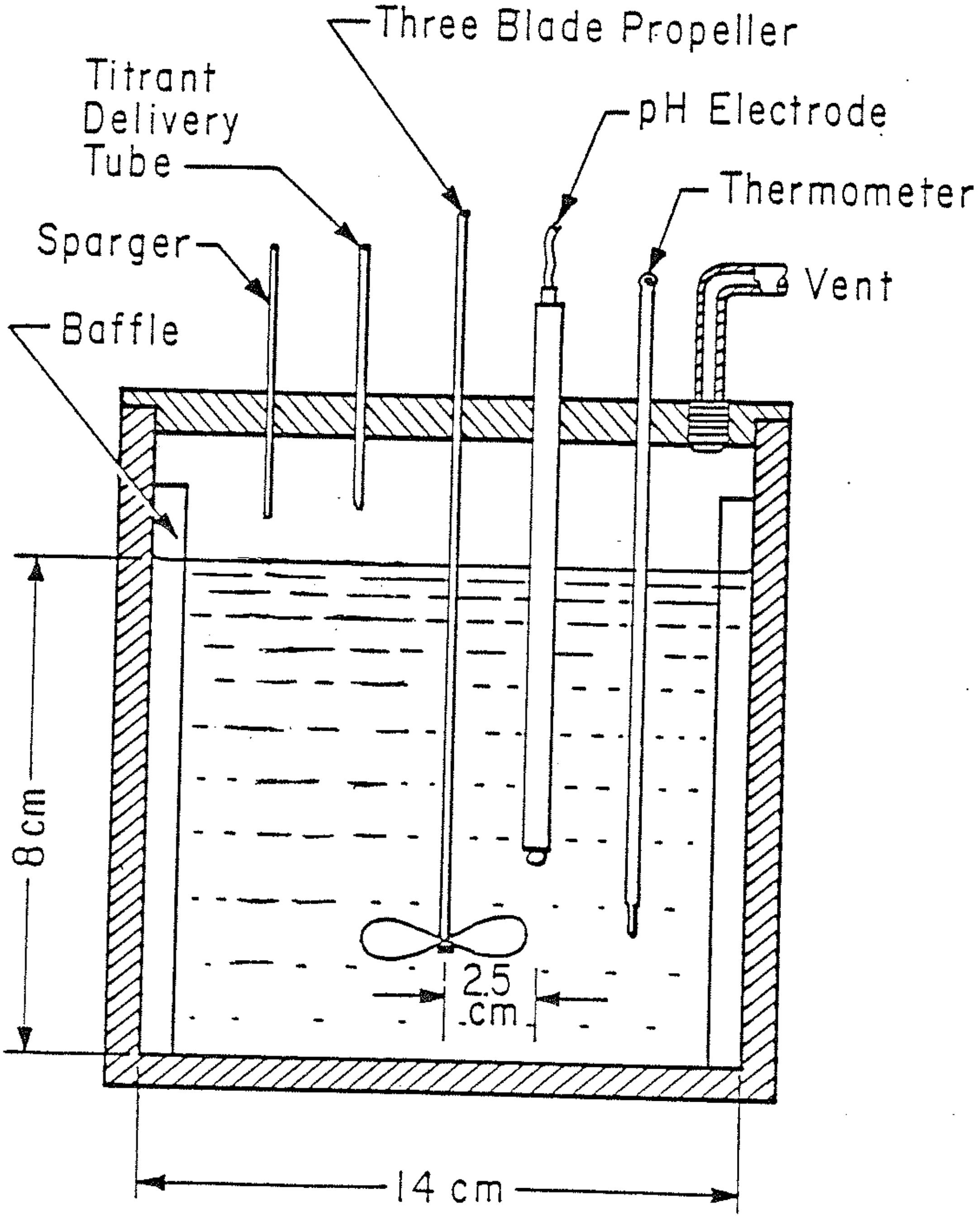
Three Blade Propeller
Titrant Delivery Tube
pH Electrode
Thermometer
Sparger
Vent
Baffle
8 cm
2.5 cm
14 cm

Figure 2.2: Detailed components of the reactor

centration of a species in the solution, such as catalyst, from a value below to a value above the default condition.

The reactor, agitator, thermometer and pH probe were first cleaned with 0.1 M sulfuric acid and rinsed with distilled/deionized water. One liter of 300 mM Na_2SO_4 solution was then heated to 50^oC on a hot plate and poured into the reactor. The thermometer, pH probe, agitator and reactor lid was added and the assembly placed in a thermostated water bath. Oxygen in the solution was stripped out by sparging with N_2 through a fritted-glass tube while the agitator was running at 400 rpm. While the sparging was underway the Na_2SO_3 titrant solution was added to the burette dispenser. After 30 minutes of sparging the fritted-glass tube was removed and the N_2 allowed to flow through the gas space in the reactor to maintain an oxygen-free atmosphere above the solution. Dry Na_2SO_3 and catalyst (as a sulfate salt) were added to the solution through a hole in the reactor lid. The pH was adjusted to the desired value with sulfuric acid and the dispenser nozzle inserted into the top of the reactor. At this point the pH-stat apparatus was turned on but would dispense no titrant if the pH had been properly adjusted to coincide with the setpoint and the gas above the solution remained oxygen-free. When the strip chart recorder was ready to record the amount of titrant added the N_2 flow was shut off and 1000 cm^3/min of air was sent into the gas space to establish a steady state O_2 concentration. After several minutes the flowrate was reduced to 300 cm^3/min for the duration of the experiment. This gas flowrate should not cause significant SO_2 stripping over a period of several hours for 10 mM S(4) at pH values as low as 3.

The absorption rate was calculated from the slope of the titrant added vs. time record. The conversion equation was:

$$\left(\frac{\text{gmols } O_2}{\text{cm}^2\ \text{s}}\right) = \left(\frac{\text{ml titrant}}{\text{s}}\right)\left(\frac{\text{gmols S(4)}}{\text{ml titrant}}\right)\left(\frac{1 \text{ mole } O_2}{2 \text{ moles S(4)}}\right)\left(\frac{1}{154\ \text{cm}^2}\right) \tag{2.1}$$

Section 3

OXYGEN ABSORPTION INTO SULFITE/CATALYST SOLUTIONS

3.1 Simultaneous Gas Absorption and Reaction

3.1.1 Physical Models

If the reaction kinetics between the gas being absorbed (O_2) and the reactive solute (S(4)) are sufficiently fast then the absorption may be described as heterogeneous. Under these conditions all of the oxygen being absorbed is consumed in a thin reaction zone at the gas-liquid interface and the bulk solution oxygen concentration is practically zero. The regions where these conditions exist may by determined by plotting the oxygen absorption flux R in moles O_2/cm^2s versus the catalyst concentration at constant total sulfite level in a stirred vessel as in Fig. 3.1. As the catalyst concentration is increased from left to right the oxidation kinetics become faster and three distinct regions of O_2 absorption are found. In region A the kinetics are too slow to maintain a bulk liquid oxygen concentration of zero and the absorption rate is given by physical absorption into an O_2-containing solution:

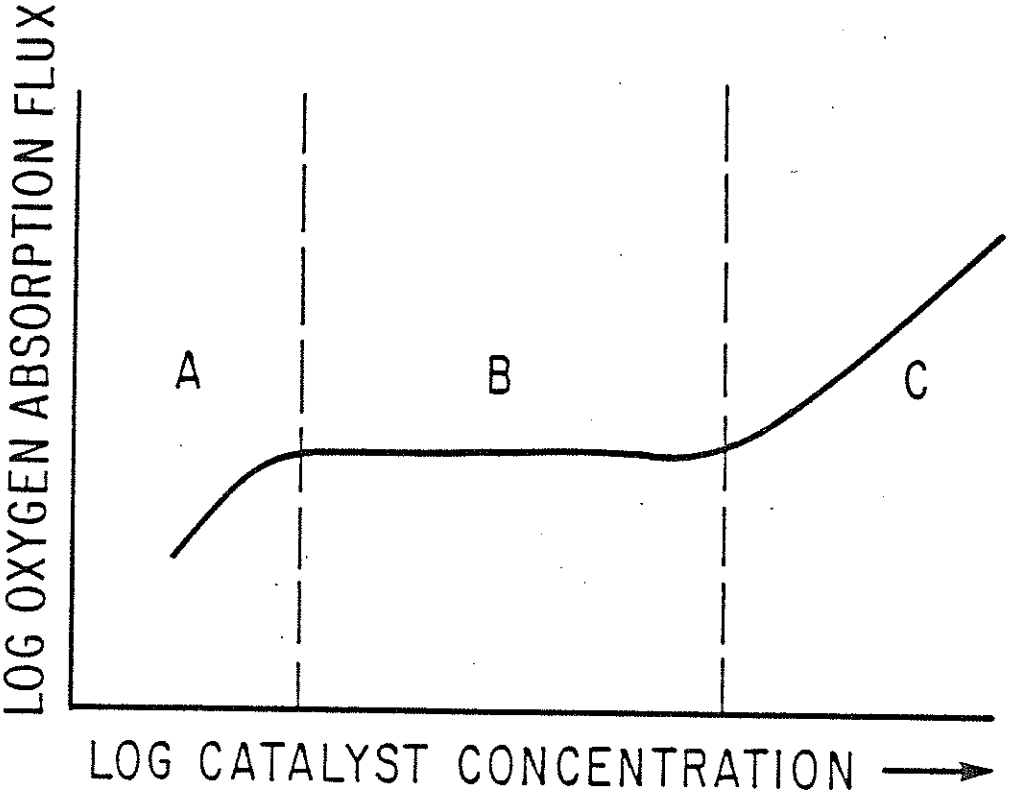

Figure 3.1: Effect of catalyst concentration on gas absorption flux

$$R = k_{ox}([O_2]_i - [O_2]_b) \tag{3.1}$$

where: k_{ox} = liquid-side mass transfer coefficient for O_2, cm/s

$[O_2]_i$ = O_2 concentration at the interface, moles/cm^3

$[O_2]_b$ = O_2 concentration in the bulk solution, moles/cm^3

In region B the kinetics are fast enough so that the bulk oxygen concentration is nearly zero but not fast enough to show any enhancement above the maximum rate of physical absorption. This highest rate of physical absorption is given the symbol R_o:

$$R_o = k_{ox}[O_2]_i \tag{3.2}$$

In region C the kinetics have become fast enough so that there is enhancement of the absorption rate above R_o. In this regime there is no bulk phase oxygen so the system is properly under heterogeneous conditions and all the incoming oxygen is consumed the in a thin reaction zone at the interface. The enhancement factor is defined as:

$$E = R/R_o \tag{3.3}$$

In practice only a very small amount of catalyst is required to achieve region B so the areas of interest for this study are B and C.

The absorption rate under heterogeneous conditions is a function of both kinetic and mass transfer effects. Therefore, if it is desired to extract kinetic information from the absorption rate it is necessary to have an accurate mathematical model that allows separation of the kinetic and mass transfer parameters. There are two main models used for this purpose: film theory and surface renewal theory.

Film theory is the simpler of the two approaches and involves a boundary layer on the liquid side of the interface (Danckwerts, 1970). A stagnant diffusion layer of thickness x_d is assumed over which, in the absence of simultaneous reaction, oxygen molecules must diffuse in order to reach the well-mixed bulk solution. If the bulk liquid O_2 concentration is zero, the physical absorption rate is given by:

$$R_o = D_{ox}\frac{[O_2]_i}{x_d} \tag{3.4}$$

Therefore, the O_2 mass transfer coefficient is D_{ox}/x_d. At higher rates of agitation the thickness of the stagnant layer decreases and so the mass transfer coefficient increases. With no reaction the O_2 concentration will fall linearly from $[O_2]_i$ at the interface (x=0) to $[O_2]_b=0$ at the edge of the diffusion layer ($x=x_d$). When simultaneous chemical reaction occurs the O_2 concentration profile becomes curved with a positive second derivative so that the concentration still falls to the bulk level at $x=x_d$ but the absorption rate, which is proportional to $d[O_2]/dx$ at x=0, is larger than that for physical absorption resulting in an enhanced absorption rate. This model is somewhat physically unrealistic since it implies a discontinuous change from transport by pure diffusion to transport by pure convection at $x=x_d$ and since a stagnant interfacial layer would not be expected, however it is mathematically simple (one adjustable parameter, x_d) and seems to perform well for engineering calculations.

Surface renewal theory (SRT) is more physically realistic but also more mathematically complex. The physical assumption behind this model is that a stagnant fluid element is brought up from the bulk solution by convection to the interface where it sticks for some residence time with one of its facets forming a small section of the interfacial area. During its residence time at the interface it absorbs gas with or without reaction as would a stagnant fluid of infinite depth. At the end of its residence time it is swept back into the bulk solution. There are two versions of SRT, those of Danckwerts (1951) and Higbie (1935). The Higbie model assumes that the residence time of any fluid element at the interface is the same and Danckwerts assumes, perhaps more realistically, that the residence time is randomly distributed about some mean. The mathematical formulation for SRT is more complex than that for film theory although it also contains only one adjustable parameter: the residence time (Higbie) or the mean residence time (Danckwerts).

The rate of gas absorption predicted by film theory and SRT are usually very close or identical. Often these differences are less than the error introduced by uncertainties in parameters such as diffusivities. Testing the relative validities of these two approaches reduces to the problem of testing the dependency of the mass transfer coefficient of the gas being absorbed upon its liquid phase diffusivity (Davies et al., 1964). Film theory predicts that k_x should vary as D_x to the first power but SRT predicts that it should vary with the square-root of D_x (Danckwerts, 1970). However, these dependencies are difficult to test since the diffusivities of dissolved gases all fall into a very narrow range around 10^{-5} cm^2/s.

The limited experimental data seems to favor the square-root approach for stirred vessels and packed columns (Kozinsky and King, 1966; Vivian and King, 1964). On the other hand, the limited range of diffusivities can be looked at as one reason that the two approaches differ so little.

For the purposes of this study, Danckwerts SRT was chosen since it is more physically realistic and has some experimental support. However, since film theory agrees so well under many conditions it is used interchangeably when the mathematical complexity precludes the use of SRT. Chan and Rochelle (1982) have shown that with equilibrium reactions film theory can be made to approximate SRT by using the square-root of diffusivities in place of diffusivities to the first power in film theory equations.

3.1.2 Danckwerts Surface Renewal Theory

The central assumptions of Danckwerts SRT are that the probability of a surface element being replaced during any given time increment is independent of the length of time it has been at the interface and during its residence time at the surface it absorbs gas as if it were a stagnant fluid of infinite depth. Implicit in the above is the assumption that the residence times are short enough so that the boundary condition which makes a fluid element seem infinitely deep is valid. That is, no unreacted gas reaches the bottom of the fluid element. This model was proposed by Danckwerts in 1951 and summarized in his classic 1970 book Gas-Liquid Reactions. In this sub-section Danckwerts SRT will be used to derive an expression for physical absorption and first-order reaction and then be extended to m-th order reactions.

The first scenario to be considered is the physical absorption of oxygen into an agitated solution where $[O_2]_b=0$ and $[O_2]_i$ is given by Henry's law. During the length of time that a fluid element is at the surface it absorbs oxygen from the gas phase as if it were a stagnant fluid of infinite depth. The equation that governs the oxygen concentration profile in such an element is:

$$\frac{\partial [O_2]}{\partial t} = D_{ox} \frac{\partial^2 [O_2]}{\partial x^2} \tag{3.5}$$

at $x = 0$ and $t > 0$, $[O_2] = [O_2]_i$

at $x > 0$ and $t = 0$, $[O_2] = 0$

as $x \to \infty$ and $t > 0$, $[O_2] \to 0$

The solution to Eq. 3.5 is:

$$[O_2] = [O_2]_i\left[1 - \mathrm{erf}\left(\frac{x}{2(D_{ox}t)^{1/2}}\right)\right] \tag{3.6}$$

The absorption rate for an individual surface element, R_{el}, is:

$$R_{el} = -D_{ox}\left.\frac{d[O_2]}{dx}\right|_{x=0} = \left(\frac{D_{ox}}{\pi t}\right)^{1/2}[O_2]_i \tag{3.7}$$

If s is the fraction of the interface renewed per second and the probability of any fluid element being replaced is independent of its age at the surface then the fraction with a residence time between time t and dt is $se^{-st}dt$. The rate of absorption is then given by summing up the rates for all the possible time increments:

$$R = \int_0^\infty R_{el}\,se^{-st}dt \tag{3.8}$$

Finally, R_o is found by substituting in R_{el} from Eq. 3.7:

$$R_o = (D_{ox}s)^{1/2}[O_2]_i \tag{3.9}$$

Therefore $k_{ox}=(D_{ox}s)^{1/2}$ and s is the adjustable parameter, a function of the agitation intensity. SRT predicts that the mass transfer coefficient varies with the square-root of the diffusivity as discussed in Sec. 3.1.1. For our apparatus at 400 rpm agitation the measured valued of k_{ox} was $8.2X10^{-3}$ cm/s and the diffusivity of oxygen in water at $50^{0}C$ is $3.72X10^{-5}$ cm^{2}/s, therefore s is 1.81 surface renewals per second or about 0.55 s per complete renewal.

For the case of simultaneous absorption and first-order reaction the procedure for deriving an expression for R is similar except that a reaction term is added to Eq. 3.5:

$$\frac{\partial [O_2]}{\partial t} = D_{ox}\frac{\partial^2 [O_2]}{\partial x^2} - k_1[O_2] \qquad (3.10)$$

This equation can be solved analytically and inserted into Eq. 3.8 to yield an absorption rate relationship:

$$R = R_0 \left[1 + \frac{D_{ox}k_1}{k_{ox}^2}\right]^{1/2} \qquad (3.11)$$

For the case of simultaneous absorption and m-th order reaction the equation describing the oxygen concentration in the surface element can only be solved analytically for m=0 or 1.

$$\frac{\partial [O_2]_i}{\partial t} = D_{ox}\frac{\partial^2 [O_2]}{\partial x^2} - k_m[O_2]^m \tag{3.12}$$

Hikita and Asai (1964) and Brian (1964) have shown that an approximate solution may be obtained by linearizing the reaction term:

$$k_m[O_2]^m \approx \left(\frac{2}{m+1}k_m[O_2]_i^{m-1}\right)[O_2] \tag{3.13}$$

This psuedo-first-order term then allows a solution analogous to Eq. 3.11:

$$R = R_o\left[1 + \frac{\frac{2}{m+1}D_{ox}k_m[O_2]_i^{m-1}}{k_{ox}^2}\right]^{1/2} \tag{3.14}$$

Comparisons with numerical evaluations for the m-th order case show that Eq. 3.14 differs by less that 6% from the rigorous solutions for m equal to integer or non-integer values between 0 and 3 (Hikita and Asai, 1964).

The reaction rate constant, k_m, is a function of the concentrations of the reactants (sulfite), catalysts and other species at the interface where the reaction occurs. So this constant may be replaced with a more generalized expression:

$$R = R_o\left[1 + \frac{\frac{2}{m+1}D_{ox}k_r[S(4)]_i^n[cat]_i^p[O_2]_i^{m-1}}{k_{ox}^2}\right]^{1/2} \qquad (3.15)$$

The estimation of the surface concentrations of various reactants and products is discussed in Sec. 4.

Eq. 3.15 may be used to explain the shape of the absorption rate vs. catalyst concentration curve shown in Fig. 3.1. At low catalyst concentrations the kinetics will be slow enough that the right-hand term inside Eq. 3.15 is much less than one so $R=R_o$ as in region B. As catalyst is added and the right-hand term rises the absorption rate becomes enhanced with the enhancement factor given by:

$$E = \frac{R}{R_o} = \left[1 + \frac{\frac{2}{m+1}D_{ox}k_r[S(4)]_i^n[cat]_i^p[O_2]_i^{m-1}}{k_{ox}^2}\right]^{1/2} \qquad (3.16)$$

As the kinetics become fast enough so that the right-hand term is much larger than one the expressions may be approximated by:

$$R = \left[\frac{2}{m+1} D_{ox} k_r\right]^{1/2} [S(4)]_i^{n/2} [cat]_i^{p/2} [O_2]_i^{(m+1)/2} \tag{3.17}$$

$$E = \frac{\left[\frac{2}{m+1} D_{ox} k_r\right]^{1/2} [S(4)]_i^{n/2} [cat]_i^{p/2} [O_2]_i^{(m-1)/2}}{k_{ox}} \tag{3.18}$$

The error introduced by this further assumption is about 11% at E=3, 7% at E=4 and 4% at E=5. From Eq. 3.17 it can be seen that the slope of the absorption rate curve in region C of Fig. 3.1 is equal to p/2. Also, in this "high enhancement" regime R becomes independent of k_{ox} and therefore independent of the agitation rate.

The method described above assumes a simple one-step irreversible reaction which may be used if the actual mechanism is not known. If the mechanism is known specialized absorption rate equations can be derived from either film theory or surface renewal theory for more complicated reaction schemes which may give better results (Brian and Beaverstock, 1965; Kuo and Huang, 1970; Matheron and Sandall, 1978; Teramoto et al., 1973).

Section 4

DIFFERENCES BETWEEN BULK AND INTERFACE CONDITIONS

4.1 Introduction

Sulfite oxidation kinetics measured in heterogeneous situations often are not the same as those measured under homogeneous conditions. One possible reason for this is differences in composition between the bulk solution and the interfacial region where the reaction takes place. The interface would be expected to be relatively depleted of reactants (sulfite and bisulfite) and relatively rich in reaction products (sulfate, bisulfate and hydrogen ions). The degree of these differences are a function of the reaction rate, the bulk solution composition and the agitation intensity. Since the rate is a function of interfacial composition and this composition is dependent on the rate, a dynamic steady state should be reached between the rate and the surface conditions for any given bulk solution composition, gas phase composition and agitation rate. Thus it would be expected that the absorption rate would correlate better with interfacial conditions than with bulk solution conditions. There is presently no satisfactory method for directly measuring interfacial pH and ionic composition without disturbing the reaction but these quantities can be estimated from transport equations.

A mathematical model is presented in this section for use in estimating the degree of differences between bulk and interface conditions for systems involving oxygen absorption into sulfite/catalyst solutions and examples of its application are given. This model is applicable to any experimental conditions but finds particular utility under FGD conditions due to the large bulk-to-interface differences that can exist for those systems.

4.2 Model of the Interfacial Region

4.2.1 Physical Model

The gas-liquid interface region is modeled with film theory as a thin stagnant film from $x=0$ to $x=x_d$ on the liquid side across which reactants from the bulk solution must diffuse to an interfacial reaction zone of thickness x_r where the oxidation occurs. The reaction products must then diffuse back to x_d to reach the bulk solution. The diffusion film becomes thinner at higher agitation rates resulting in faster mass transfer. This assumption that the molecules must diffuse a distance to and from the reaction zone is fulfilled in the fast reaction regime where the reaction zone is much thinner than this stagnant fluid layer ($x_r << x_d$). A combination of Eqs. 3.4 and 5.10 indicates that $E=x_d/x_r$. The interfacial concentration is some average value over the reaction zone for all species diffusing to and from the bulk. The value of $[O_2]_i$ is taken at x=0 because of its applicability in surface renewal equations and the usefulness of Henry's constants to predict it.

As stated in Sec. 3.1, surface renewal theory is more physically realistic than film theory but calculated values for the absorption rate of the gas being consumed as a function of the homogeneous rate constant and the interfacial concentration are identical in the limits of slow kinetics (E=1) and fast kinetics (E>3). From the viewpoint of surface renewal theory the chemical composition of the interface is the same as that in the bulk solution at the time the fluid element arrives at the surface but the interfacial composition for that element changes as oxygen is absorbed, sulfite is consumed and hydrogen ions are produced, reaching a maximum difference at the time the fluid element is pulled back into the depths. Thus, any stationary point on the surface undergoes an ocillatory change in composition. From the viewpoint of film theory the conditions at the surface are static and equal to some average value of the cyclic conditions predicted by renewal theory.

There are five unknowns to be solved for: the interfacial concentrations of sulfite, bisulfite, sulfate, bisulfate and hydrogen ions. The five physical assumptions consist of two mass balances, one charge balance and two equilibrium relationships:

1. the rate of S(4) consumption equals the rate of S(4) transport to the interface
2. the rate of S(6) production equals the rate of S(6) transport away from the interface
3. the flux of positive charges to the interface equals the flux of negative charges to the interface
4. sulfite and bisulfite are in equilibrium at the interface
5. sulfate and bisulfate are in equilibrium at the interface

4.2.2 Mathematical Model

The flux of species X to the interface is given by:

$$N_x = D_x \frac{[X]_b - [X]_i}{x_d} \qquad (4.1)$$

where: N_x = flux of X to the interface, moles/cm^{2}s

D_x = diffusivity of X, cm^2/s

$[X]_b$ = bulk liquid concentration of X, moles/cm^3

$[X]_i$ = interfacial concentration of X, moles/cm^3

This may be rewritten with a defined mass transfer coefficient:

$$N_x = k_x([X]_b - [X]_i) \qquad (4.2)$$

where: k_x = mass transfer coefficient for species X = D_x/x_d, cm/s

The mass transfer coefficient for O_2, k_{ox}, may be directly measured experimentally so it is convenient to be able to derive the coefficient for any species from k_{ox}. By the definition of k_{ox} in Eq. 4.2:

$$k_x = k_{ox}\left[\frac{D_x}{D_{ox}}\right] \tag{4.3}$$

However, Kozinsky and King (1966) has shown that the mass transfer coefficients for mechanically agitated vessels are better correlated if they vary with the square-root of diffusivity as in surface renewal theory:

$$k_x = k_{ox}\left[\frac{D_x}{D_{ox}}\right]^{1/2} \tag{4.4}$$

Film theory predicts that the liquid-phase mass transfer coefficient changes with the first power of diffusivity as in Eq. 4.3 while surface renewal theory predicts the one-half order dependency of Eq. 4.4. It is very difficult to test these two assumptions since the diffusivity for any solute tends to fall into a narrow range. The limited experimental data has been interpreted to show that the absorption rate is, in general, better correlated with the square root approach (Davies et al., 1964; Vivian and King 1964).

The consumption rate of S(4) per square cm of interface equals the production rate of S(6) and is twice the absorption rate of oxygen.

The five physical assumptions from Sec. 4.2.1 may now be cast into quantitative form:

1. $2R = N_{US4} + N_{BS4}$ (4.5)

2. $2R = -(N_{US6} + N_{BS6})$ (4.6)

3. $N_{H+} = 2(N_{US4} + N_{US6}) + (N_{BS4} + N_{BS6})$ (4.7)

4. $K_{S4} = [SO_3^{-2}]_i[H^+]_i/[HSO_3^-]_i$ (4.8)

5. $K_{S6} = [SO_4^{-2}]_i[H^+]_i/[HSO_4^-]_i$ (4.9)

where the subscripts are: BS4 = bisulfite

US4 = sulfite (unprotonated)

S4 = total sulfite

H+ = hydrogen ion

Substituting in Eq. 4.2 yields a nonlinear set of five equations for the five unknowns.

The equations may be rearranged to facilitate a numerical solution by eliminating the sulfite and sulfate unknowns from Eqs. 4.5 and 4.6 with the equilibrium relationships and then solving them for bisulfite and bisulfate, respectively. There are then three equations and three unknowns: bisulfite, bisulfate and hydrogen ion concentrations at the interface.

$$[HSO_3^-]_i = \frac{k_{BS4}[HSO_3^-]_b + k_{US4}[SO_3^{-2}]_b - 2R}{k_{BS4} + k_{US4}K_{S4}(1/[H^+]_i)} \tag{4.10}$$

$$[HSO_4^-]_i = \frac{k_{BS6}[HSO_4^-]_b + k_{US6}[SO_4^{-2}]_b + 2R}{k_{BS6} + k_{US6}K_{S6}(1/[H^+]_i)} \tag{4.11}$$

$$\begin{aligned}[H^+]_i = [H^+]_b &+ (k_{BS4}/k_{H+})([HSO_3^-]_b - [HSO_3^-]_i) \\ &+ (k_{BS6}/k_{H+})([HSO_4^-]_b - [HSO_4^-]_i)\end{aligned} \tag{4.12}$$

The equations were solved by guessing a value for $[H^+]_i$ and then calculating values of $[HSO_3^-]_i$ and $[HSO_4^-]_i$ from Eqs. 4.10 and 4.11 . These numbers were then used to obtain a new value of $[H^+]_i$ with Eq. 4.12 for comparison to the guess. When convergence was achieved, $[SO_3^{-2}]_i$ and $[SO_4^{-2}]_i$ were found from the equilibrium relationships.

The interfacial concentrations of these ionic species are a function of the bulk conditions and the absorption rate and are independent of the catalyst used to achieve a given rate.

4.2.3 Transport and Equilibrium Constants

Two types of constants are needed for the solution of Eqs. 4.5 through 4.9: liquid phase mass transfer coefficients for sulfite, bisulfite, sulfate, bisulfate and hydrogen ions and equilibrium constants for the sulfite/bisulfite and sulfate/bisulfate systems.

The mass transfer coefficients were calculated from the measured value of k_{ox} ($8.2X10^{-3}$ cm/s at 400 rpm) via Eq. 4.4 with the diffusivity of oxygen in water at 50^oC equal to $3.72X10^{-5} cm^2/s$. Ionic diffusivities at 25^oC were estimated from the following relationship (Reid et al., 1977):

$$D_x = \frac{R_g T L}{z F^2} \tag{4.13}$$

where: R_g = gas constant, 8.314 J/mole K

T = K

L = limiting ionic mobility, A/cm^2

z = ionic charge

F = Faraday's constant, 96,500 C/mole

The D_x calculations were done at 25°C since limiting ionic mobilities were available only at that temperature (Landolt and Bornstein, 1960) and corrected to 50°C with the Stokes-Einstien relationship:

$$\frac{D_x v}{T} = \text{constant} \tag{4.14}$$

where v: = viscosity of water, gm/cm s

The results of these calculations are given in Table 4.1.

The equilibrium constants K_{S4} and K_{S6} were needed at 50°C and 0.93 M ionic strength. The values at 25°C and I=0.93 M were taken from Smith and Martell (1976) and corrected to 50°C with:

Table 4.1

Liquid phase diffusion and mass transfer coefficients of the dissolved species

Species (X)	Limiting Ionic Mobility (A/cm^2)	$D_x X10^5$ 25^oC (cm^2/s)	$D_x X10^5$ 50^oC (cm^2/s)	$k_x X10^3$ 50^oC 400 rpm (cm/s)
O_2	--	2.10	3.72	8.2
SO_3^{-2}	72	0.94	1.66	5.5
HSO_3^-	50	1.30	2.30	6.5
SO_4^{-2}	80	1.04	1.84	5.8
HSO_4^-	50	1.30	2.30	6.5
H^+	350	9.11	16.1	17.0

$$\ln \frac{K_2}{K_1} = \frac{-\Delta H}{R_g}\left[\frac{1}{T_2} - \frac{1}{T_1}\right] \tag{4.15}$$

where: R_g = gas constant

ΔH = -3.0 kcal/mole for the S(4) system

= -5.6 kcal/mole for the S(6) system

The equilibrium constants were calculated to be:

$pK_{S4} = 6.57$

$pK_{S6} = 1.45$

4.3 Results and Discussion

Numerical solutions of Eqs. 4.5 through 4.9 as a function of the absorption rate at pH_b 5, $[S(4)]_b$=10 mM, $[S(6)]_b$=300 mM and k_{ox}=8.2 X 10^{-3} cm/s (400 rpm) are given in Table 4.2. The absorption rate was varied from physical absorption (0.98X10^{-9} moles O_2/cm^2 s) to R_{lim} (32.4X10^{-9}), the rate limited by S(4) transport from the bulk solution. Since the physical absorption rate is so close to 10^{-9} moles O_2/cm^2s numerical values of RX10^9 may be read as E with very little error. Significant differences between bulk and interface conditions are indicated for pH and for the concentrations of sulfite, bisulfite, S(4) and bisulfate. Once the bulk solution composition is set and R is specified there are no further degrees of

Table 4.2

Interface conditions as a function of the absorption rate at pH_b 5, 10 mM S(4) and 400 rpm agitation

E	pH_i	$[SO_3^{-2}]_i$	$[HSO_3^-]_i$	$[S(4)]_i$	$[SO_4^{-2}]_i$	$[HSO_4^-]_i$	$[S(6)]_i$
0	5.00	0.26	9.74	10.00	299.9	0.085	300
1	4.59	0.10	9.57	9.67	300.0	0.220	300
1.5	4.43	0.069	9.44	9.51	300.0	0.31	300
2	4.30	0.050	9.30	9.35	300.0	0.42	300
3	4.12	0.032	9.01	9.04	300.0	0.64	301
4	3.99	0.023	8.71	8.73	300.0	0.87	301
6	3.80	0.014	8.10	8.11	301	1.3	302
8	3.67	0.009	7.48	7.49	301	1.8	303
10	3.57	0.007	6.87	6.88	301	2.3	303
15	3.39	0.004	5.33	5.33	301	3.4	304
20	3.26	0.002	3.79	3.79	302	4.6	307
30	3.09	0.001	0.70	0.70	303	7.0	310
32.4	3.06	0.000	0.00	0.00	303	7.5	311

concentrations are in mM

freedom remaining for the interfacial concentrations so any change in the interfacial concentration of some species due to a change in R or a bulk concentration will be reflected as changes in the concentration of all the other species at the interface. For example, if the absorption rate is increased, $[S(4)]_i$ will drop by some amount while $[S(6)]_i$ and $[H^+]_i$ would rise by an amount of the same order of magnitude. The specific amounts by which the individual S(4) species, sulfite and bisulfite, are depleted at the interface and the division of the S(6) products into sulfate and bisulfate are functions of transport considerations and local pH. It is apparent then that the concentration of the more dilute species would undergo the largest proportional changes. In Table 4.2 it can be seen that the surface concentrations of the most dilute components do in fact show the most percent of change: H^+ (initially 0.01 mM), SO_3^{-2} (0.26 mM) and HSO_4^{-2}(0.085 mM). HSO_3^- (9.74 mM) and S(4) (10 mM) show less relative change at any given value of R while SO_4^{-2} and S(6) (both about 300 mM) show only a few percent of change from R_o to R_{lim}. Despite the large differences in proportional change the absolute changes are limited to about 1 to 10 mM for each species.

In the case of FGD conditions, such as those of this study, the S(4) concentration is relatively low and the slightly acid solution results in $[HSO_3^-]>>[SO_3^{-2}]$ and $[HSO_4^-]<<[SO_4^{-2}]$. Thus it can be expected that significant S(4) depletion, particularly for sulfite, could occur at the interface at modest enhancement factors and that transport of acidity away from the interface by bisulfate would be less important than transport by hydrated protons. The relationships between R and bulk conditions and the interfacial conditions in FGD-like systems are further complicated because one of the species that would be expected to undergo large proportional change, S(4), functions as both a buffer (sulfite/bisulfite at pH 6.6) and as a reactant for the system. Therefore pH_i and $[S(4)]_i$ are strong functions of R and bulk conditions for typical FGD solutions.

Eq. 4.5, rewritten below, expresses the amounts of S(4) species at the interface as a function of the rate and the bulk concentrations:

$$R = (1/2)k_{US4}([SO_3^{-2}]_b - [SO_3^{-2}]_i) + (1/2)k_{BS4}([HSO_3^-]_b - [HSO_3^-]_i) \qquad (4.5)$$

The S(4)-limited rate would be R evaluated at interfacial S(4) concentrations of zero:

$$R_{lim} = 0.72X10^{-9} + 31.7X10^{-9} = 32.4X10^{-9} \text{ moles } O_2/cm^2 s$$

Thus, the great majority of S(4) transport to the interface at pH_b 5 is by bisulfite. Eq. 4.5 may be approximated in simpler terms by expressing it in terms of total sulfite:

$$R = (1/2)k_{S4}([S(4)]_b - [S(4)]_i) \tag{4.16}$$

where: k_{S4} = concentration weighted average of k_{US4} and k_{BS4}

The S(4)-limited rate calculated from Eq. 4.16 is 32.5×10^{-9}, almost exactly the same as the one from Eq. 4.5 since nearly all the S(4) can be considered to be bisulfite. Rearranging Eq. 4.16 and using the definition of R_{lim} shows that the fractional $[S(4)]_i$ depletion is a linear function of the rate's fraction of R_{lim}:

$$\frac{[S(4)]_i}{[S(4)]_b} = 1 - \frac{R}{R_{lim}} \tag{4.17}$$

The S(4) and HSO^- columns in Table 4.2 are very nearly linear in R but the SO_3^{-2} column is not since it is at a relatively low concentration.

Interfacial pH plotted against R in Fig. 4.1 shows similar behavior for any value of bulk pH. As the absorption rate increases pH_i drops slowly from pH_b but at some point begins to drop very rapidly before leveling off near a common pH_i of about 3. The downward break occurs at higher values of R for higher bulk pH values and at $pH_b<6$ the initial slow decrease region is so small that it is practically nonexistent. These near-level regions around pH_b are main-

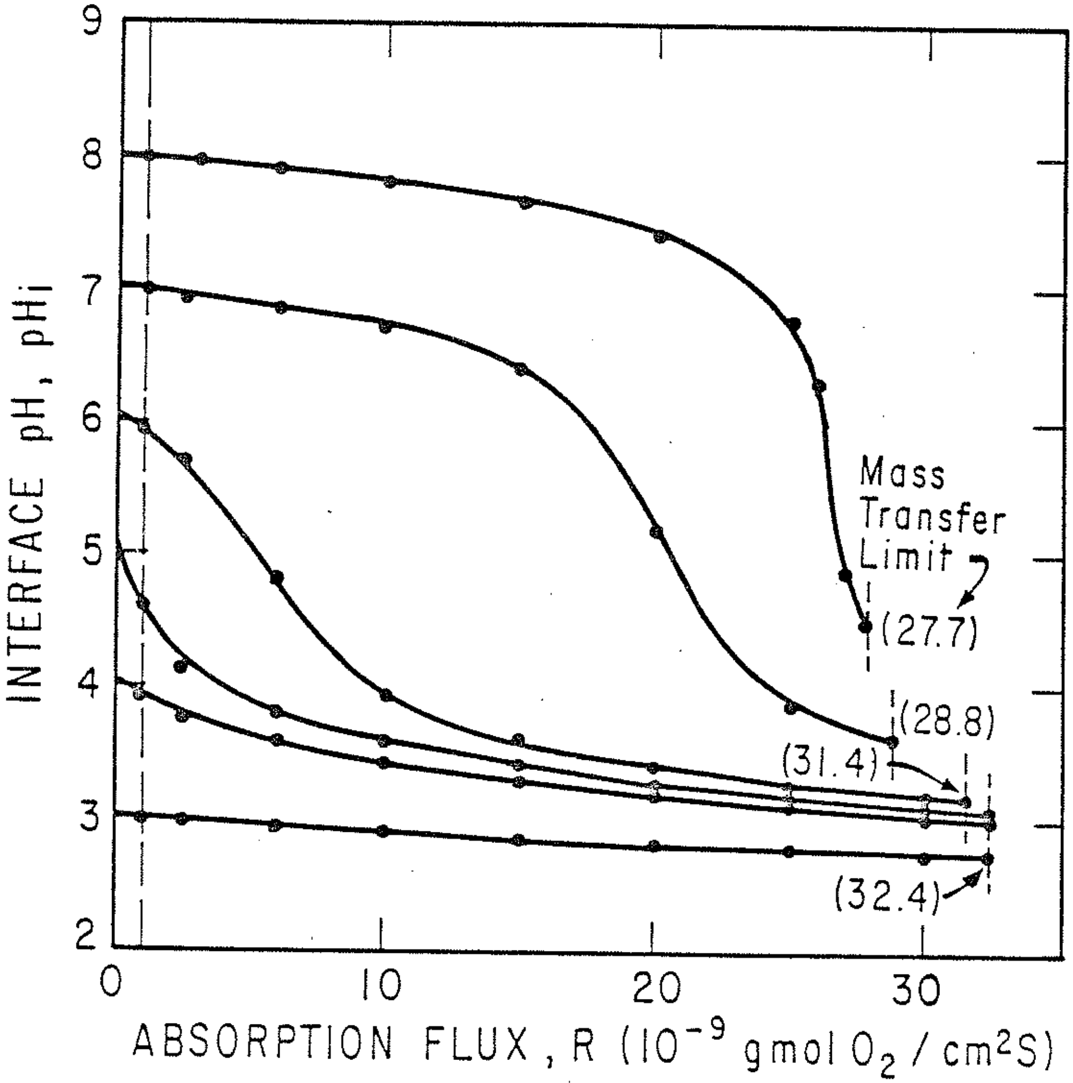

Figure 4.1: Depression of interfacial pH due to sulfite oxidation at 10 mM S(4)

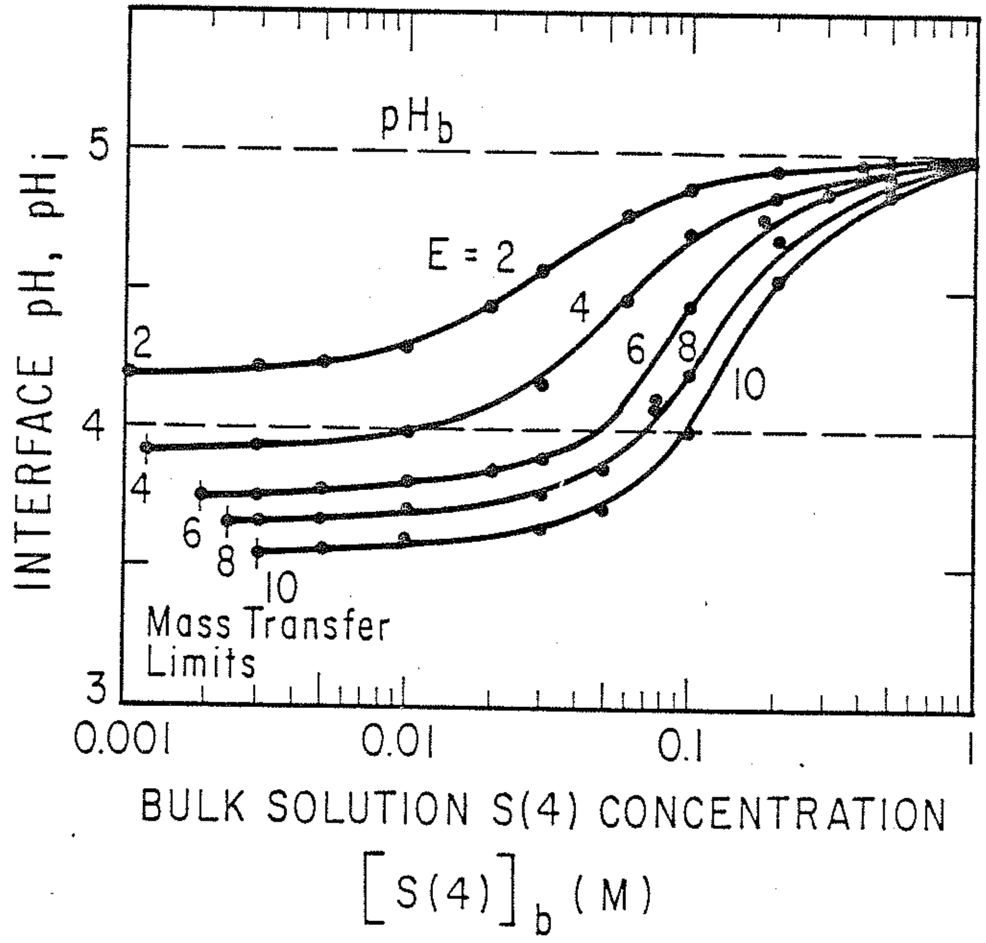

Figure 4.2: Effect of bulk sulfite concentration on the depression of interfacial pH at bulk pH 5

tained by sulfite/bisulfite buffering at the interface which occurs as long as the interfacial sulfite and bisulfite concentrations are fairly high and of comparable magnitude. When the buffering effect is removed due to decreases in $[SO_3^{-2}]_i$ (caused by interfacial S(4) depletion and pH_i drop) the sudden drop in interfacial pH occurs. At $pH_b<6$ there is never enough sulfite present at the interface to provide significant buffer capacity so there is no region where pH_i is maintained near pH_b. For the cases of $pH_b = 7$ and 8 this $[SO_3^{-2}]$ depletion is reflected by large increases in the ratio $[HSO_3^-]/[SO_3^{-2}]$ at the breakpoint indicating the loss of buffer capacity. The decrease in R_{lim} with increasing pH_b is due to the greater contribution to S(4) transport by sulfite which has a slightly lower diffusivity than bisulfite due to its higher charge. Near R_{lim} each line seems to be converging near a common pH_i of about 3. At this point the rate of H^+ production at the interface is about the same for any value of pH_b: $2R_{lim}$ or about $65X10^{-9}$ moles H^+/cm^2s. In order to maintain steady state, H^+ must be transported away from the interface at the same rate. If we assume that the only transport mechanism is the diffusion of protons then:

$$65X10^{-9} = k_{H+}([H^+]_i - [H^+]_b) \tag{4.18}$$

where: $[H^+]$ is in moles/cm^3

This equation shows that the limiting interfacial hydrogen ion concentration will be much larger than the bulk concentration and so will be fairly constant with respect to pH_b.

pH_b	limiting pH_i by Eq. 4.18
3	2.34
5	2.45
7	2.45

The solution of the more rigorous model indicates a limiting pH_i of 3.06 for pH_b 5. This difference of about half a pH unit is due to acidity transport by bisulfate; at low pH_i values the interfacial bisulfate concentration can be large enough compared to its bulk concentration to provide significant transport.

As mentioned above, the main reason for the sensitivity of pH_i and $[S(4)]_i$ to R is the low concentration of S(4) in the bulk solution leading to depletion of interfacial S(4) species at moderate absorption rates. The depression of pH_i at enhanced absorption rates is greatly diminished as $[S(4)]_b$ is increased (Fig. 4.2) since higher S(4) levels provide more buffering capacity and a higher S(4)-limited rate. Most previous sulfite oxidation work has been applied to mass transfer characterization or to mechanism studies which are usually carried out at $[S(4)]_b$ values of 0.5 M or higher. Thus, it can be seen from Fig. 4.2 that differences in bulk and interface conditions would not be a problem for studies conducted at such high S(4) levels but would be a concern for heterogeneous experiments done under FGD conditions.

The partial pressure of SO_2 over an S(4) solution (Fig. 4.3) may be a strong function of bulk-to-interface conditions. This could be especially important in the design of units for simultaneous scrubbing and oxidation. The following equation was used to determine P_{SO2} (Rochelle, 1980):

$$\log \frac{P_{SO2}}{P_{H2O}[S(4)]_i} = 3.24 - pH_i \tag{4.19}$$

where: P_{SO2} and P_{H2O} are in atm and $[S(4)]_i$ is in M

The peaks in P_{SO2} are caused by two competing effects: decreasing pH_i and decreasing $[S(4)]_i$. Flue gas from coal-fired boilers averages 500 to 5000 ppm SO_2. This range is acheived at about $(1/2)R_{lim}$ at pH_b 5.

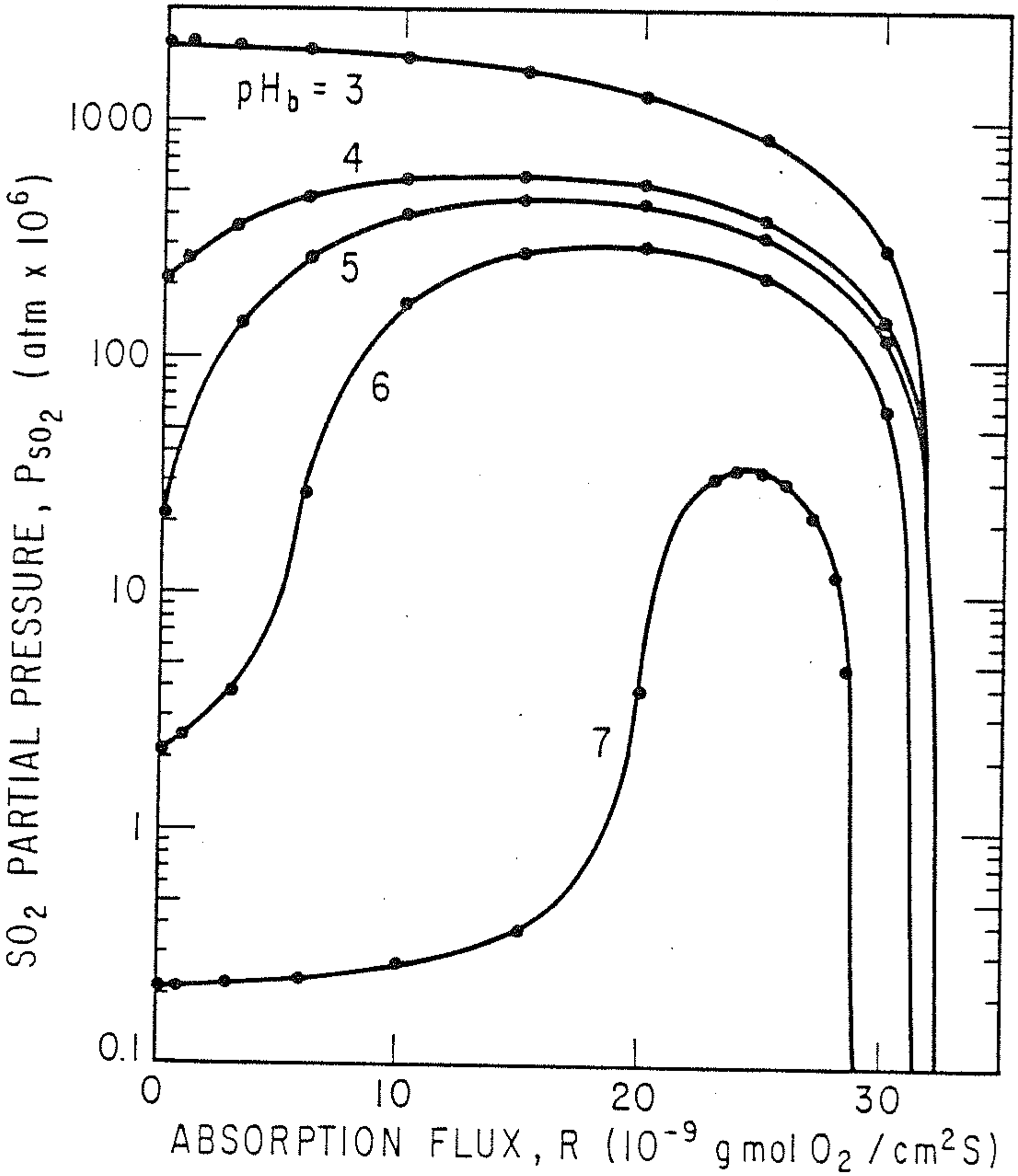

Figure 4.3: Effect of interfacial sulfite oxidation on the partial pressure of sulfur dioxide above the solution at 10 mM S(4)

Section 5

KINETICS AND MECHANISMS

5.1 Mathematical Model of Enhancement due to Free Radical Reactions

A quantitative relationship between the observed absorption rate and proposed reaction steps must be derived in order to evaluate the validity of candidate mechanisms. Such a model is necessarily part of the proposed mechanism itself since it relies on physical assumptions and can be imagined, in its most basic form, to be a mathematical relationship between the gas absorption rate and the interfacial concentrations that are calculated by the methods of Sec. 4. Reactant and catalyst concentrations will vary with position in the reaction zone so the interfacial concentrations are some integrated average from $x=0$ to $x=x_r$. This type of model is derived in the first part of this section on the basis of film theory and employing a generalized free radical reaction mechanism. Experimental data is then evaluated with the model in order to ascertain characteristics of the sulfite oxidation mechanism. The model is presented in context with sulfite oxidation but should be applicable to other complex reactions under heterogeneous conditions.

Since a detailed free radical mechanism is not available, the model must employ a generalized sequence consisting of initiation, propagation, termination and perhaps inhibition steps. The effects of catalysts are easier to model than the effects of reactants because the initiation and termination reactions are much less numerous and interrelated than propagation reactions and therefore are better understood. Because there are so many possible propagation reactions they are more prone to change with changing conditions.

The initiation step is assumed to be a Backstrom-type reaction (Backstrom, 1934; Backstrom and O'Hern, 1966; Chen and Barron, 1972) as given in Sec. 1.3.3:

$$Me^{U} + X \longrightarrow Me^{L} + R^{\bullet} \qquad \text{(Rxn. 5.1)}$$

where: $Me^{U,L}$ = a metal ion in its upper,lower state

X = some non-radical ion or molecule

$R^{\bullet}$ = a radical

The initiation rate at constant local [X] is then:

$$r_{init} = k_{init}[Me^U] \qquad (5.1)$$

where: $[Me^U]$ = the local Me^U concentration

The free radical created in Rxn. 5.1 then participates in a cyclic set of propagation reactions that involves other radical intermediates being generated and consumed. The typical propagation reaction does not change the number of free radicals but passes the radical character on to another species:

$$R^{\bullet}_A + X_B \longrightarrow X_A + R^{\bullet}_B \qquad \text{(Rxn. 5.2)}$$

There will be a number of reactions like 5.2 operating in a cyclic series, the radical product of one being the radical reactant of the next. Therefore, if propagation steps are not competing for the same radicals, the concentrations of all radicals in the reaction zone would be proportional to one another and the reactions would be first order so the generalized expression for the propagation rate would be:

$$r_{prop} = k_{prop}[R^{\bullet}] \quad \text{at constant } [X] \qquad (5.2)$$

The product, S(6), is formed from the further reaction of non-radical propagation products such as the reaction of SO_5^{-2} with sulfite to form two sulfates. The rate of sulfite oxidation in the reaction zone, r_{S4}, is proportional or equal to r_{prop} since some constant integer number of S(4) ions will be oxidized by each complete propagation cycle (2 for Backstrom's mechanism). The number of times that the propagation sequence cycles before termination is defined as the "chain length" and was first measured for sulfite oxidation by Backstrom (1927). The value of the chain length and the effects of changing conditions upon it can be used to determine aspects of the mechanism (Huyser et al., 1973; Twigg, 1962; Walling, 1957).

Termination reactions consume free radicals and therefore stop propagation chains. This reaction can be first order in $R^{\bullet}$ if the radical combines with a non-radical to become a non-reactive radical or second order if two radicals combine into a non-radical.

$$r_{term} = k_{t1}[R^{\bullet}] \quad \text{1st order termination} \tag{5.3}$$

$$= k_{t2}[R^{\bullet}]^2 \quad \text{2nd order termination} \tag{5.4}$$

Termination occurs either chemically, by the above reactions, or by dispersion, where a radical from a propagation cycle moves away from the oxygen-rich surface and, therefore, no longer contributes to the oxidation process. These radicals are eventually converted to non-radicals or consumed in the bulk solution but their rate of departure from the reaction zone is mass transfer controlled and therefore first order.

If the free radical concentration is at steady state $r_{init}=r_{term}$ so:

$$[R^{\cdot}] = (k_{init}/k_{t1})[Me^U] \qquad \text{1st order termination} \qquad (5.5)$$

$$= (k_{init}/k_{t2})^{1/2}[Me^U]^{1/2} \qquad \text{2nd order termination} \qquad (5.6)$$

The propagation rate, proportional to the oxidation rate, is given via Eq. 5.2:

$$r_{prop} = k_{prop}\left[\frac{k_{init}}{k_{t1}}\right][Me^U] \qquad \text{1st order termination} \qquad (5.7)$$

$$= k_{prop}\left[\frac{k_{init}}{k_{t2}}\right]^{1/2}[Me^U]^{1/2} \qquad \text{2nd order termination} \qquad (5.8)$$

The next task is to relate R to r_{prop} via film theory. Although surface renewal theory is more physically realistic than film theory (Sec. 3) it will be shown that the results are identical for the two approaches above an enhancement factor of about three. Although surface renewal theory should be used for E<3, the derivation of an absorption rate expression via film theory serves to illustrate the relationships between the rapidity of the homogeneous kinetics, the thickness of the reaction zone and the absorption flux.

The physical model (Fig. 5.1) involves a stagnant reaction zone of thickness x_r (as described in Sec. 3.1.1) in which all the incoming oxygen is consumed. The oxygen concentration profile is assumed to be straight between x=0 and x_r in contrast to the more realistic profile which would show a positive second derivative. An oxygen balance gives:

$$R = 1/2\ r_{S4}\ x_r \tag{5.9}$$

where: r_{S4} is in gmols S(4)/cm^3 s

The flux of oxygen at the surface is:

$$R = -D_{ox}\left.\frac{d[O_2]}{dx}\right|_{x=0} = D_{ox}\frac{[O_2]_i}{x_r} \tag{5.10}$$

Eliminating x_r gives the desired expression:

$$R = \left[\frac{D_{ox}[O_2]_i}{2}\right]^{1/2} r_{S4}^{1/2} = (1.49X10^{-6}) r_{S4}^{1/2} \quad \text{gmols } O_2/\text{cm}^2\text{s} \qquad (5.11)$$

Inspection of the above equations shows that the thickness of the reaction zone is inversely proportional to the absorption rate or inversely proportional to the square-root of r_{S4}. This film theory result is identical to the surface renewal theory expression at high enhancement factors but predicts lower values of R in the "knee region" between E=1 and E=3 (transition from region B to C in Fig. 3.1). Above E=3 the error is less than 10% but, under the conditions of this study, enhancements often fall in the knee region so surface renewal theory is used to relate R to r_{S4}, the homogeneous rate, and to k_1, the first order (in O_2) rate constant. These slight errors will be ignored for the purposes of relating the presumed reaction steps described at the beginning of this section since the basis of comparison between the model and the observed absorption rates will be trends (such as reaction orders and forms of the absorption rate equations) instead of absolute rates of absorption.

Substitution of r_{prop} from Eqs. 5.7 and 5.8 for r_{S4} in Eq. 5.11 gives:

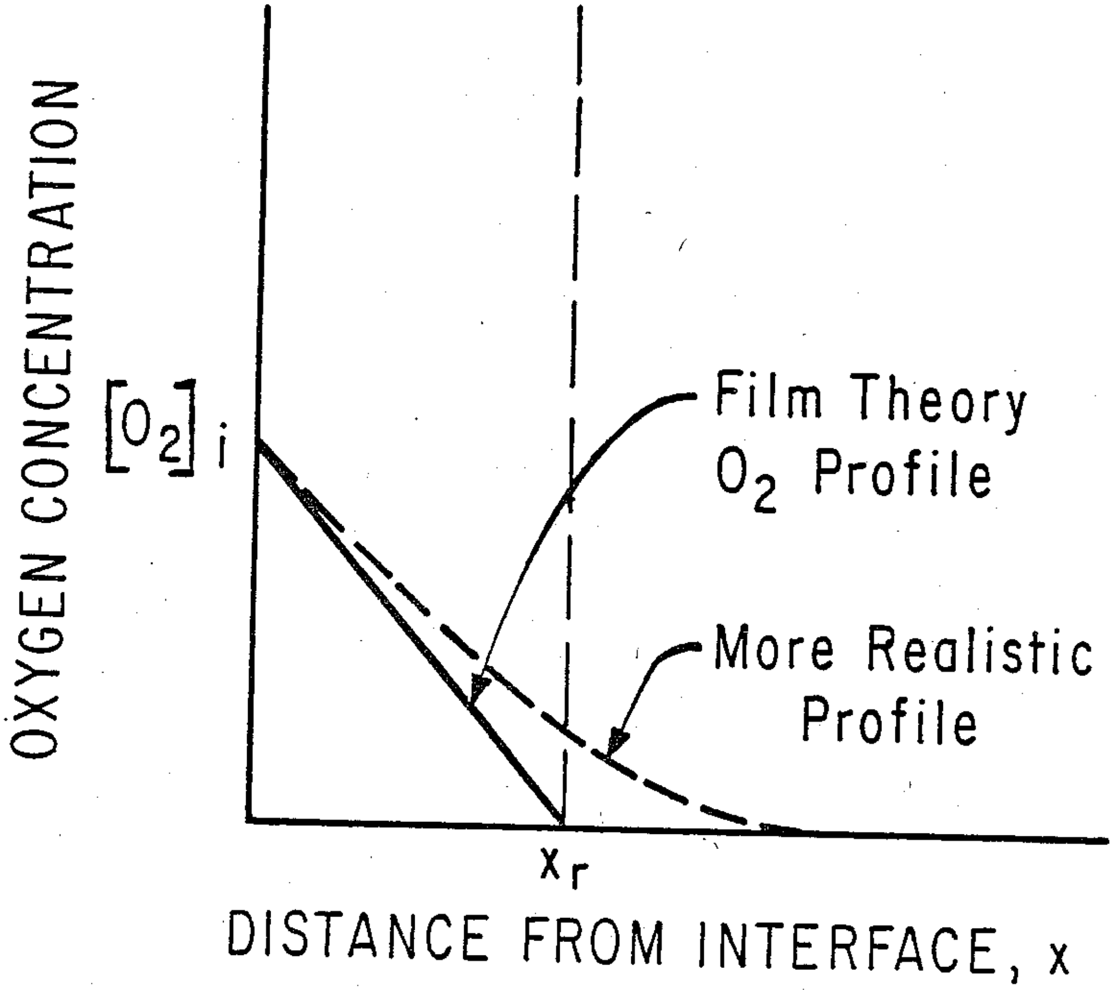

Figure 5.1: Oxygen profile in the interfacial reaction zone

$$R = \left(\frac{D_{ox}[O_2]_i}{2}\right)^{\frac{1}{2}}\left(\frac{k_{prop}k_{init}}{k_{t1}}\right)^{1/2}[Me^U]^{1/2} \quad \text{1st order termination} \quad (5.12)$$

$$= \left(\frac{D_{ox}[O_2]_i}{2}\right)^{\frac{1}{2}} k_{prop}^{1/2}\left(\frac{k_{init}}{k_{t2}}\right)^{1/4}[Me^U]^{1/4} \quad \text{2nd order termination} \quad (5.13)$$

The applicable expression will depend on the termination mechanism but 5.13 would be expected to hold at higher rates since the higher radical concentration would preferentially accelerate the second order reaction over the first order step. These equations are modified for the actions of inhibitors in Sec. 5.3.

Catalytic activities may be compared by determining r_{S4} and k_1 from R via surface renewal theory. In the absence of information on m, the homogeneous reaction order with respect to oxygen, m=1 is assumed to give pseudo-first order data. Rearrangement of Eq. 3.11 gives:

$$k_1 = \frac{k_{ox}^2}{D_{ox}}\ (E^2 - 1) = (1.81)(E^2 - 1) \quad s^{-1} \qquad (5.14)$$

This constant and the oxygen concentration in the reaction zone, assumed to be $[O_2]_i/2$, fixes the homogeneous rates of oxygen and S(4) comsumption:

$$r_{ox} = k_1([O_2]_i/2) = (1/2)r_{S4} \tag{5.15}$$

where: $[O_2]_i = 1.2X10^{-4}$ M

r_{ox} and r_{S4} are in M/s

Elimination of k_1 relates E and r_{S4}:

$$r_{S4} = \frac{k_{ox}^2}{D_{ox}}[O_2]_i(E^2 - 1) = (2.17X10^{-4})(E^2 - 1)\ \frac{M\ S(4)}{s} \tag{5.16}$$

5.2 Catalysis by Dissolved Metal Ions

5.2.1 Comparison of Catalysts

Table 5.1 shows the relative catalytic abilities of 10 mM of the six transition metals at the default conditions of this project (given in Sec. 2.2). The pseudo-first order rate constants (in O_2) were calculated from data in Figs. 5.2, 5.3 and 5.4 via Eq. 5.14. The average homogeneous rate of sulfite consumption, r_{S4}, was calculated from Eq. 5.16. The physical absorption rate at 400 rpm was measured at $0.98X10^{-9}$ moles O_2/cm^2s so, at this agitation intensity, the quantity $RX10^9$ can be assumed to be numerically equal to E with very little error. It was found that the rates for Cu and Cr, which were added in their upper states, started out very high ($E\approx15$ and 35) and decreased to a steady state in one to three hours. Greenhalgh et al. (1975) observed similar transients following the addition of cupric ions. Mn, Co and Ni, which were added in their lower states, reached steady state in under 10 minutes and may have risen slightly to the final values. Iron was added in both states and showed similar behavior, dropping from E=4.2 to steady state, E=2.4, in two hours when added as 1 mM ferric chloride and rising less than 10% in only a few minutes to about the same value when added as ferrous sulfate. Also, other investigators have found higher rates in rapid mixing experiments when Co or Cu is added with the oxygen-carrying steam instead of being in the sulfite stream (Mishra and Srivastava, 1976; Altwicker, 1976; Chen and Barron, 1972). Barron and O'Hern (1965) have found that copper in the cupric form was a strong catalyst while cuprous copper was a mild inhibitor. Furthermore, all sulfite oxidation catalysts exhibit more that one significant oxidation state. All of this evidence lends credence to the idea that it is the upper valence state of the ion that is catalytically active, probably via Rxn. 5.1. Ni, which has only one significant valence state in solution, was the most inactive catalyst and its slight activity could have been due to Fe impurities.

Table 5.1

Comparison of catalytic activities during enhanced oxygen absorption into 10 mM S(4) and 300 mM S(6) at pH 5, 50°C and 400 rpm agitation

k_1 = first order (in O_2) rate constant, s^{-1}
r_{S4} = average homogeneous oxidation rate in the reaction zone, gmols S(4)/liter sec.

mM catalyst		E	k_1	r_{S4}
5	Mn	2.5	9.5	0.0011
10	Mn	5.0	43	0.0050
50	Mn	7.5	99	0.0120
0.1	Fe	3.1	16	0.0019
0.5	Fe	3.1	16	0.0019
5	Fe	2.6	10	0.0012
10	Fe	2.4	8.6	0.0010
50	Fe	2.4	8.6	0.0010
5	Co	1.5	2.3	0.0003
10	Co	1.9	4.7	0.0005
50	Co	3.2	17	0.0020
10	Ni	1.1		
50	Ni	1.2		
10	Cr	2.7	11	0.0013
10	Cu	7.3	94	0.0110

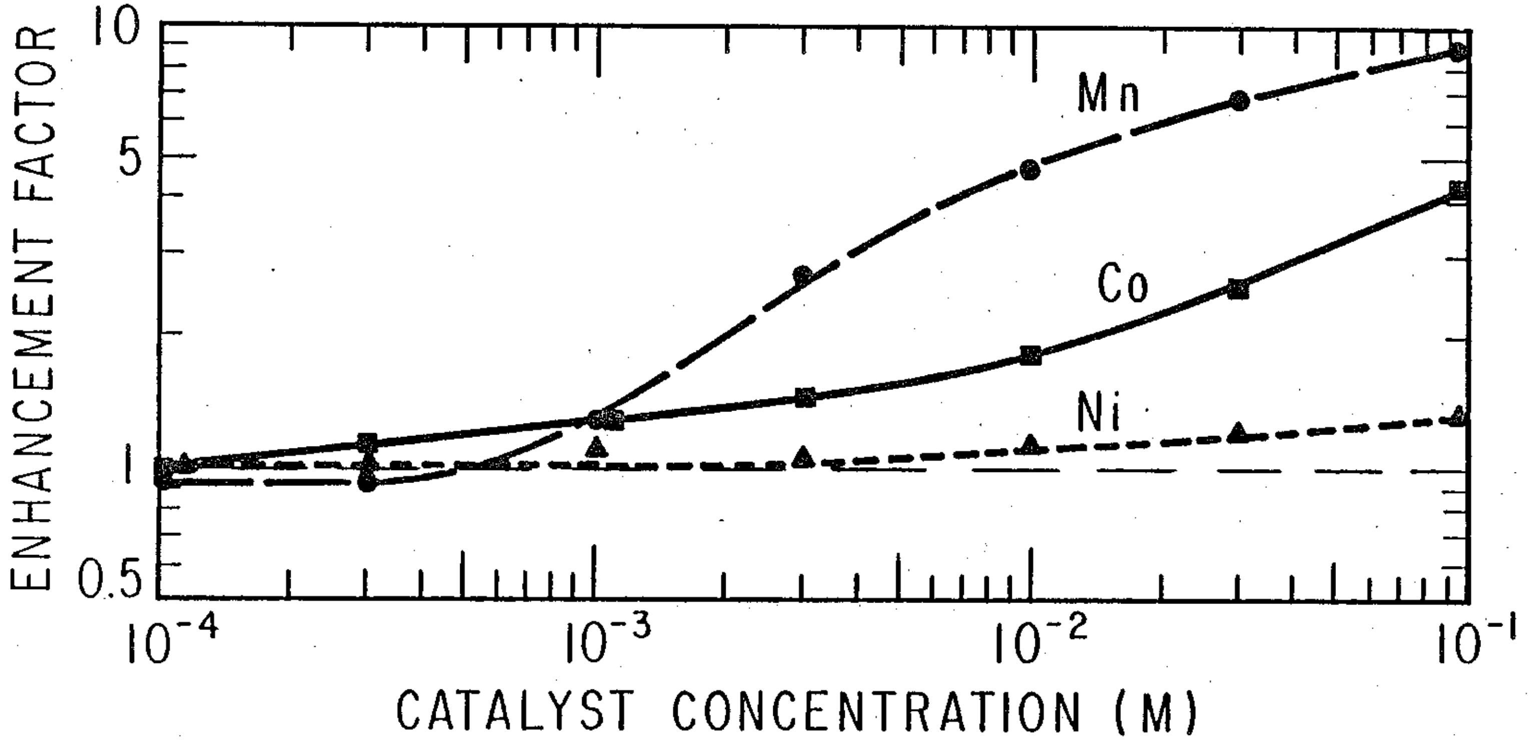

Figure 5.2: Effect of Mn, Co and Ni catalyst concentration on the enhancement factor at 10 mM S(4) and pH 5

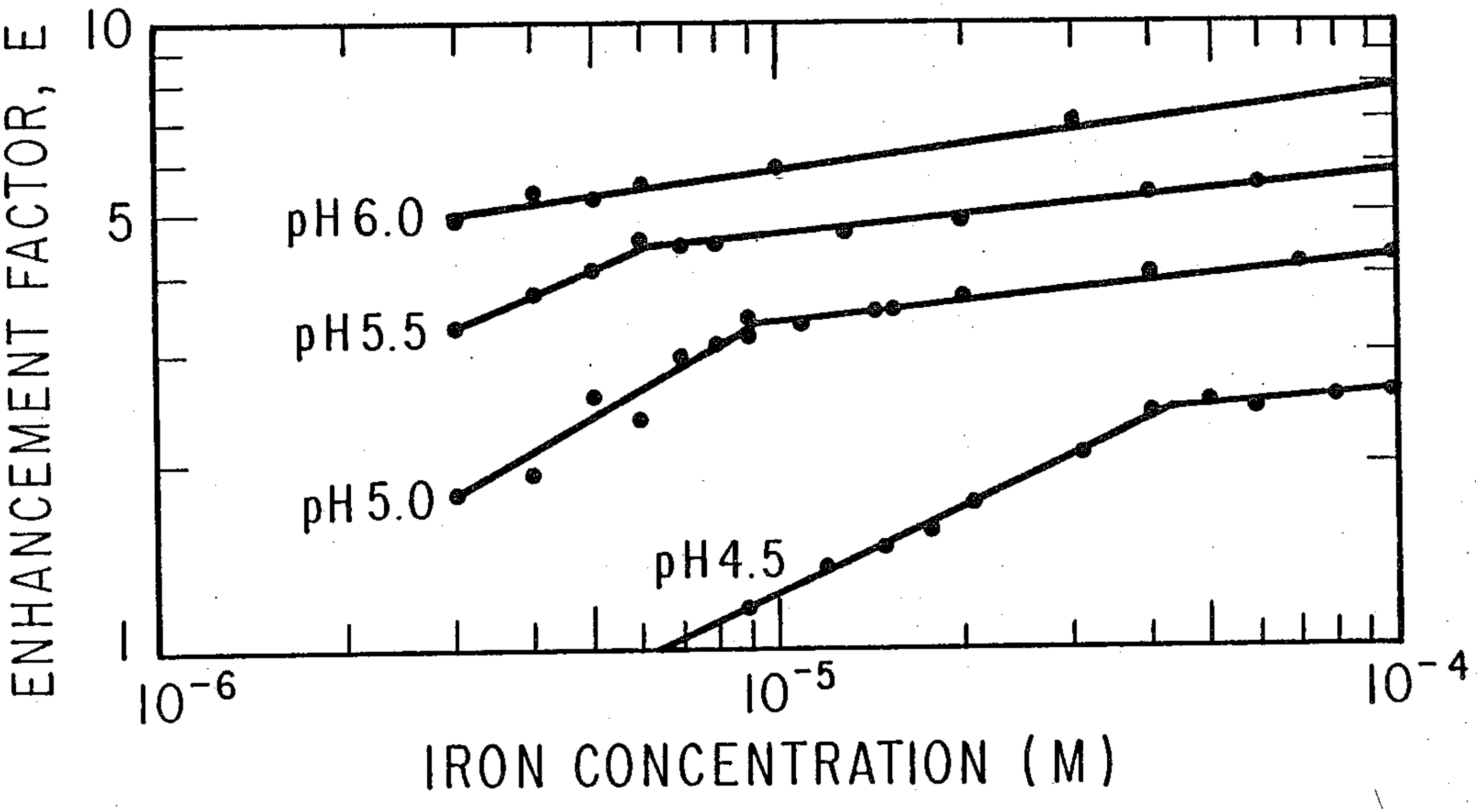

Figure 5.3: Effect of low Fe concentration on the enhancement factor at 30 mM S(4) and various pH values

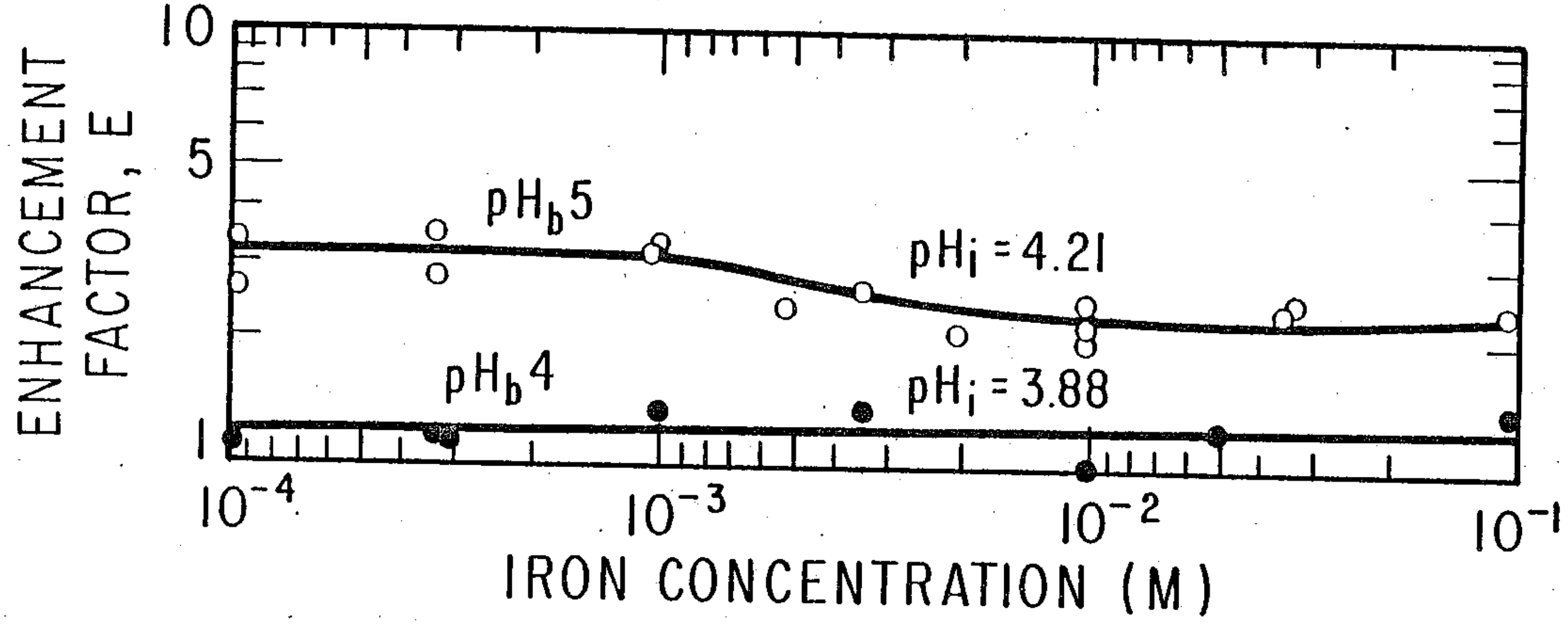

Figure 5.4: Effect of high Fe concentration on the enhancement factor at 10 mM S(4) and pH 4 and 5

The homogeneous rates from Table 5.1, r_{S4}, were compared with homogeneous rates from the literature. Published rate expressions were evaluated at 5 mM catalyst for Mn and Co, 0.1 mM catalyst for Fe, 10 mM total sulfite, 0.12 mM oxygen and pH 5. This lower level for iron was used since the catalytically active species seems to be solubility limited at this concentration of total iron (Fig. 5.3). Hoffmann and Jacob (1982) have published a review of rate expressions derived from experiments at low pH but the sulfite and catalyst levels were smaller than those in this project. These expressions predict reaction rates of at least two orders of magnitude too high for Mn in four out of the five comparisons. Table 5.1 gives r_{S4}=0.0011 M S(4)/s for 5 mM Mn while Hoffmann and Jacob's relationships predict 250, 47, 0.50, 0.16 and 0.0013. The expressions for iron agreed much better with one high (0.25), one low (0.00001) and three of the right magnitude (0.0082, 0.004, 0.008) compared to 0.0019. All three comparisons were high for Co: 2.0, 0.09 and 0.007 compared to 0.0003. Bengtsson (1974) studied Co at pH 5 and his expression, extrapolated to the higher catalyst concentrations in this study, predicts a rate about two orders of magnitude too high (0.057). Martin (1983) studied Mn and Fe catalysis at pH 0 to 3, 0.1 mM catalyst and 1 mM sulfite. Again, the expression for Mn is at least five orders too high while the predicted rate for iron is of the same order. Therefore, the published homogeneous rates seem to be higher than those observed for 5 mM Mn and Co but about equal to those for 0.1 mM Fe. However, most of the published expressions were derived from data at catalyst concentrations closer to 0.1 mM than 5 mM.

Although ferric seems to be more directly active in initiating free radical chains, ferrous ions may participate in the production of radicals by decomposing hydroperoxides into radicals (Walling, 1957; Huyser, 1973; Twigg, 1962). Branching reactions such as the following are common in the solution phase free radical oxidation of hydrocarbons:

$$Me^{L} + XOOH \longrightarrow Me^{U} + XO^{\bullet} + OH^{-} \qquad \text{(Rxn. 5.3)}$$

The result of branching reactions is a higher free radical concentration which serves to decrease the yield of hydroperoxides in the reaction products, increase the reaction rate and shorten the propagation chain length by consuming chain carriers (Turney, 1965). In the case of sulfite oxidation the most probable participants in Rxn. 5.3 would be the decomposition of HSO_5^- to $SO_4^{\dot{-}}$. Also, the ferrous ions will effect the solution equilibrium and the average valence number.

The effect of Mn, Co and Ni catalyst concentrations on the absorption rate is shown in Fig. 5.2. All three curves converge at

R_0 below 1 mM. The curve for Mn changes slope from 0.54 to 0.27 at 10 mM indicating a change in homogeneous order from about unity to about one-half. Coughanower and Krause (1965) have observed similar behavior with this catalyst. The generalized reaction model presented above predicts one-half and one-quarter slopes for the cases of first and second order termination, respectively, so the observed change in slope may be due to the shift to a second order termination reaction as the free radical concentration becomes high enough to favor this step. Co seems to exhibit a slope of one-half above 30 mM and Ni never shows enough enhancement to determine its order.

An estimate of the free radical concentration in the reaction zone may be made from kinetic data. Hayon (1972) gives the second order rate constant for the combination of O_2 and the sulfite radical (the first propagation reaction in the Backstrom mechanism, Sec. 1.3.3) as 10^9 $(M\ s)^{-1}$. If a typical homogeneous rate of 10^{-3} moles S(4)/l s is assumed and the oxygen concentration is taken to be 10^{-4} M then the sulfite radical concentration is about 10^{-8} M.

5.2.2 Catalysis by Iron

Similar experiments with Fe gave a quite different kind of result; the curves showed significant slope only at concentrations below 0.1 mM (Fig. 5.3) and exhibited zero order above that level

(Fig. 5.4). 0.1 mM Fe gave as much enhancement as 3 mM Mn at pH 5 so it is at least 30 times more potent as a catalyst judged on the basis of causing enhanced oxygen absorption. However, under homogeneous reaction conditions, the relative catalytic power would be $30^2=900$ due to the square root dependency of the absorption rate upon the homogeneous velocity. These results are explained if the catalytically active species is a ferric ion--probably complexed-- and if its concentration is solubility-limited at or below the breakpoints in Fig. 5.3. Justification for the first assumption comes from the experiments described above involving addition of Fe in its two valence states and literature support for chain initiation by upper states. If some ferric species is the only catalytically active agent then the apparent zero order behavior would be due to solubility limitations on sparingly soluble ferric ions. The breakpoints move up with lower pH due to the increased solubility limit. The solubility of ferric or ferrous iron if difficult to determine because of the many hydrolysis and precipitation reactions that can occur, some of which are slow in going to completion (Tamura et al., 1976; Gayer and Woontner, 1956; Siddall and Vasburgh, 1951; Leussing and Kolthoff, 1953). Ferric iron can exist as hydrated and complexed Fe^{+3}, $Fe(OH)_2^-$ or FeOOH as well as several other forms. These species can exist as free ions or neutral molecules, floc or solid precipitates. The relative catalytic activities of these species are not known although it has been claimed that some hydrolyzed ferric forms are better reactants for the initiation step because they can have a higher redox potential, particularly those formed at high pH. (Brimblecombe and Spedding, 1974). The solutions containing Fe and sulfite were observed to turn an opaque red-brown at 1 mM Fe and were at least red-tinted at 0.1 mM indicating the presence of some sort of suspended ferric floc. After each experiment with iron the inside of the reaction vessel as well as the impeller, pH probe and thermometer were coated with brown precipitate which seemed to increase in quantity with both pH and time. The solubility of ferric oxides and hydroxides are well below the breakpoints of Fig. 5.3 while the solubility of ferrous species would be much higher. At pH 5 the solubility of FeOOH is about 10^{-9} M, typical of most ferric ions, while the breakpoint occurs at 10^{-5} M total iron. When the total Fe concentration is less than 10^{-5} M the concentration of the catalytically active species is below its solubility limit and in equilibrium with other Fe species. As the total Fe concentration rises the concentration of the active species also rises until it hits its limit at a total Fe concentration of 10^{-5} M.

Some ferric species have higher redox potentials than hydrated ferric ions and, therefore, may be better initiation agents (Gayer and Woontner, 1956; Brimblecombe and Spedding, 1974; Huss et al., 1982). The redox potential for the sulfite/sulfite radical couple is estimated at 0.89 V (Hoffmann and Jacob, 1982) so the ferric/ferrous couple at 0.77 V would not be as effective an initiator as FeOOH (0.908 V). Both of these iron couples are below 1.23 V so the ferric forms would be thermodynamically favored in the presence of dissolved oxygen.

The iron-catalyzed rate was higher at higher pH, possibly because the catalyst regeneration reaction, ferrous to ferric, is faster at more basic conditions. Ferrous oxidation is a short chain reaction possibly employing some radicals such as hydroxyl and is first order in pH from 2 to 5 and second order above 6 (Tamura et al., 1976; Stumm and Lee, 1961) Therefore, under these conditions, the catalyst regeneration reaction should be between one and two orders of magnitude faster per unit of pH rise.

Fig. 5.5 shows the results of varying the total sulfite concentration in the presence of Fe catalyst. The observed phenomena may be the result of either kinetic effects caused by the changing interfacial concentration or pH effects caused by changing bulk S(4) concentrations. The question is resolved by using the interfacial model to determine pH_i at several points along the curves. These calculations indicate that there are no profound variations of interfacial pH along either curve and therefore the shapes of these curves are due to kinetic effects. The interfacial pH does not vary much in this kind of S(4) scan because of competing actions: as the bulk lev-

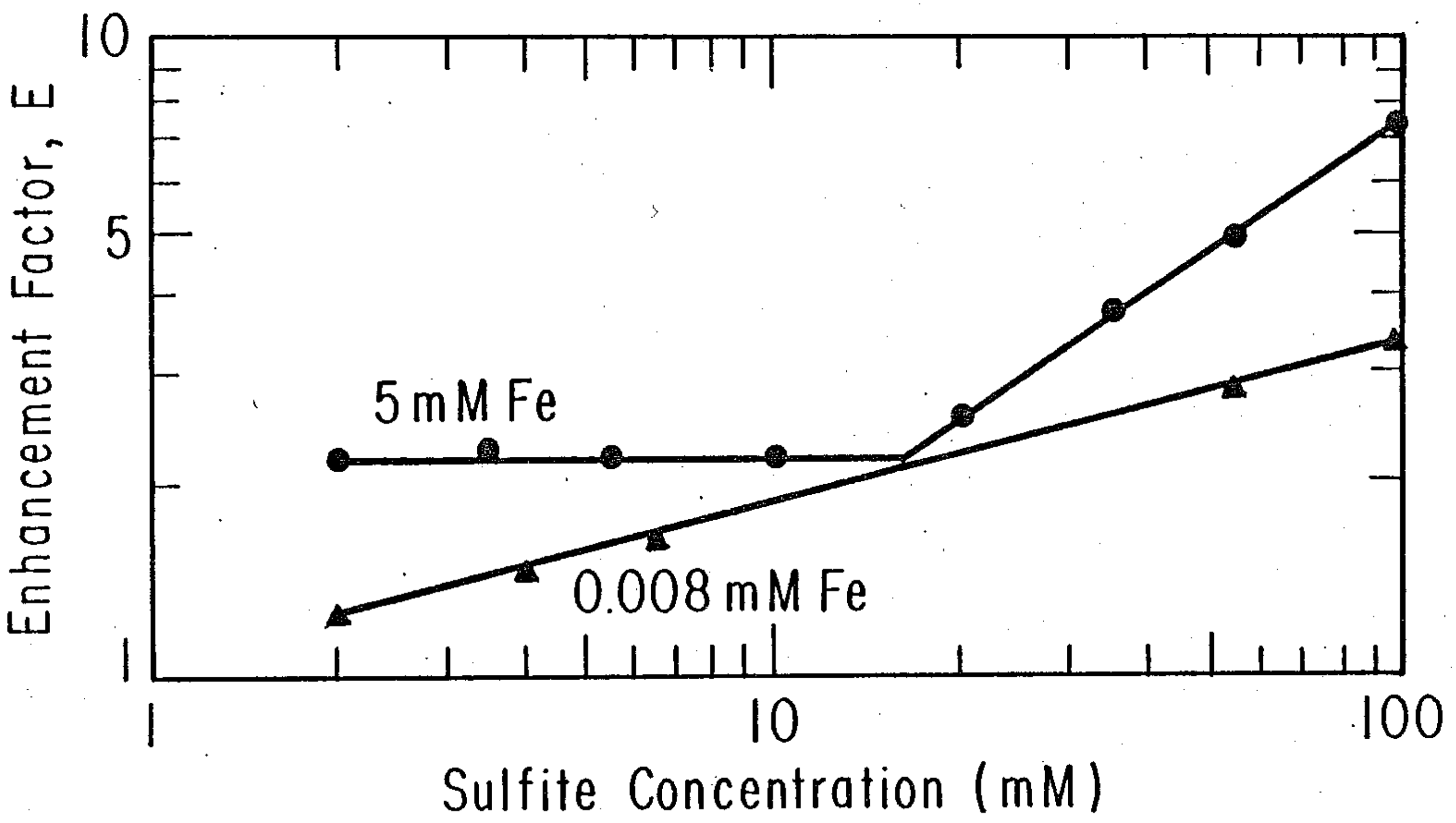

Figure 5.5: Effect of sulfite concentration on the enhancement factor at low and high Fe concentrations

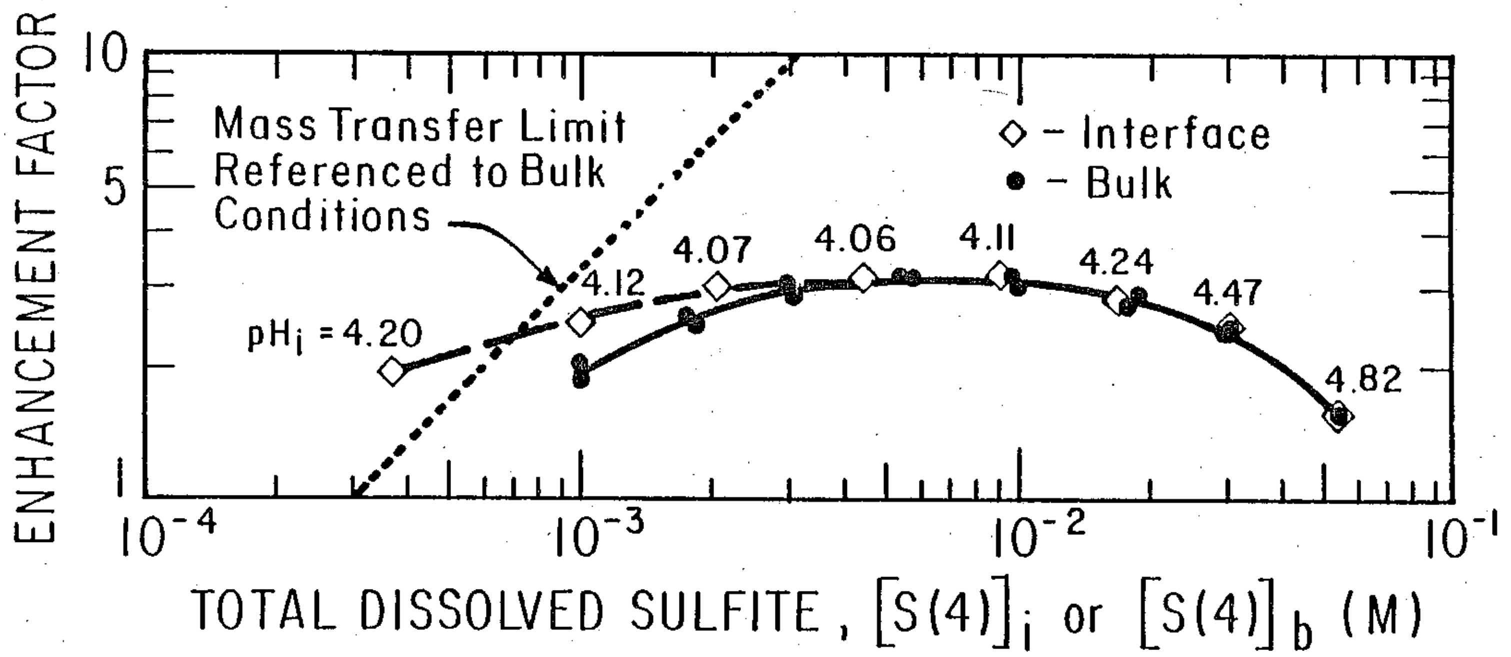

Figure 5.6: Effect of sulfite concentration on the enhancement factor at 30 mM Mn catalyst and pH 5

el of total sulfite is raised the interfacial region is more strongly buffered but the absorption rate is also generally higher. Therefore, interfacial pH variation tends to be less of a concern in S(4) scans than in catalyst scans.

The reaction order with respect to S(4) (Fig. 5.5) at an iron concentration of 0.008 and pH_b 5 showed a one-half order dependence but at 5 mM Fe the order changed abruptly from zero to about 1.5 at 17 mM S(4). In addition to this order change there was a change from one-half to zero and 1.5 at some Fe concentration between these two cases. Changes of reaction order such as these are typical of complex reactions with many intermediates and indicates a change in importance of certain elementary steps as the solution concentration is altered. Although the ferric concentration in the solution would be expected to be the same for the two total Fe concentrations it seems that the total amount of iron in the solution or the concentration of some other component that is proportional to total iron does have some effect upon the mechanism. This may be due to increased branching caused by ferrous ions (Rxn. 5.3) or by effects upon the catalytic regeneration reaction. Fig. 5.6 shows an approximate zero order dependency on S(4) at 30 mM Mn catalyst. The solid line is with respect to bulk S(4) concentration and the dashed line is for interfacial S(4) levels as calculated by Eq. 4.17 which diverge significantly from the bulk concentrations only when R approaches R_{lim}. Interfacial pH values are listed above the data points.

An FGD oxidation system operating under the conditions of this project would be expected to show enhancement factors that are independent of pH. At a constant S(4) concentration of 30 mM the enhancement factor for an Fe-saturated system drops from 4.5 at pH 5.5 (at the breakpoints of Fig. 5.3) to 2.5 at pH 4.5. However, the S(4) concentration for a saturated $CaSO_3$ solution would rise by a factor of 10 as a result of a one unit pH drop. Fig. 5.5 indicated a 0.26 order dependency of E on [S(4)] for an Fe-catalyzed system at the breakpoint at pH 5. Therefore, the net change in enhancement is:

$$E(\text{pH } 4.5)/E(\text{pH } 5.5) = (2.5/4.5)10^{0.26} = 1.01$$

5.3 Inhibition by Free Radical Scavengers: Thiosulfate

The effects of various types of inhibitors can give information on the mechanisms of complex chemical reactions. There are basically two types of inhibitors, those that are consumed so that they have temporary effects such as free radical scavengers and those that are not consumed and have a permanent effect such as complexing agents. This section is concerned with the former which may include organic compounds with hydroxyl groups such as mannitol (Fuller and Crist, 1941), hydroquinone (Altwicker, 1977) and ethanol (Braga and Connick, 1982). Mechanistic information from inhibitor studies can be garnered from the amount of retardation produced, the rate of recovery and the degree of recovery. For example, ethanol is a good test for the presence of sulfate radicals during the reaction since it reacts about 10,000 times faster with sulfate radicals than with $SO_3^{\dot{-}}$ or $SO_5^{\dot{-}}$ radicals (Hayon et al., 1972). Although the chemistry of thiosulfate is not well understood it is believed to act in the same way as organic inhibitors: it reacts with a free radical and takes on the odd electron becoming a radical itself. However, it is much less reactive than the radical it scavenged and the propagation chain is terminated. Thiosulfate radicals have been detected spectroscopically (Dogliotti and Hayon, 1968).

Fig. 5.7 shows the effects of thiosulfate addition to a system catalyzed by 30 mM Mn. The rate dropped immediately to a lower value and then rose linearly with time back to its original level. The 0.150 mM addition dropped the kinetics into the physical absorption region so the absorption rate remained at E=1 for a time before the kinetics recovered enough to move back into the enhancement region. The recovery rate was found to be generally independent of thiosulfate or Mn concentration and averaged out at 0.0176 enhance-

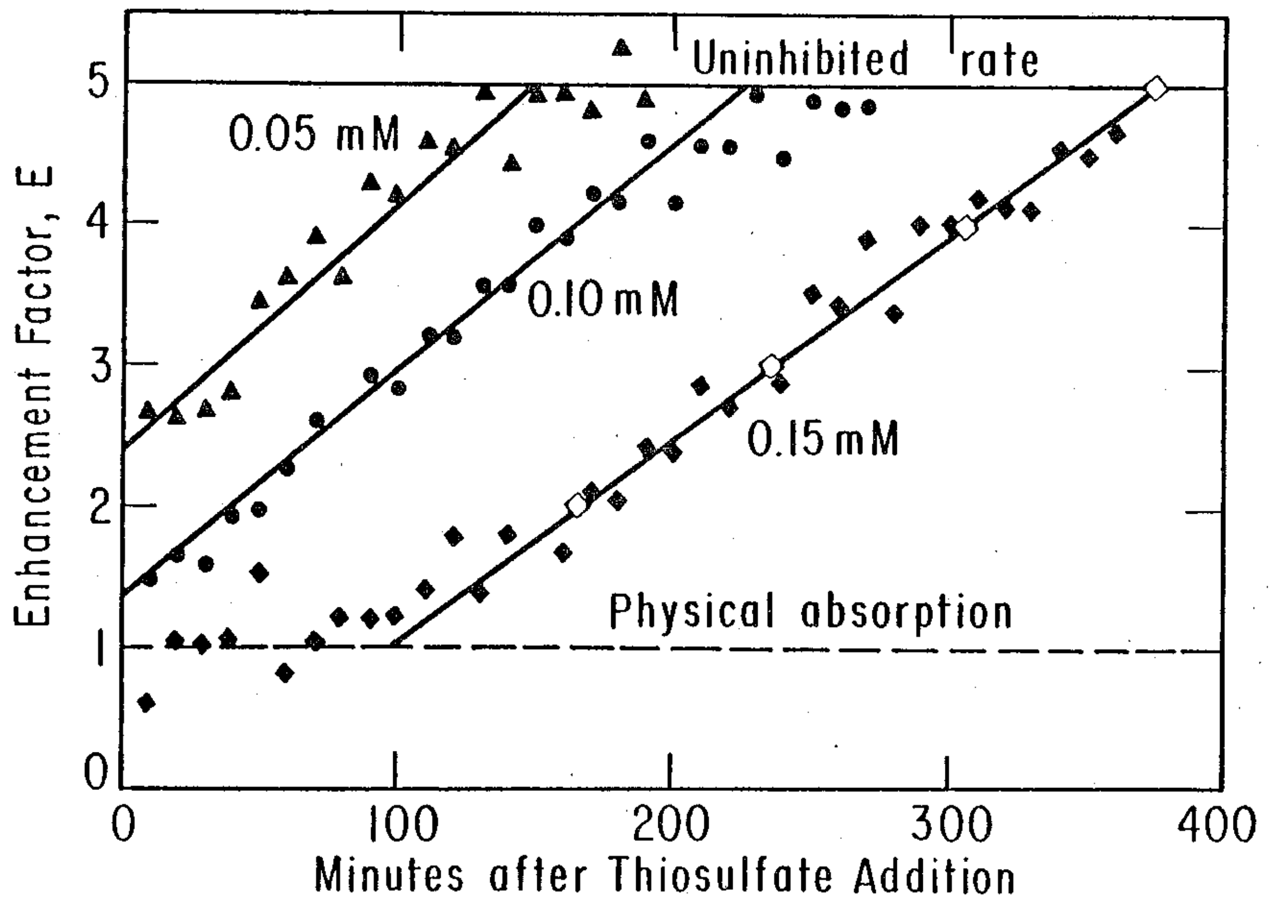

Figure 5.7: The absorption rate recovering from inhibition by thiosulfate at 30 mM Mn catalyst, 10 mM S(4) and pH 5

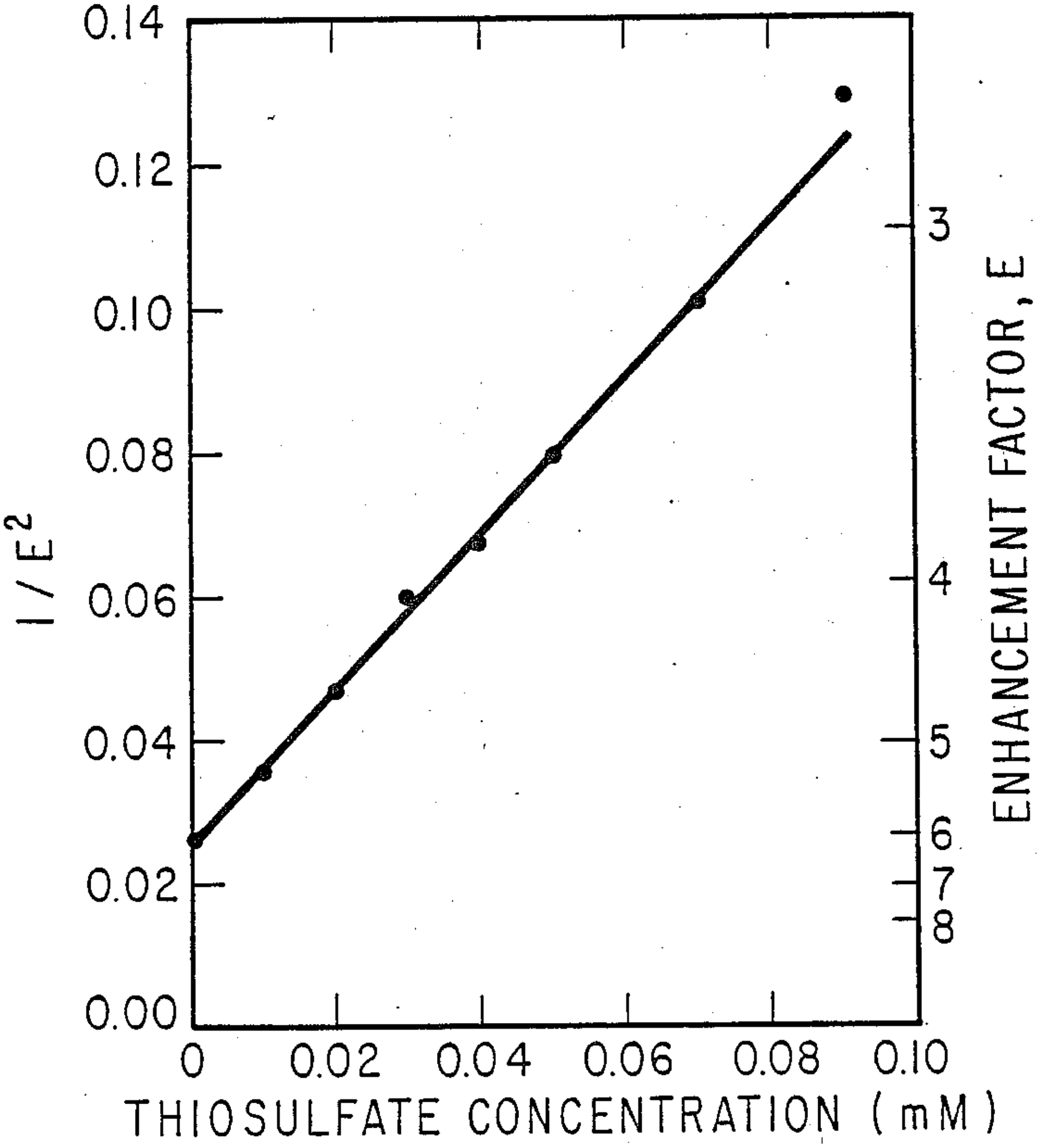

Figure 5.8: Decrease of enhancement due to the addition of thiosulfate at 30 mM Mn, 10 mM S(4) and pH 5

ment units per minute with a standard deviation of 0.0031 over 10 measurements.

Fig. 5.8 shows the effect of thiosulfate concentration on the absorption rate with 30 mM Mn catalyst. The line is made straight if the ordinate is expressed as $1/E^2$ leading to the empirical correlation:

$$E = \frac{6.17}{(1 + 46.8[S_2O_3^{-2}, \text{mM}])^{1/2}} \tag{5.17}$$

Since the absorption rate is proportional to the square-root of what the homogeneous kinetics would be at interface solution conditions it may be concluded that the reaction kinetics vary inversely with the thiosulfate concentration. This type of behavior is often observed with inhibition by alcohols (Backstrom, 1927; Walling, 1957).

Eq. 5.17 may be derived from the film theory equations given at the beginning of this section by assuming first order termination and by adding an inhibition step:

$$R^{\bullet} + I \longrightarrow \text{inert} \qquad \text{(Rxn. 5.4)}$$

$$r_{inh} = k_{inh}[R^{\bullet}][I] \qquad (5.18)$$

A free radical balance gives:

$$r_{init} = r_{term} + r_{inh} \qquad (5.19)$$

$$E = \frac{\left(\frac{D_{ox}[O_2]_i}{2}\right)^{1/2} \left(\frac{k_{prop}k_{init}}{k_{t1}}\right)^{1/2} [Me^U]^{1/2}}{(1 + (k_{inh}/k_{t1})[I])^{1/2}} \times 10^9 \qquad (5.20)$$

The numerator is the uninhibited rate (Eq. 5.12) and the factor 46.8 mM^{-1} is k_{inh}/k_{t1}. First order termination would be expected during inhibited oxidation due to the lowered radical concentration.

An experiment was conducted to determine if the thiosulfate was being consumed in the bulk solution or in the reaction zone. A system catalyzed by 30 mM Mn was allowed to reach steady state at E=5.2 and then 0.050 mM thiosulfate was added. The rate immediately dropped to 1.5 and proceeded to rise normally at 0.0188 E units/minute. After rising for 90 minutes to E=3.15 the reactor was blanketed with nitrogen causing the reaction to stop. After 60 minutes of delay, air was once again passed into the reactor and the reaction resumed. The absorption rate picked up where it had left off prior to the interruption and rose back up to steady state with a slope of 0.0182. The conclusion is that the thiosulfate causes inhibition, as expected, in the reaction zone where the free radicals are concentrated and is itself not degraded, in this time frame, in the absence of reaction. This does not contradict the earlier claim that radicals can exist in the bulk solution since there was no incoming oxygen during the interuption to produce them.

Information on the kinetics of thiosulfate degradation can be deduced from the findings that E is approximately proportional to $1/[S_2O_3^{-2}]^{1/2}$ and that, during recovery, dE/dt is equal to a constant. Eliminating E from these two expressions shows that the rate of thiosulfate degradation in moles per liter per second is proportional to the thiosulfate concentration to the three-halves power. This fractional reaction order suggests that thiosulfate is degraded in a multi-step chain reaction of its own into an inert species.

Some indication of the chain length may be derived from the inhibition efficiency for a given system. The inhibition efficiency is defined as the moles of S(4) that was prevented from being oxidized by the addition of an inhibitor divided by the moles of inhibitor added. The number of moles of S(4) that was prevented from being oxidized is proportional to the area of the triangular-shaped indentation of the rate produced by the addition of thiosulfate (Fig. 5.7). Fig. 5.9 shows that the inhibition efficiency is not a function of the amount of thiosulfate added and for the case of 30 mM Mn the efficiency was about 39 moles S(4) not oxidized per mole of thiosulfate added. This number can be identified with the chain length since an inhibitor that terminates a longer chain would necessarily have a higher efficiency.

Fig. 5.10 shows that the inhibition efficiency, and hence the chain length, drops with increasing manganese catalyst concentration. An increase in catalyst concentration can shorten the chain length in two ways: the increase in initiation reactions causes a higher concentration of free radicals and thus accelerates the termination reactions which are usually second order in radical concentration, or the increase of branching reactions can have the same net effect upon the radical concentration (Huyser et al., 1973; Twigg, 1962; Walling, 1957).

Experiments with iron catalysts show that these systems are much less susceptable to thiosulfate inhibition than are manganese-catalyzed systems but still recovered linearly as in Fig. 5.7.

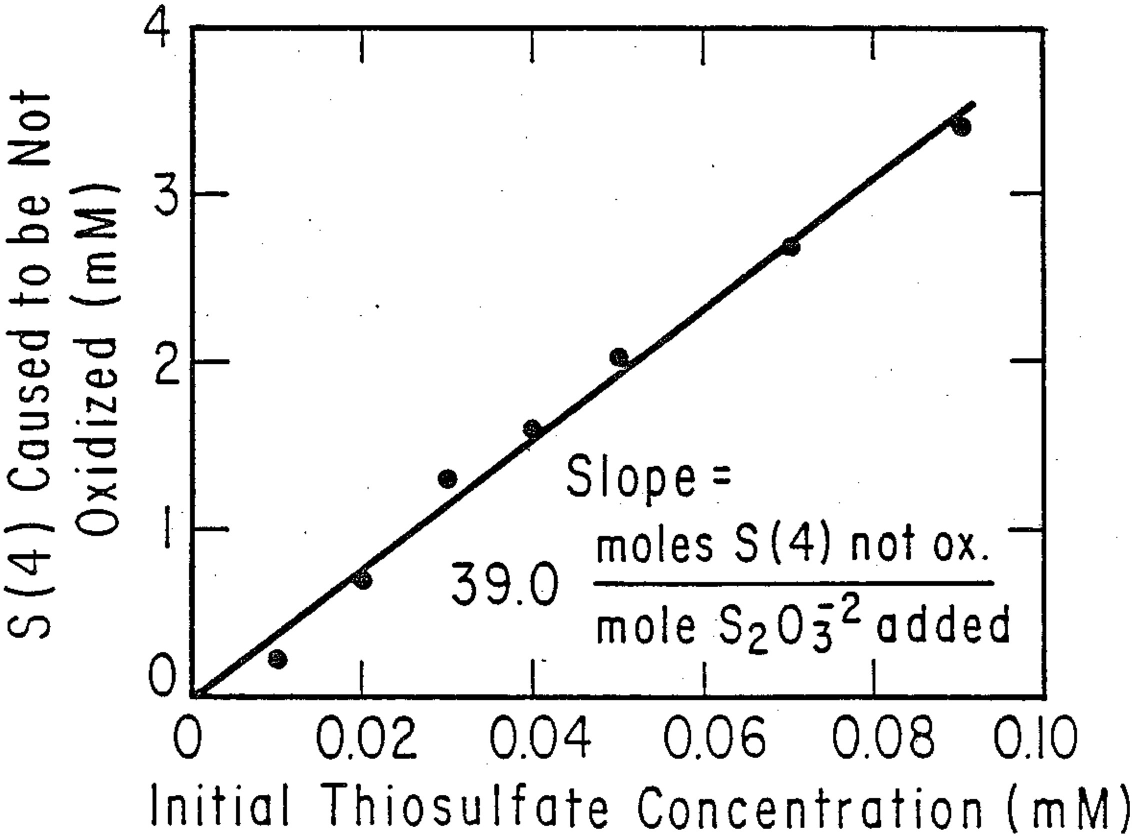

Figure 5.9: Determination of the inhibition efficiency of thiosulfate at 30 mM Mn, 10 mM S(4) and pH 5

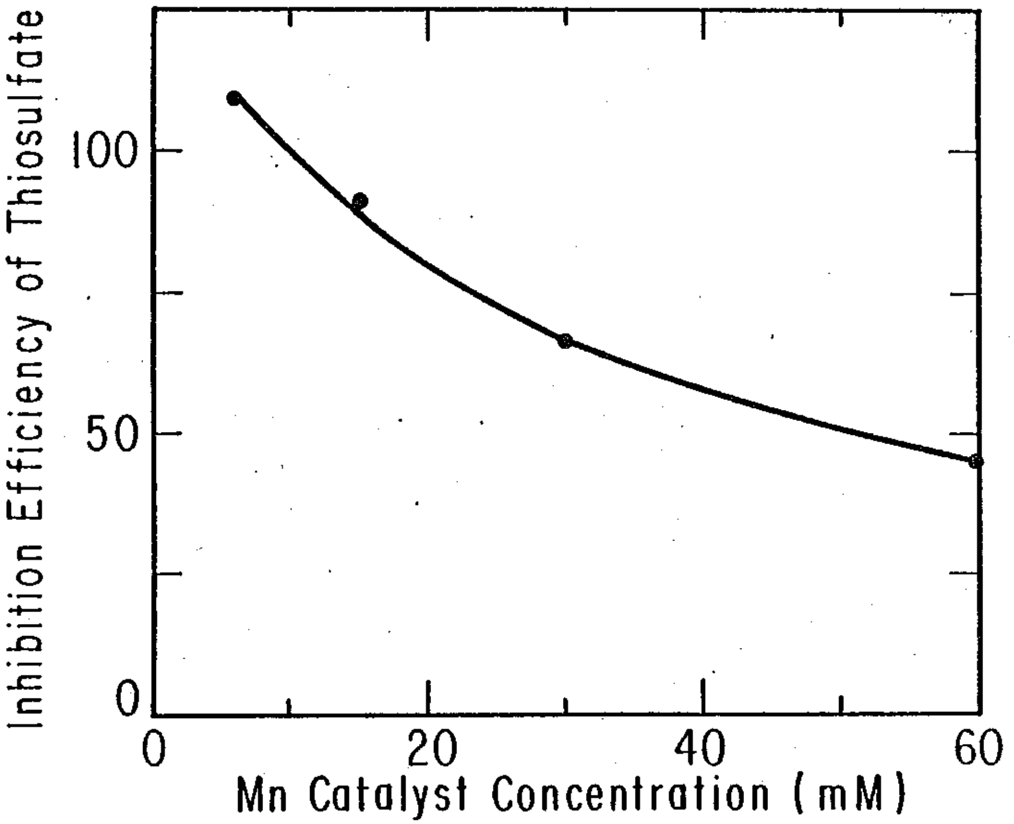

Figure 5.10: Decrease in thiosulfate inhibition efficiency as Mn concentration increases at 10 mM S(4) and pH 5

The iron-catalyzed system required between one and two orders of magnitude more thiosulfate to achieve the same percentage of absorption rate decrease. 0.1 mM thiosulfate added to a system catalyzed by 30 mM Mn caused a drop in E from 5.5 to 1.6 (70% reduction) while the same amount of thiosulfate added to a 30 mM Fe system caused a decrease of only 17% from 2.3 to 1.9. The addition of 0.01 mM thiosulfate into a 6 mM Mn system retarded the enhancement factor by about 37% from 3.64 to 2.32 while a 65% reduction for a 3 mM Fe system (2.40 to 1.55) required 0.30 mM. Lim et al. (1982) found similar behavior under quite different experimental conditions. Also, the recovery rate was about twice as slow for Fe at about 0.0074 E units/minute and the inhibition efficiency was much lower at about 3. The shorter chain length and faster thiosulfate degradation with Fe indicates that there are more free radicals generated during Fe catalysis.

5.4 Inhibition by Complexing Agents: EDTA

EDTA belongs to a class of inhibitors that are not consumed by the reaction and impart more or less permanent retardation. Some anionic ligands can inhibit by shifting the redox potential of the ferric/ferrous couple to values too low for the initiation reaction (Huss et al. 1982; Bailar and Emeleus, 1973). The ammonium ion is a ligand that has a low capacity for facilitating electron transfer between substrates (Mishra and Srivastava, 1976; Taube, 1970) and probably blocks some free radical reactions. EDTA is a particularly strong chelating agent that produces stable complexes with virtually every metal ion except alkali metals. Its inhibition action is due to steric hinderances produced by wrapping around the metal ion and enclosing it within all six of its ligand sites. The stability constants for EDTA and Fe are large relative to that for other metal ions: $2.1X10^{14}$ for ferrous and 10^{25} for ferric (Schwarzenbach, 1957). Thus, virtually all the EDTA in solution will be tied up to any available iron.

Fig. 5.11 shows that the progressive addition of EDTA to a system catalyzed by 0.01 mM Fe causes a slight drop in absorption rate up to the point where the EDTA and Fe concentrations are about equal. At this crossing point the rate drops suddenly into the physical absorption range where it remains at least until the EDTA concentration is ten times that of Fe. Thus it seems that even trace amounts of Fe can have considerable catalytic activity since the rate does not fall off strongly until the concentrations are within $2X10^{-6}$ M of each other at pH 6. The solution remained transparant throughout the experiment although there must be some very dilute solids present since 0.01 mM Fe is to the right of the pH 6 breakpoint in Fig. 5.3. The same experiment was conducted at 1 mM Fe with the same results except that the rate fell to about zero when [EDTA]/[Fe] was

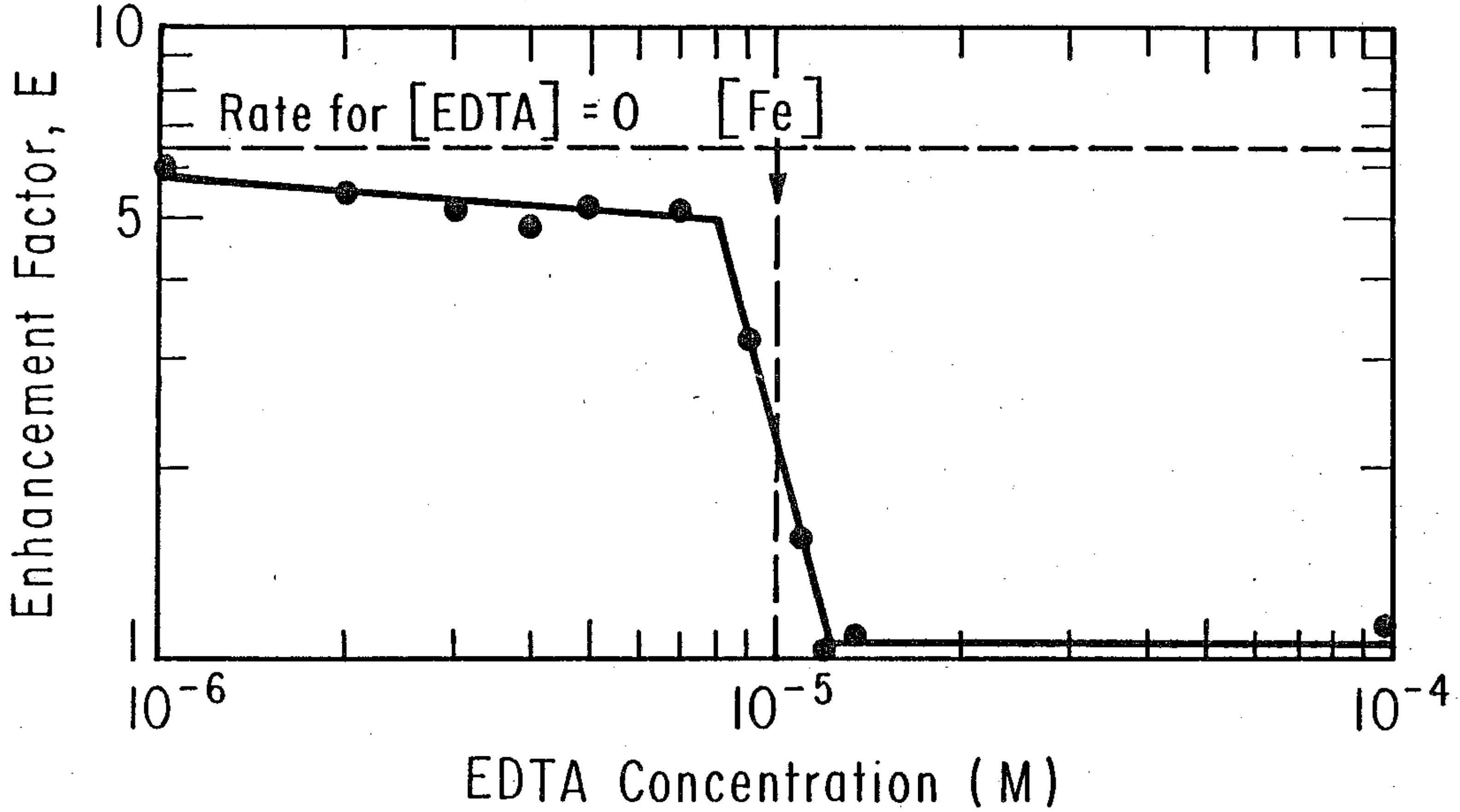

Figure 5.11: Effect of EDTA additions on the enhancement factor at 0.01 mM Fe, 30 mM S(4) and pH 6

equal to 10. Under these higher concentrations the solution was barely opaque with finley-divided red-brown solids.

The time-dependent absorption rate following the addition of EDTA provides some information on the role and rapidity of the dissolution of these Fe-containing solids. 0.1 and 0.2 mM aliquots of EDTA were added to the solution in the presence of 1 mM Fe to produce the diagram similar to Fig. 5.11. When the total amount of EDTA was less than the total Fe concentration the addition of the EDTA caused the rate to drop immediately to zero and remain there for about 15 minutes before climbing back up to steady state in about 5 minutes. At the same time the red-brown color of the solution, thought to be caused by an iron (mostly ferric) precipitate, cleared slightly during this time. Once the EDTA concentration passed the Fe concentration the rate did not recover from the immediate inhibition. This effect was not observed for the 0.01 mM Fe case; the absorption rate rapidly reached steady state following the addition of EDTA either near the uninhibited rate (for less than 0.01 mM EDTA) or at the physical absorption region (for more than 0.01 mM EDTA). The 0.01 mM Fe solution was clear at all times. In the presence of a visible solid precipitate during the 1 mM Fe experiments the added 0.1 mM EDTA apparently exceeded the concentration of dissolved catalytically active ferric species and complexed them to send the rate to zero. As iron species dissolved from the floc they were immediately complexed by the remaining EDTA until all the free EDTA was consumed and the dissolving iron remained free and therefore catalytically active. The ferric must have been replaced by dissolving ferric solids and not by the liquid phase oxidation of ferrous since the amount of precipitate was observed to decrease. This type of behavior was not observed in the case of 0.01 mM Fe probably because the added EDTA was much smaller in comparison to the ferric concentration than in the 1 mM Fe experiments. EDTA aliquots for the latter was 100 times larger but, since the ferric concentration is solubility limited, it is the same for both cases. And, although the total iron concentration for the second case is 100 times larger, it may have a greater fraction of its total iron tied up as solids due to the intersection of the solubility limits of more species.

When the EDTA concentration was ten times the Fe level the rate dropped into the physical absorption range for the 0.01 mM Fe run but went to zero for the 1 mM run. The observed rate was probably caused by other transition metal ions in the solution that are not complexed as strongly as ferric. These ions might escape complexation at the low EDTA levels but not at the higher concentrations.

The addition of 0.002 mM increments of EDTA to the system catalyzed by 0.01 mM Fe seemed to have little effect upon the rate up to the time that the total EDTA and Fe concentrations were comparable. This indicates that the fraction of catalytically active iron out of the total amount added is actually very small. The rate curve in Fig. 5.10 begins to drop off suddenly when the EDTA concentration is within about 0.002 mM of the total Fe concentration indicating that the actual concentration of catalytically active species is at least this small. The remainder of the iron is tied up as ferrous or inactive solids. This magnitude of ferric solubility is more in line with the literature values stated earlier and the upper limit of the pH 6 breakpoint (Fig. 5.3) of 0.002 mM Fe.

5.5 The Catalyst Cycle for Iron

Fig. 5.12 shows the possible reaction steps for Fe catalyst in the sulfite oxidation reaction. The liquid and solid phase ferrous oxidation steps must take place in the reaction zone since this is the only place that dissolved oxygen is available. The branching step can serve to increase the reaction rate if it occurs in the reaction zone or will be involved in solution equilibria in the bulk region. Likewise, the reverse of the initiation reaction can be viewed as a "chain restart" reaction if it occurs in the reaction zone if the new ferric ion goes on to create a radical before leaving the zone or else this step plays a role in bulk phase equilibria.

This approach to modelling can be carried one step further if it is assumed that the ferric ion is just another radical and that Rxn. 5.1 is just another propagation reaction. Then the actual initiation reaction would be the oxidation of ferrous to ferric. In fact, the ferric ion is a free radical since it has an unpaired electron although its radical character is weak.

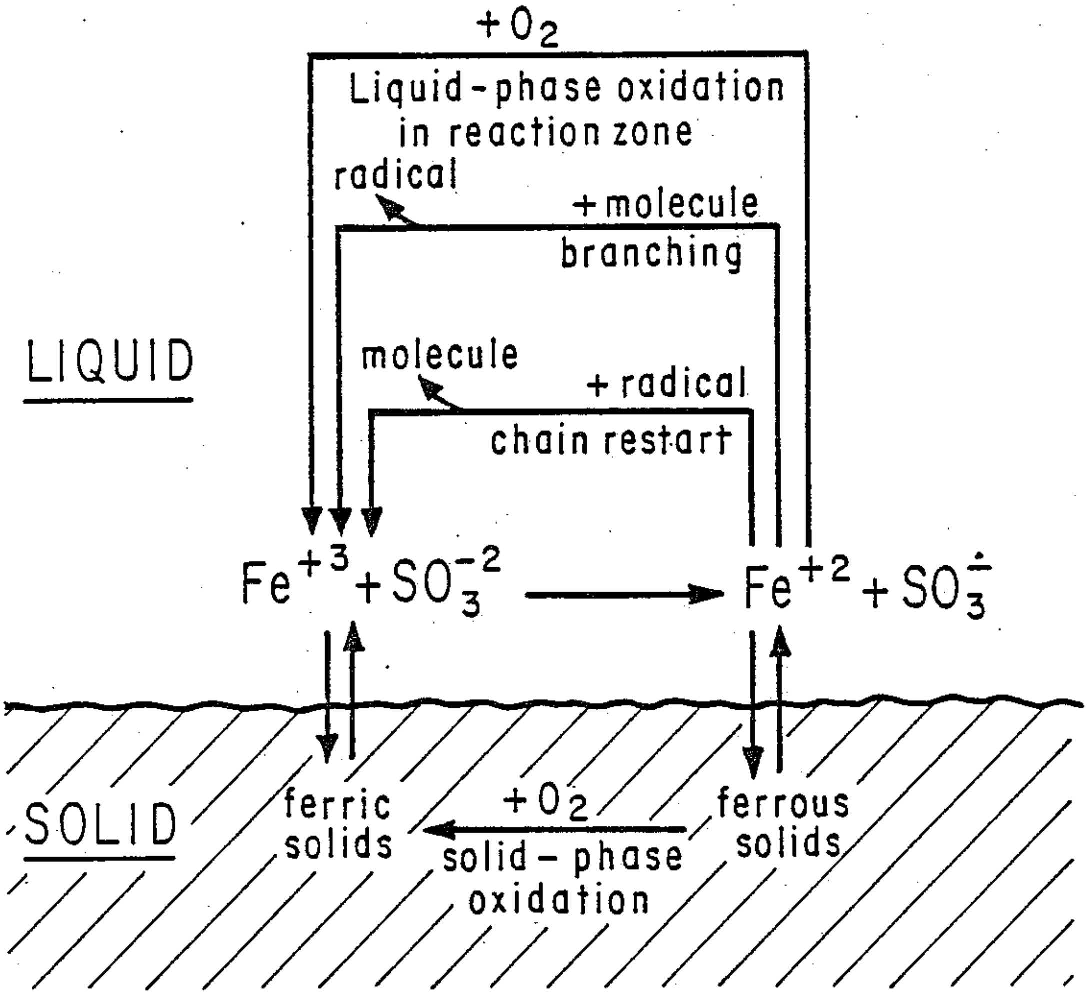
+O2
Liquid-phase oxidation in reaction zone
radical
+molecule
branching
LIQUID
molecule
+radical
chain restart
Fe+3 + SO3-2
Fe+2 + SO3-
SOLID
ferric solids
+O2
solid-phase oxidation
ferrous solids

Figure 5.12: The catalytic cycle for Fe

Section 6

DETERMINATION OF MASS TRANSFER CHARACTERISTICS

6.1 Introduction

The measurement of mass transfer characteristics in gas-liquid contactors is of such great practical importance that numerous studies on the determination of k_x, the liquid phase mass transfer coefficient of species X, and A, the interfacial contact area, are available in the literature. However, it is usually not possible to predict these parameters accurately from published correlations due to the large number of system effects that makes the generalization of contacting schemes difficult (Metha and Sharma, 1971). Therefore, most published studies present practical methods for directly measuring these quantities in full-scale equipment rather that attempting to present equations for their calculation. In general it is relatively easy to measure k_xA but more difficult to separate the two parameters (Reith and Beek, 1973). The product k_xA is nearly always measured via a chemical method whereby some gas is absorbed into a solution under physical absorption conditions to give a total physical absorption rate, AR_o, in moles/s. Then if $[X]_i$ is known from Henry's law and $[X]_b=0$:

$$(k_xA) = \frac{(AR_o)}{[X]_i} \tag{6.1}$$

The separation into k_x and A may be accomplished by measuring A with a chemical method where the reaction kinetics are so fast that the absorption flux R is independent of k_{ox} as in Eq. 3.17 or, in some circumstances, by estimating A with an optical method such as photography or light scattering (Uhl and Grey, 1967; Nagata, 1975). Some chemical systems that have gained acceptance for mass transfer characterization include the absorption of carbon dioxide or nitrogen oxides into alkaline solutions (Sherwood et al., 1978) and the absorption of oxygen into sulfite/catalyst solutions (Linek and Vacek, 1981; DeWaal and Okeson, 1966; Westerterp and Van Dierendonck, 1963).

Sulfite oxidation is attractive as a chemical method since the solutions are non-toxic, non-corrosive, inexpensive and since air can often be used as the gas phase. Furthermore, the low solubility of oxygen in aqueous solutions can prevent the problem of gas phase depletion and gas film resistance that sometimes occurs in carbon dioxide systems (Wesselingh and Van't Hoog, 1970). However, sulfite oxidation has a disadvantage in that the kinetics are not well understood and literature values of kinetic constants are nearly always hard to reproduce and cannot be extrapolated with confidence. Furthermore, kinetic information from homogeneous reactors usually does not apply to the heterogeneous conditions that are present in contacting equipment, probably due to initiation times associated with the free radical chain reactions (Bengtsson and Bjerle, 1975; Chen and Barron, 1972; Johnstone and Coughanower, 1958). There is also some evidence that the kinetics can be affected by changes in the agitation rate (Schultz and Gaden, 1956; Phillips and Johnson, 1959).

Most of the previous work on methods of estimating mass transfer characteristics via sulfite oxidation has been performed at total sulfite concentrations between one and two orders of magnitude higher than those in this study. These lower S(4) concentrations were necessitated by the desire to approximate conditions in flue gas desulfurization units. Correspondingly higher catalyst concentrations are used here to achieve comparable absorption rates.

6.2 Theory

The liquid phase mass transfer coefficient in stirred tanks and bubble columns is a weak function of the agitation intensity; the rise in k_xA with agitation speed is almost entirely due to increases in the contact area (Westerterp and Van Dierendonck, 1963; Sideman et al., 1966). In sparged contactors the interfacial area is usually expressed as area per reactor volume but since the stirred tank in this study was unsparged the contact area is expressed in cm^2. At high agitation rates, however, this system approximated a sparged tank closely due to the entrainment of air bubbles.

The mass transfer characteristics of our reactor were determined by first rearranging Eq. 3.15 as follows:

$$(AR) = A[O_2]_i(k_{ox}^2 + \frac{2}{m+1}D_{ox}k_r[S(4)]_i^n[cat]_i^p[O_2]^{m-1})^{1/2} \qquad (6.2)$$

In the experiments of Secs. 3, 4, 5 and 7 the quantity R could be measured directly since the agitation rate was low enough so that the interface was smooth and unbroken and A could be assumed to be the cross-sectional area of the reactor (154 cm^2). However, in this section the agitation will be varied into regions of surface rippling and bubble entrainment so that this area assumption cannot be made and the total absorption rate, AR in moles/s, is the only quantity that can be measured. Now the assumption is made that none of the parameters in the right-hand side of the parentheses in Eq. 6.2 are a function of the agitation rate. This will certainly be true for D_{ox}, the catalyst concentration and the oxygen concentration and also for the total sulfite concentration provided that $R<<R_{lim}$. So, for constant temperature and bulk solution concentrations, the right- hand term can be considered to be a constant, c_r^2, and Eq. 6.2 becomes:

$$(AR) = A[O_2]_i(k_{ox}^2 + c_r^2)^{1/2} \tag{6.3}$$

where: c_r = the lumped kinetic constant, cm/s

The first step in determining k_{ox} and A is to measure their product. This is done by using a solution that contains a low enough level of catalyst so that the system is under physical absorption yet enough to maintain the bulk solution concentration of oxygen at zero (region B in Fig. 3.1). Under these conditions $k_{ox}^2>>c_r^2$ and $k_{ox}A$ is found from an equation analogous to 6.1:

$$(k_{ox}A) = \frac{AR_o}{[O_2]_i} \tag{6.4}$$

The lumped kinetic constant c_r is determined from AR at an agitation rate low enough so that A may be assumed to be equal to the reactor's cross-sectional area. This allows k_{ox} to be calculated at the low agitation rate and then Eq. 6.3 can be used to obtain c_r which is assumed to be independent of agitation. The product $k_{ox}A$ may be separated by measuring the total absorption rate with enough catalyst present so that there is significant enhancement. Eqs. 6.3 and 6.4 are rearranged to:

$$k_{ox} = \frac{c_r}{(E^2 - 1)^{1/2}} \tag{6.5}$$

where: $E = AR/AR_o$ at any agitation rate

The above method facilitates the estimation of k_{ox} and A as a function of the agitation intensity from the total absorption rate vs. agitation rate at low and high catalyst concentrations and without the necessity of detailed prior knowlege of the kinetics.

6.3 Results and Discussion

The total absorption rate as a function of agitator speed was measured for 0.1 (curve A, Fig. 6.1), 10 (curve B) and 100 mM Mn (curve C) at 10 mM S(4), for the synergistic couple 100 mM Mn plus 1 mM Fe at 50 mM S(4) (curve D) and for 0.01 (curve B, Fig. 6.2) and 1 mM Fe (curve C) at 30 mM S(4). The 0.1 mM Mn curve from Fig. 6.1 appears again as curve A in Fig. 6.2. 0.1 mM Mn was earlier found to be in the physical absorption regime at 400 rpm (Fig. 5.2) so this lower curve was used to determine $k_{ox}A$ via Eq. 6.4 with the interfacial oxygen concentration equal to the saturation value for 0.184 atm

O_2 at 50^0C in a 0.3 M sulfate solution: $1.19X10^{-7}$ moles/cm^3 (Linek and Vacek, 1981). The resulting curve of $k_{ox}A$ vs. agitation speed may be read off of the right-hand ordinate of Fig. 6.1 and is valid only in regions where the bulk phase concentration of oxygen is zero. k_{ox} may be calculated at low agitation rates where the area may be assumed to be 154 cm^2. At 400 rpm $k_{ox}A$ was 1.26 cm^3/s so k_{ox} is $8.2X10^{-3}$ cm/s. Now, this value may be used in Eq. 6.3 to calculate c_r at 400 rpm for the physical absorption case and the five catalyst systems that showed enhancement (Table 6.1). Finally, the product $k_{ox}A$ may be separated by using these values of c_r in Eq. 6.5 (Fig. 6.3). The same values of k_{ox} and A as a function of agitation intensity were obtained with each of the five catalyst systems from 300 to 800 rpm.

Although k_{ox} and A were not measured by a different method some clear inferences about the validity of the values from the sulfite oxidation method can be made. Although the measurement of $k_{ox}A$ is probably accurate except possibly at the highest agitation intensities, the product almost certainly was not correctly separated by this method; the values for A do not seem to rise fast enough with increased agitator speed and k_{ox} seems to rise too fast. The unsparged stirred tank used in this study began to entrain air bubbles at about 600 rpm, probably causing the rise in $k_{ox}A$ above this point, and appeared to be thoroughly sparged with bubbles by 800 rpm. The

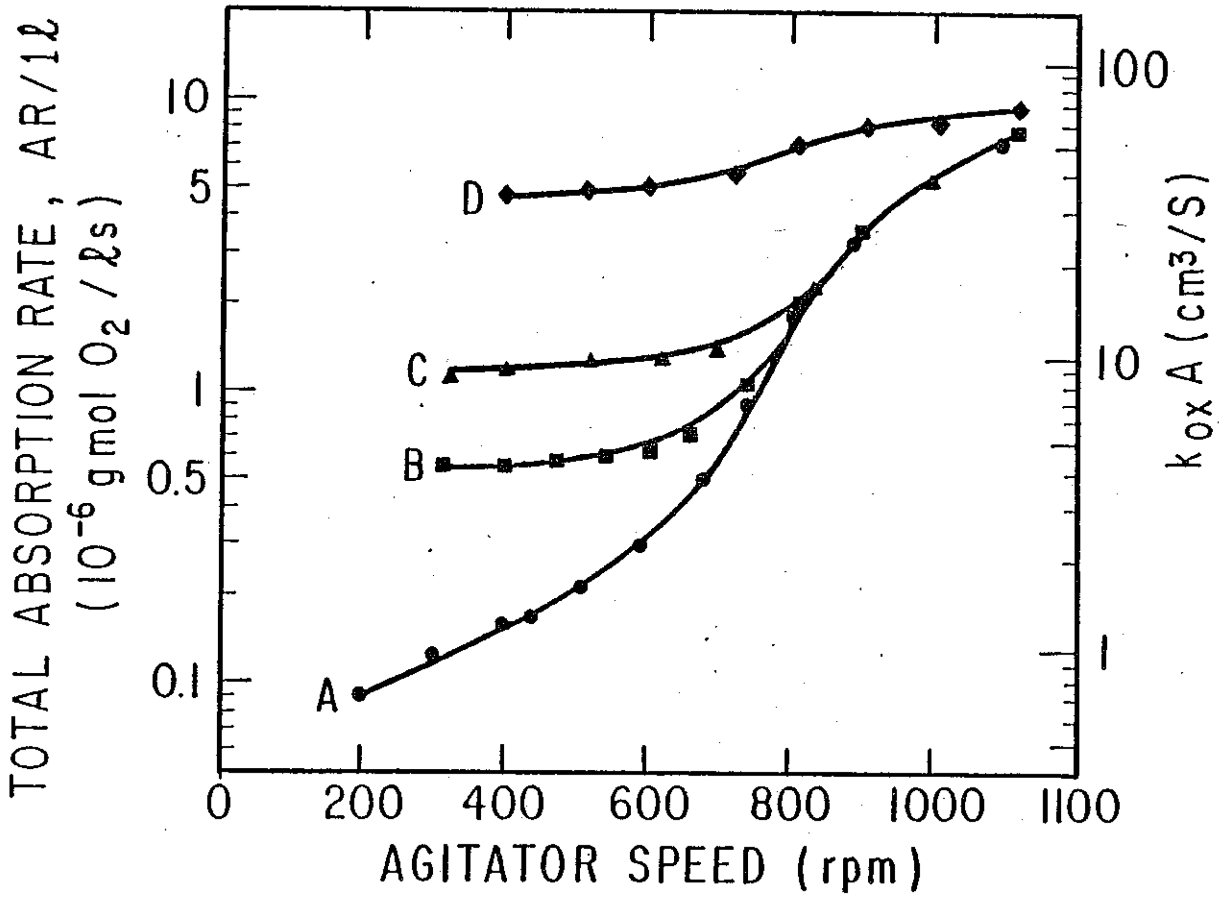

Figure 6.1: Effect of agitator speed on the total oxygen absorption rate, Mn and Mn-Fe synergistic catalysts at pH 5

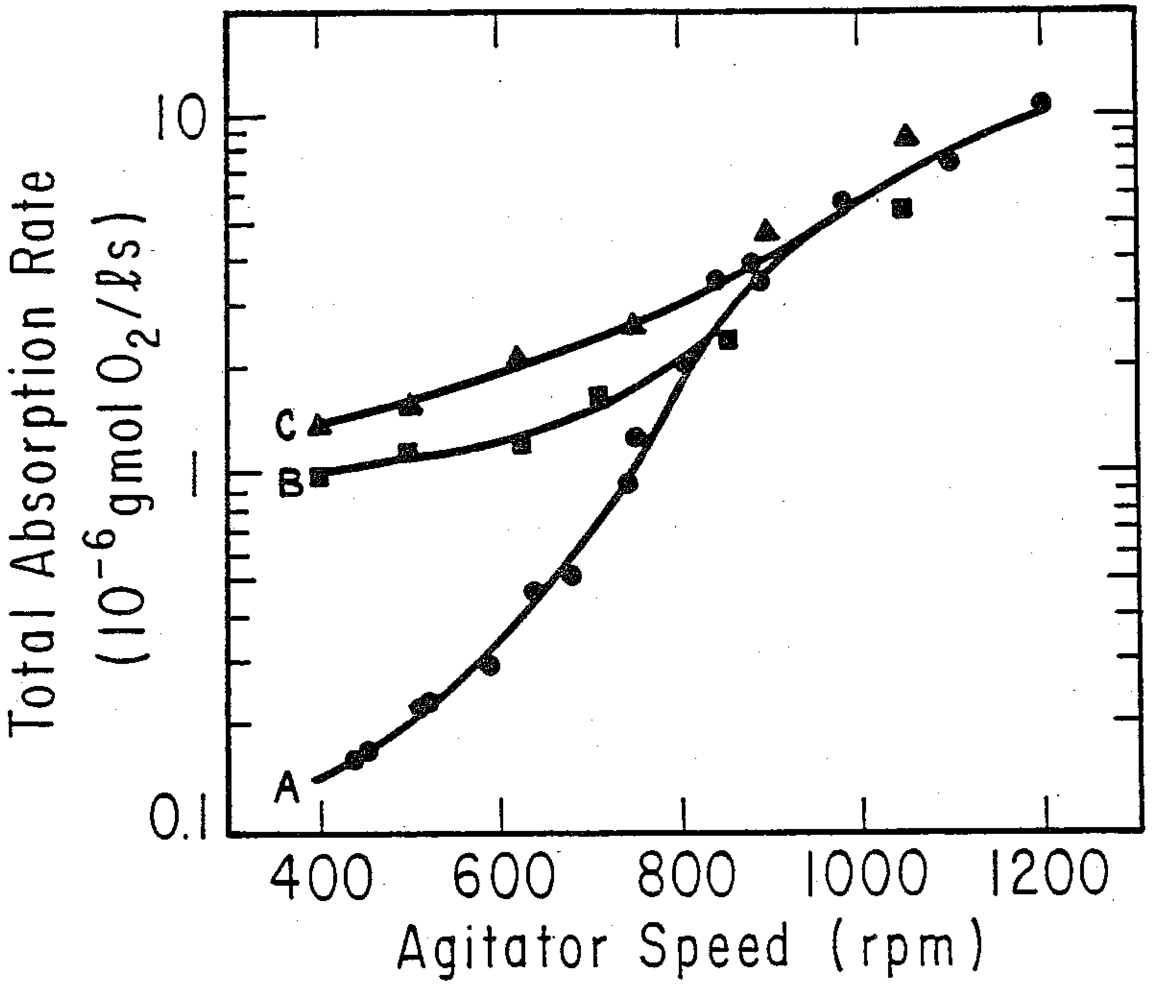

Figure 6.2: Effect of agitator speed on the total oxygen absorption rate, Fe catalysts at 30 mM S(4) and pH 6

Table 6.1

Catalytic activities used to determine mass transfer characteristics of a one liter stirred tank vessel

solution composition	$AR \times 10^6$ 400 rpm (gmols O_2/s)	E 400 rpm	c_r (cm/s)	c_r^2/k_{ox}^2 400 rpm
0.1 mM Mn 10 mM S(4)	0.16	1.0	$<<k_{ox}$	<<1
10 mM Mn 10 mM S(4)	0.55	3.7	2.9×10^{-2}	13
100 mM Mn 10 mM S(4)	1.2	8.0	6.5×10^{-2}	63
100 mM Mn 1 mM Fe 50 mM S(4)	4.7	31	25×10^{-2}	930
0.01 mM Fe 30 mM S(4)	1.0	6.6	5.3×10^{-2}	43
1 mM Fe 30 mM S(4)	1.4	9.3	7.6×10^{-2}	85

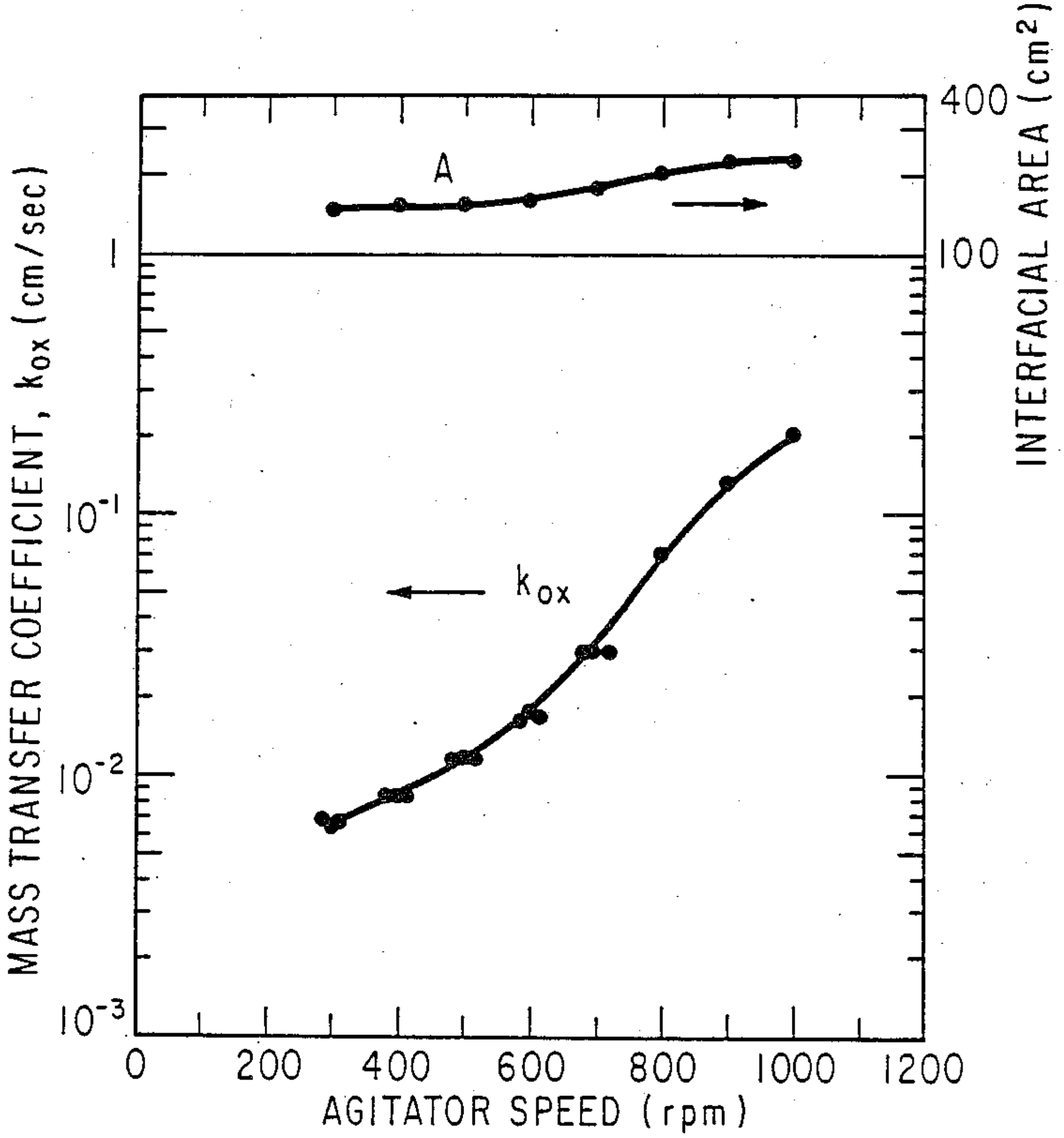

Figure 6.3: Calculated values of the oxygen mass transfer coefficient and interfacial contact area

measured contact area rose by only 65% over this transition region where the hydrodynamics in the reactor were observed to change from a gently rippled surface to a violent froth. If the average diameter of an entrained bubble is 0.3 cm then 180 bubbles would be required to produce the change in contact area of 50 cm^2 indicated in Fig. 6.3 between 400 and 800 rpm. But the volume of these 180 bubbles would be 2.54 cm^3 indicating a gas holdup of only 0.25%, an impossibly low value for the level of agitation observed at 800 rpm. Metha and Sharma (1971) give typical values of A/V for sparged agitated vessels as 4 to 7 cm^{-1}. Our reactor was unsparged but at high agitation rates should approach these numbers. If 4 cm^{-1} is assumed then $A=4000\ cm^2$ and $k_{ox}=11.3X10^{-3}$ cm/s, a much more reasonable value since k_{ox} is much less sensitive to changes in the agitation rate than is A. For sparged stirred vessels in general A has been observed to rise linearly above a critical agitation rate while k_x tends to rise with a much weaker power, on the order of 0.1 to 0.3 (Metha and Sharma, 1971; Westerterp and Van Dierendonck, 1963).

Depletion of S(4) reactant at the interface has been suggested as a cause of this type of error (Sec. 4) but sufficient amounts of sulfite were used to prevent the absorption rate from becoming larger than 0.2 of the limiting rate. Besides, the reaction under these conditions seems to be about zero order in S(4) for Mn catalyst (Fig. 5.6). If the assumption that $[O_2]_b=0$ during the measurement of $k_{ox}A$ is incorrect the error produced would cause the calculated values of k_{ox} to be too small, not too large. Also, calculations show that typical bubbles do not have sufficient residence time in the solution to be depleted of their oxygen; a 0.2 cm bubble with a k_{ox} of 0.020 cm/s would require 60 s for 50% depletion at its initial (maximum) rate of oxygen flux.

This type of error in k_{ox} and A can occur if the kinetics of the reaction become slower at higher agitation rates, resulting in a drop in c_r. At any given agitator speed the measured enhancement factor sets the ratio of c_r/k_{ox}:

$$\frac{c_r}{k_{ox}} = (E^2 - 1)^{1/2} \tag{6.6}$$

An enhancement factor that is decreasing towards unity is indicated on Figs. 6.1 and 6.2 when the highly catalyzed curves move towards the weakly catalyzed physical absorption line, the bottom one. As E approaches one the ratio of c_r/k_{ox} falls towards zero. In this method of determining mass transfer characteristics, c_r was assumed to be constant at all agitator speeds so that the decrease of the ratio was considered to be due to large increases in k_{ox}. The apparent area, found by division from $k_{ox}A$, is then found to rise very little. Therefore, it seems that the assumption of constant kinetics with changing agitation rates may not valid; the reaction slows down at higher rates. Schultz and Gaden (1956) measured the apparent mass transfer coefficient of oxygen in aerated vessels filled with sulfite/catalyst solutions under similar conditions and found that it dropped as the agitation rate increased. Since this apparent coefficient is given by $(k_{ox}^2+c_r^2)^{1/2}$ from Eq. 6.3 the actual coefficient, k_{ox}, may have been rising slowly as expected but c_r may have been falling more rapidly.

If the reason for this behavior is due to lowered reaction rates, then this retardation is probably caused by the fluid elements being at the interface for a time that is shorter than the induction time for the free radical reaction. The same reason is often given for differences in reaction kinetics between homogeneous and heterogeneous reactors containing the same solutions (Bengtsson and Bjerle, 1975; Chen and Barron, 1972). This approach is a surface renewal viewpoint and seems the most physically reasonable explanation of the phemomena although it does not easily explain the fact that the same values of k_{ox} and A are obtained with five different catalyst systems and three S(4) concentrations. It is possible that all five catalyzed systems were responding to the decreased oxygen exposure times by shifting from one common mechanism to another. Phillips and Johnson (1959) observed that the reaction order with respect to oxygen dropped from 1.5 to 1.0 at high agitation rates indicating a change in reaction mechanism and changes in oxygen reaction order with P_{ox} have been reported in the literature (Linek and Vacek, 1981).

The apparatus used here is not ideal for this type of study because the nature of the surface hydrodynamics changes as the agitation increases. Different areas may have different values of k_{ox} so the measured value is an integrated average over the entire surface. A more consistent contactor such as a wetted-wall column or a liquid jet may be preferable.

The conclusion from this section is that the mass transfer characteristics of our reactor were not accurately measured by oxygen absorption into sulfite/catalyst solutions under FGD conditions. The reason may be due to decreased reaction rates at high agitation intensities. If so, then this effect is probably caused by induction time undercutting but further quantitative treatment of the problem necessitates some knowledge of the detailed reaction steps to support the assumption that this phenomena is due to the buildup of a steady-state concentration of some reaction intermediate. The best way to accomplish this would be by time-resolved spectroscopy to measure the concentrations of various radicals as the reaction rate accelerates.

Section 7

CATALYTIC SYNERGISM

7.1 Introduction

The phenomena of catalytic synergism in sulfite oxidation is particularly interesting due to the profound and unmistakable effects that multiple catalysts can have on the total oxidation rate. Two or more metal ion catalysts can exhibit a catalytic activity that is much greater or lesser than what would be expected from the sum of their individual activities. This action was first noticed by Johnstone (1931) but has received only a small amount of attention since then compared to the amount of work that has been done on catalysis by single species (Altwicker and Nass, 1983; Martin et al., 1981; Barrie and Georgii, 1976; Martin, 1983). There is no generally accepted mechanism and very few proposed reaction steps have been put forth in the literature, primarily as a result of the limited amount of research that has been done on the subject. Catalytic synergism has not received the attention it deserves and remains a promising and wide-open area for research.

7.2 The Synergism Coefficient

In order to quantify the degree of interaction between two dissolved catalysts the synergism coefficient is defined as the ratio of the observed absorption rate with two catalysts present simultaneously (A and B) to the absorption rate that would be expected from surface renewal theory if the two catalysts did not interact:

$$S = \frac{R_{obs}}{R_{AB}} \tag{7.1}$$

All other conditions being constant, the absorption rate, R_A, for concentration C_A of catalyst A is given by:

$$R_A = R_o(1 + W_A C_A^p)^{1/2} \tag{7.2}$$

where: W_A = a function of conditions other than catalyst concentration

p = reaction order of the catalyst

The reaction rate with catalysts A and B present but not interacting, R_{AB}, is not simply R_A+R_B but is:

$$R_{AB} = R_o(1 + W_A C_A^p + W_B C_B^p)^{1/2} \tag{7.3}$$

This may be rearranged to a form that is a function of what the separate rates for the two catalysts would be:

$$R_{AB} = (R_A^2 + R_B^2 - R_o^2)^{1/2} \tag{7.4}$$

Therefore the synergism coefficient is given by:

$$S = \frac{R_{obs}}{(R_A^2 + R_B^2 - R_o^2)^{1/2}} \tag{7.5}$$

The above equation may be expressed in terms of enhancement factors.

The procedure for determining S from Eq. 7.5 requires the measurement of the absorption rate with A and B only, the rate with A and B present together in the same concentrations as in the measurement of the individual rates and the physical absorption rate. The interpretation of S involves both sign and magnitude:

$S>1$, positive synergism

$S=1$, no interaction

$S<1$, negative synergism

Similar synergism coefficients can be derived for homogeneous reactions as well.

7.3 Results and Discussion

Scanning the Mn concentration from 0.1 to 100 mM, as in the previous experiments, but this time in the presence of 10 mM of some other catalyst results is synergistic effects with some of the second species. For reference, the dotted line in Fig. 7.1 is the absorption rate with Mn alone, the same curve as in Fig. 3.2. The rates indicated on the left side of the diagram, corresponding to 10 mM of the second catalyst and 0.1 mM Mn, will be shown later to be a region of no synergism, probably owing to the relatively small amount of Mn present, and these are the rates that would be expected from 10 mM of the second species alone. As the concentrations become more comparable some obvious synergistic effects occur. The rate with 10 mM Fe is the most interesting, dipping below the Mn-alone rate from 5 to 10 mM Mn and then turning sharply upward above 10 mM. The flattening of this curve is due to the mass transfer limitation imposed by the solution phase transport of S(4) to the reactive interface. This R_{lim} was calculated in Sec. 4 to be about E=33. As usual, $RX10^9$ is almost exactly numerically equal to E. There is no way to tell from this data how much higher the curve would have gone without the mass transfer limitation since no kinetic information is available in the high or low limited regions. On the other hand, Cu and Mn show strong negative synergism; at 100 mM Mn and 10 mM Cu the rate is almost down to the physical absorption region. The Cr-Mn system seems to exhibit some negative interaction as well.

While the strong Fe-Mn and Cu-Mn synergisms are readily apparent from a diagram like Fig. 7.1 it is difficult to make even qualitative judgements on the interaction between Mn and Ni or Co. Application of the synergism coefficient seems to provide effective quantitative correlation for the degree of interaction (Fig. 7.2). The expected negative-then-positive behavior of the Fe-Mn couple is present as well as the expected trends for Mn and Cr or Cu. Co and Ni show some weak positive interaction with Mn, perhaps surprisingly so in the case of Ni which has almost no catalytic activity of its own. This observed synergism may actually be between Mn and Fe impurities in the $NiSO_4$. At 10 mM Ni and 1 mM Mn the observed absorption rate is about twice that which would be expected in the two catalysts did not interact.

The Fe-Mn couple was chosen for more detailed study due to its profound positive synergism. Figs. 7.3 and 7.4 are analogous to Fig. 7.1, they are Mn scans at several different constant values of Fe concentration between 0.1 and 100 mM. Fig. 7.3 is at pH_b 5 and Fig. 7.4 is at pH_b 4. Although some of the flattening of rates at

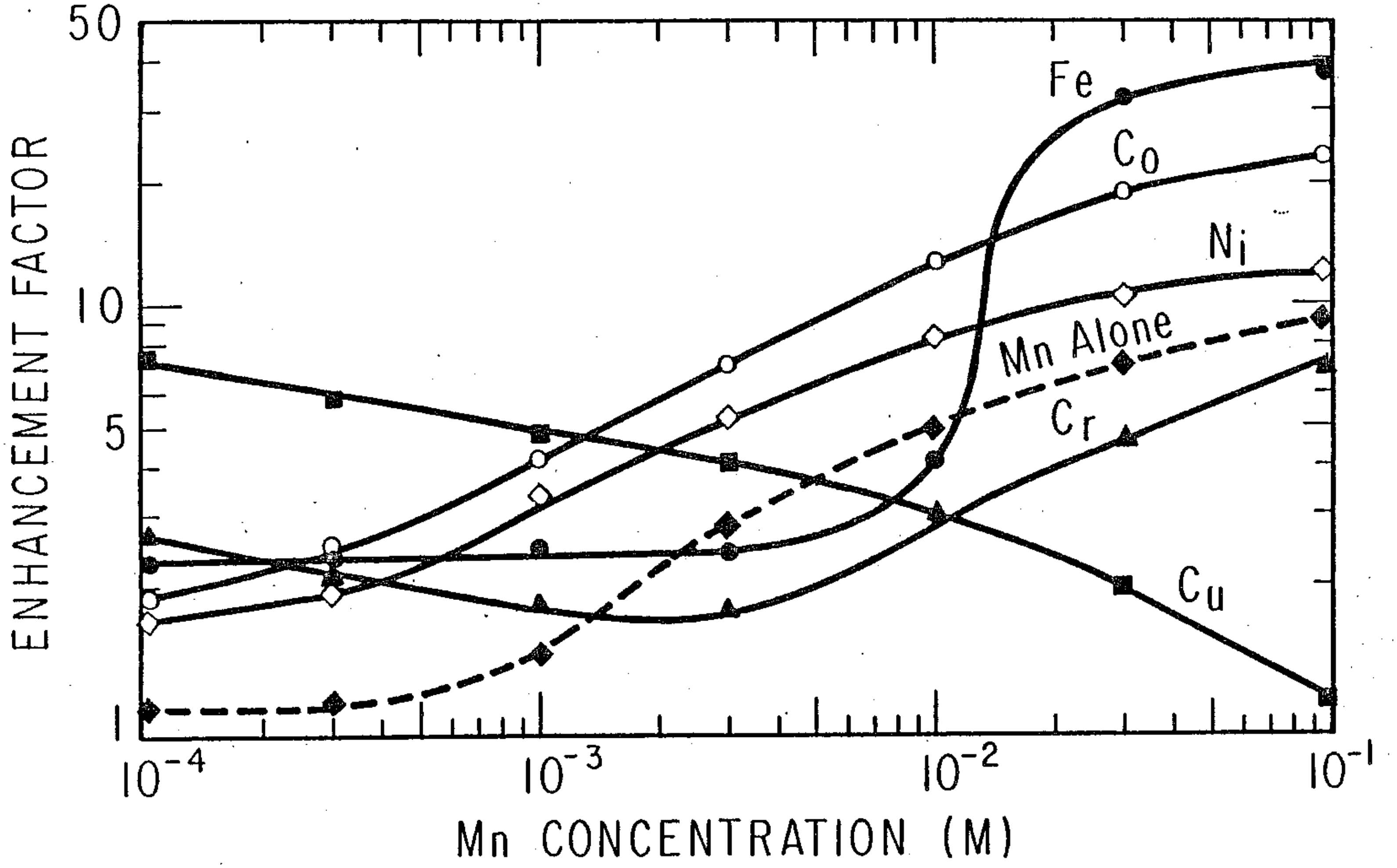

Figure 7.1: Enhancement factors during a Mn scan with 10 mM of a second catalyst present at 10 mM S(4) and pH 5

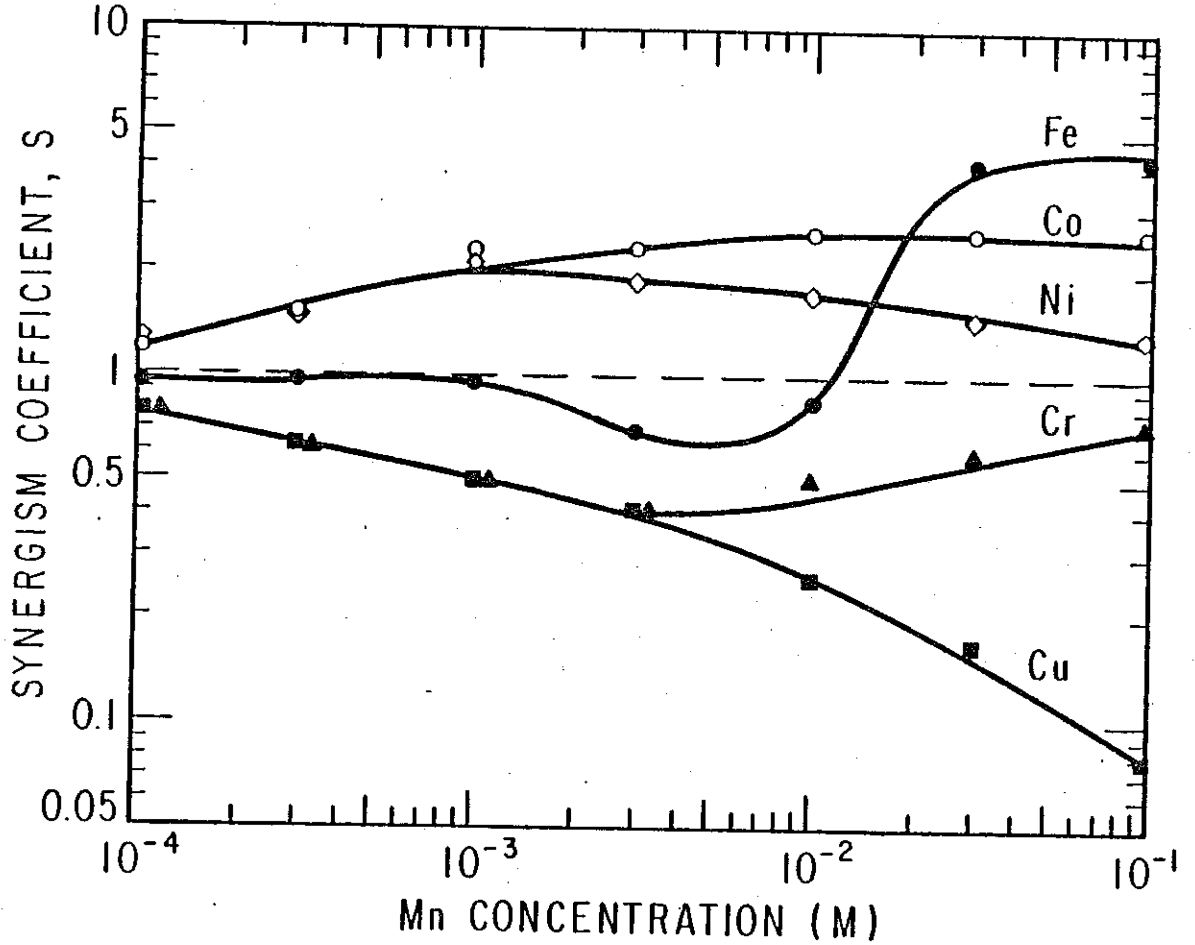

Figure 7.2: Synergism coefficients as a function on Mn concentration at 10 mM of a second catalyst at 10 mM S(4) and pH 5

high Mn concentrations is due to the mass transfer limitation at E=33 the flattening of several of the other curves at enhancement factors of 10 to 20 must be due to kinetic reasons.

Figs. 7.5 and 7.6 are plots of the synergism coefficient for the previous two figures. In Fig. 7.5 the 5 and 10 mM Fe curves are transport limited and in Fig. 7.6 the 10 mM curve is limited but the other curves indicate that the synergism coefficient tends to show a maximum at certain concentrations of Fe and Mn. Also, S seems to fall off sharply with increasing Fe concentration after the maximum, even dipping below the S=1 line. It was previously reported that the rate for Fe alone was significantly decreased by a drop in pH from 5 to 4 and that the rate for Mn alone was unaffected by the same change. It appears that neither the rates nor S is profoundly affected by the drop from 5 to 4 except for the appearance of positive S peaks at <1 mM Mn concentrations and >20 mM Fe.

This exploratory study did not provide enough information to make any definitive statements about the mechanism of synergism. There seems to be two possible mechanistic schemes: chain crossing and electrochemical oxidation of one catalyst by the other. Chain crossing involves the sharing of one or more free radicals that are common to the mechanisms of both catalysts. For instance, the reaction rate by one catalyst might be limited by the supply of a

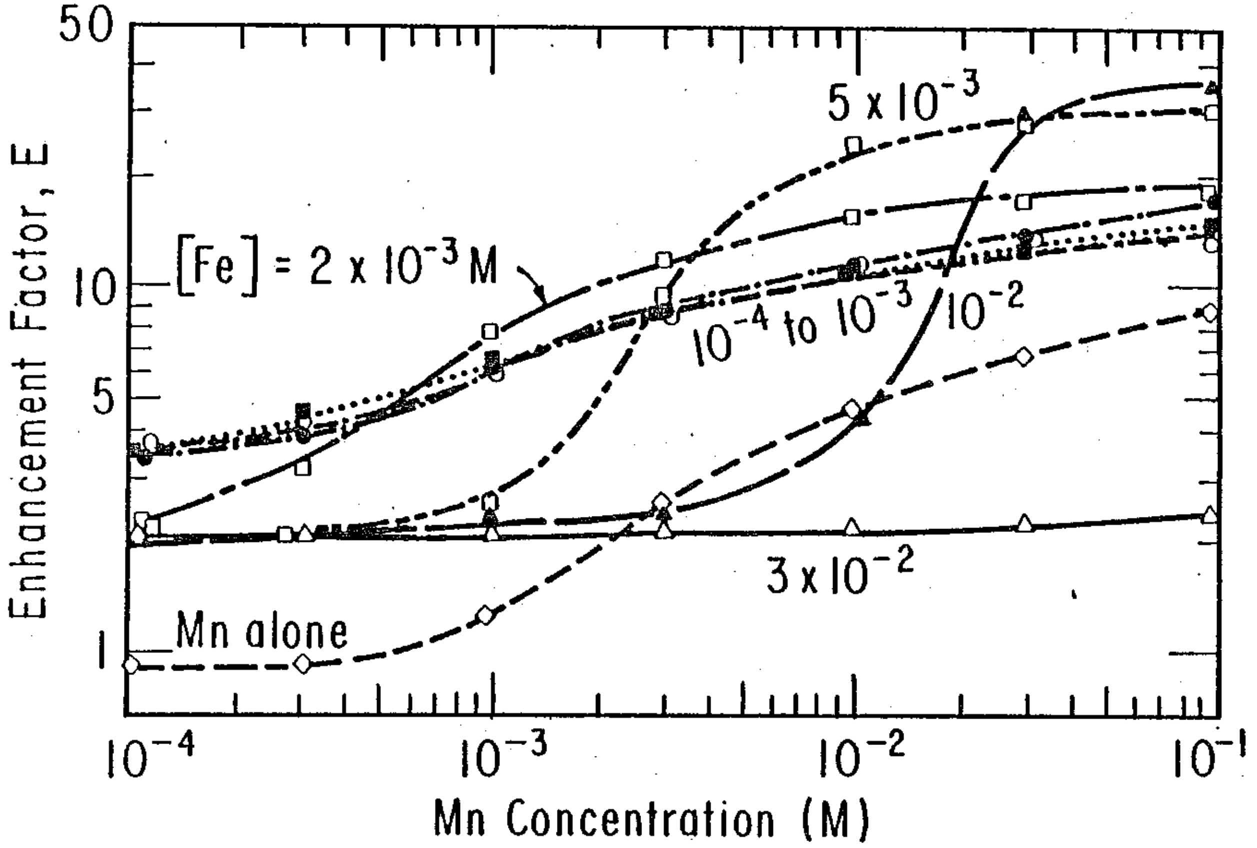

Figure 7.3: Synergistic enhancement factors for

Mn-Fe systems at 10 mM S(4) and pH 5

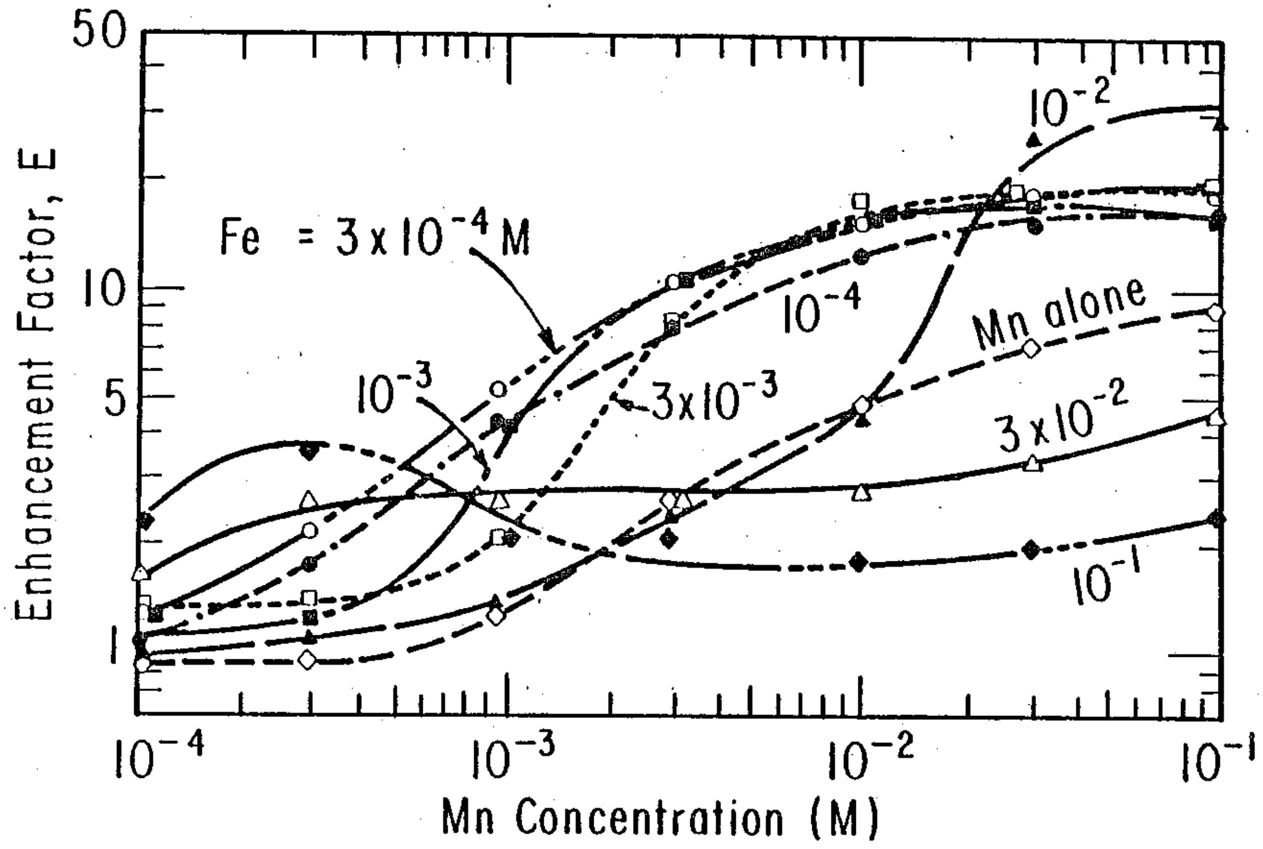

Figure 7.4: Synergistic enhancement factors for Mn-Fe systems at 10 mM S(4) and pH 4

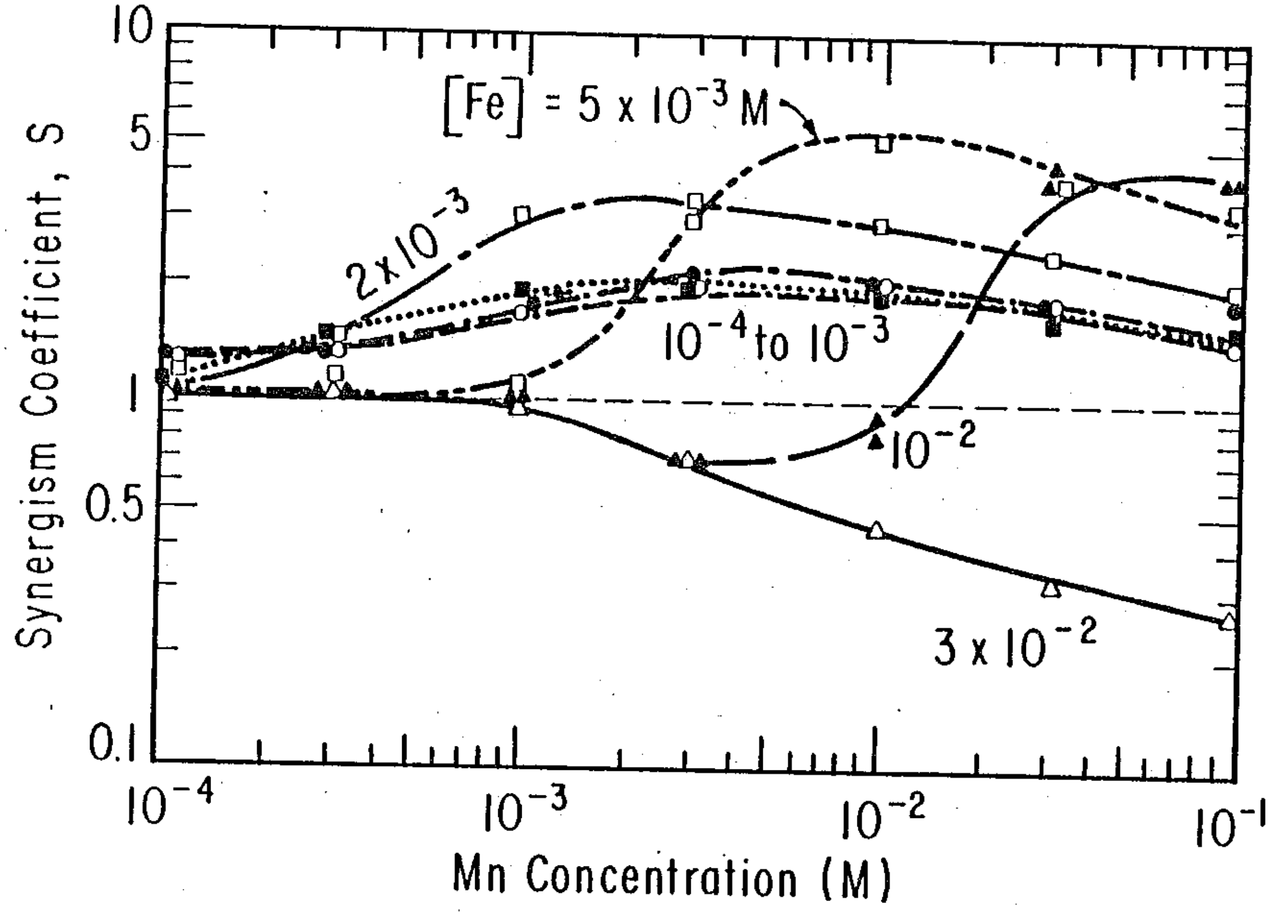

Figure 7.5: Synergism coefficients for Mn-Fe systems at 10 mM S(4) and pH 5

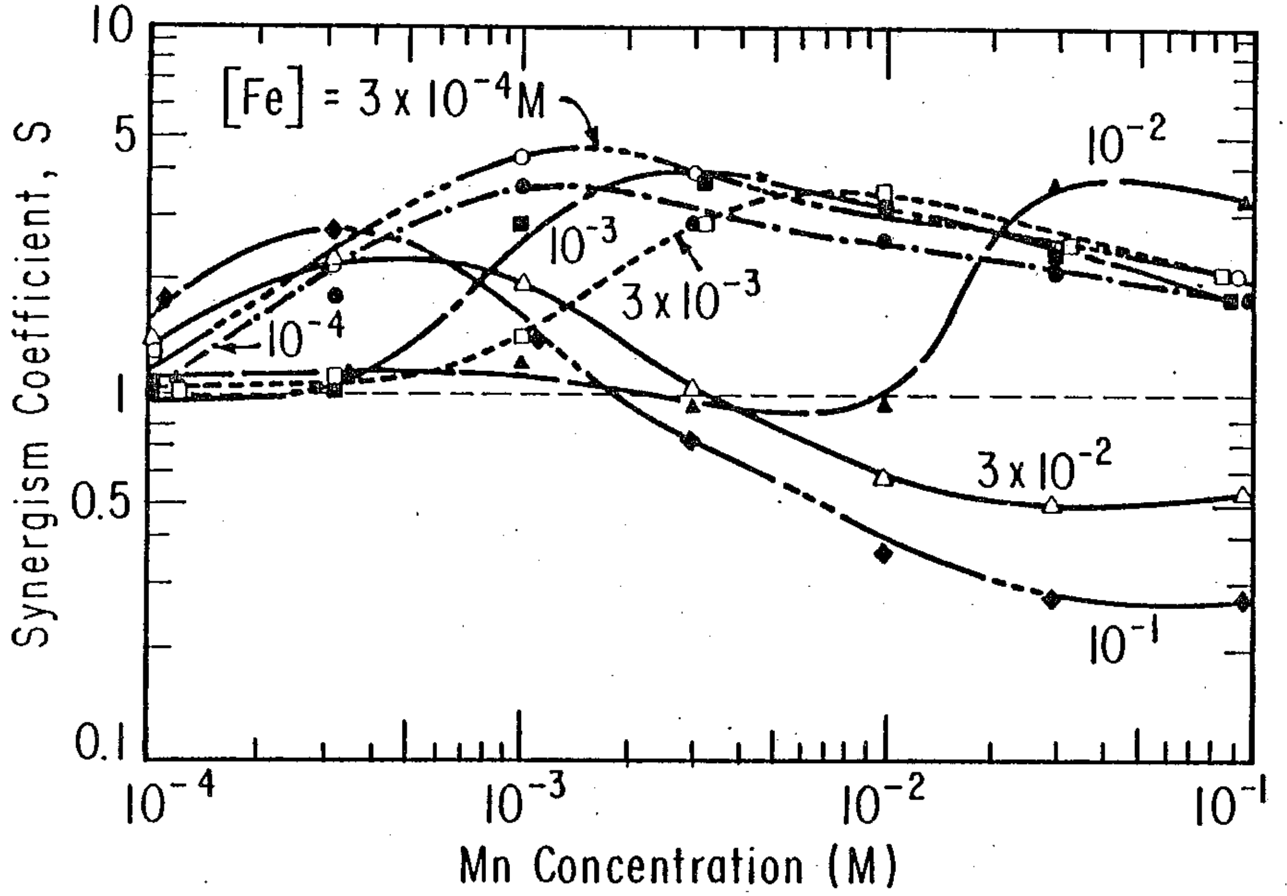

Figure 7.6: Synergism coefficients for Mn-Fe systems at 10 mM S(4) and pH 4

certain radical that is produced by a certain propagation reaction. The other catalyst, when acting alone, might not be limited by this radical but by another species and may make the former in large quantities. When the two are acting simultaneously the radicals produced by the second catalyst could greatly enhance the rate from the first catalyst. Thus, one metal ion would actually act as the catalyst and the other as a promoter. The idea of electrochemical oxidation of one catalyst by the other is related to the theory that it is the upper state of the ion that is catalytically active. One catalyst might have a rate limited by how fast it can be regenerated into its upper state but another catalyst might be limited by something else, say by a certain propagation reaction, and be very easily oxidized to its upper state. Then it might be possible for the second catalyst to oxidize the first to its upper state at the expense of losing a valence state itself and becoming inactive as an initiator but with the gain of an increased overall reaction rate. Once again, one species acts as the catalyst and one as the promoter and the electrochemical scheme can even be considered a case of chain crossing if one considers the catalyst in its upper (active) state as a radical.

The absorption behavior of the Fe-Mn pair shows some characteristics that would be expected from one catalyst oxidizing the other. The $Mn^{+2/+3}$ couple (1.51 V) has a higher redox potential than does the $Fe^{+2/+3}$ couple (0.77 V) so, when they are both present in solution, the following equilibrium would be shifted to the right:

$$Fe^{+2} + Mn^{+3} \rightleftarrows Fe^{+3} + Mn^{+2} \qquad \text{(Rxn. 7.1)}$$

Therefore, it may be possible that Mn^{+3} is a weaker initiation catalyst than Fe^{+3} (it was shown in Sec. 6.2 that Mn is a weaker catalyst than Fe) but that the kinetics for Rxn. 7.1 is very fast to the right so that the relatively inactive manganic ions can oxidize the ferrous to the more potent ferric ions. Figs. 7.3 and 7.4 show that for >30 mM Fe the effect of Mn is removed and the net rate is equal to that of the Fe alone, resulting in a negative synergism. At these high Fe concentrations practically all of the Mn may be forced into its inactive lower state.

Section 8

RECOMMENDATIONS

It seems that the best way to elucidate the sulfite oxidation mechanism is through spectroscopic methods because of their ability to give an accurate free radical census. The measurement of free radical species distribution and concentrations can be given sufficient temporal resolution to enable the calculation of radical reaction rate constants, which is the kind of information needed to determine the types and rates of the propagation reactions. The lack of this type of information currently limits the theoretical treatment of the mechanism.

Results from this study and from the literature suggest the presence of induction times for this reaction that are long enough to adversely affect heterogeneous rates. This phenomena should be further investigated since it is of importance to the design of flue gas desulfurization equipment and in the determination of mass transfer characteristics. Experiments could be performed with time-dependent spectroscopy to determine what radical species are slow to reach steady state or the rate of oxygen absorption into sulfite/catalyst solutions could be measured for short exposure times. A cell could be constructed for the latter purpose by closing the gas space and leaving open only one small diameter glass or teflon tube. A single soap bubble wall could then be used to close this tube near the top and would drop with a velocity proportional to the total absorption rate. Such a bubble in a 0.1 cm tube with $R=10^{-9}$ gmols O_2/cm^2 s and $A=154$ cm^2 would move at 0.43 cm/s.

Catalysis by dissolved metal ions should be studied from the viewpoint of the electrochemical environment in the solution since it appears that specific valence states of these ions are the catalytically active species. Electrochemical reactors could be used for this purpose by introducing into the solution, instead of a dissolved catalyst, carbon or platinum electrodes. For example, if the electrochemical oxidation of the sulfite ion to form a sulfite radical is an effective initiation reaction then the oxidation rate in an oxygen/sulfite solution should rise markedly at 0.89 V on the anode. Synergism is a wide-open area for investigation; little work has been done on it to date and its effects upon the reaction rate are profound enough to warrant more attention than it is getting.

Further study of the effects of agitation intensity on heterogeneous reaction and gas absorption rate is closely connected to the study of induction times. An unsparged stirred tank reactor is not ideal for this purpose. A better system would be one in which the contact area can remain known at all agitation rates such as a wetted-wall column or a bubble column.

Differences of conditions between the interface and bulk solution should be studied to determine the importance of transport effects on the reaction conditions and rates in heterogeneous reactors. It was shown in Sec. 4 that these differences may be substantial under FGD conditions. Since the partial pressure of sulfur dioxide over the solution was predicted to be profoundly affected by the interfacial pH depression it may be possible to construct a reactor cell upsteam from an sulfur dioxide analyzer to get an indirect measure of surface pH.

SUMMARY

Introduction

The liquid-phase sulfite oxidation reaction involves the addition of an oxygen atom supplied by dissolved oxygen to an S(4) species, sulfite or bisulfite, to produce S(6), sulfate or bisulfate. The pH fixes the distribution among protonated and unprotonated species but the reactants and products are usually referred to as simply "sulfite" and "sulfate". This reaction is a very complex free radical sequence involving a number of highly reactive intermediate species. It is catalyzed by micro-molar or higher amounts of dissolved transition metal ions having more than one valence state and is very sensitive to impurities in general (Linek and Mayrhoferova, 1970). Recent studies indicate that the reaction does not proceed at all in the absence of a catalyst (Huss et al., 1978). The observed kinetics are also sensitive to experimental conditions so that there is no common agreement on rate equation forms, rate constants or even reaction orders. This widely varying behavior indicates that different elementary reactions become important at different conditions and control the rate, contributing to the complexity of the problem. An excellent review of the subject has been written by Linek and Vacek (1981).

The two main engineering uses of sulfite oxidation are the determination of mass transfer characteristics in gas-liquid contacting equipment (DeWaal and Okeson, 1966; Westerterp et al., 1963; Metha and Sharma, 1971), and the oxidation of calcium sulfite waste products in flue gas desulfurization (Rochelle, 1977; Borgwardt, 1978; Hudson, 1980; Gleason, 1977). Scientific interests focus on the reaction's role in acid precipitation and in free radical reactions in general (Chen and Barron, 1972; Hayon et al., 1972; Hoffmann and Jacob, 1982; Martin, 1983). Also, the sulfite oxidation reaction has many features in common with the solution phase free radical oxidation of hydrocarbons so there are some opportunities for information crossover (Twigg, 1962; Turney, 1965).

The purpose of this project was to study sulfite oxidation under flue gas desulfurization (FGD) conditions. These conditions differ from those usually employed in other studies which tend to be either mass transfer characterization projects at higher S(4) concentrations and pH but lower catalyst levels or acid precipitation studies at trace amounts of S(4) and catalyst and lower pH. The experiments were performed at pH 4 to 6 and 0.01-0.03 M sulfite to simulate the conditions in typical FGD oxidizing units. The reaction occurred under heterogeneous conditions where oxygen was absorbed out of air at $50^{o}C$ into an agitated, unsparged sulfite/catalyst solution typically containing 0.1 to 100 mM of Mn, Fe, Co, Cu, Cr or Ni. Under these conditions the reaction kinetics were so fast that all of the incoming oxygen was consumed in a thin reaction zone at the gas-liquid interface and the bulk solution oxygen concentration was maintained near zero. The absorption rate was measured via the pH-stat method (Chan and Rochelle, 1982) since this technique allows solution concentrations to remain constant indefinitely while the absorption rate comes to steady state.

The scope of this project was to determine what factors are important in fixing the reaction rate, and therefore the absorption rate, under FGD conditions and to elucidate some aspects of the reaction mechanism when common FGD catalysts are present. The principal solution effects that were considered included catalyst concentration, S(4) concentration, pH and agitation rate. Catalytic synergism was studied by having two catalysts present simultaneously in the solution. The results of these experiments were correlated to hypothesized reaction steps with equations describing simultaneous reaction and mass transfer under these conditions in order to judge the validity of proposed reaction steps.

Theory

Both surface renewal theory and film theory were used to model the processes occurring in the system according to the suitability of each to specific applications (Hikita and Asai, 1964; Danckwerts, 1970; Brian, 1964). Reaction rate constants and reaction orders were correlated with a Danckwerts surface renewal equation that is generalized to include any values of reaction orders:

$$R = R_o \left[1 + \frac{\frac{2}{m+1} D_{ox} k_r [S(4)]_i^n [cat]_i^p [O_2]_i^{m-1}}{k_{ox}^2} \right]^{1/2} \qquad (S\text{-}1)$$

where: R = the absorption flux, gmols O_2/cm^2 s

R_o = the physical absorption flux = $k_{ox}[O_2]_i$, $1X10^{-9}$ at 400 rpm agitation

k_r = the homogeneous reaction rate constant

m, n, p = homogeneous reaction rate orders

k_{ox} = the unenhanced liquid-phase mass transfer coefficient, $8.2X10^{-3}$ cm/s at 400 rpm

The right-hand term in the brackets dominates the unity at enhancement factors above about three. One basis for comparing catalysts was the first order rate constant with respect to oxygen, $k_1 = k_r[S(4)]_i^n[cat]_i^p$ in Eq. S-1. Rearranging this equation gives:

$$k_1 = \frac{k_{ox}^2}{D_{ox}}(E^2 - 1) = 1.81(E^2 - 1)\ s^{-1} \qquad \text{(S-2)}$$

E = the enhancement factor, R/R_o

Another basis of comparison was established so the absorption rate data from these experiments could be converted to a homogeneous reaction rate for comparison to literature values. The quantity r_{S4} is defined as the average homogeneous rate of S(4) consumption in the interfacial reaction zone in gmols S(4)/l s and is equal to twice the rate of oxygen consumption, r_{ox}. r_{ox} is equal to k_1 times the concentration of oxygen in the reaction zone, $[O_2]_i/2$:

$$r_{S4} = 2k_1([O_2]_i/2)(E^2 - 1) = (2.71X10^{-4})(E^2-1)\ M\ S(4)/s \qquad \text{(S-3)}$$

Two coupled film theory models were written for the interfacial region, one describing the reaction zone at the interface and one describing transport between the bulk solution and the reaction zone.

Since the detailed mechanism of sulfite oxidation is not known, a generalized free radical mechanism was derived and used in conjunction with equations relating the oxygen absorption flux (R) to the velocity of the homogeneous reactions (r_{S4}) to model the effects of changing catalyst and inhibitor concentrations upon r_{S4} and therefore upon the observed absorption rate. This generalized mechanism employs some hypothesized initiation and termination reactions, which are understood to some extent, and uses a generalized form for the propagation reactions, which are very numerous and almost never known with any certainty in sulfite oxidation. This model suggests that the observed change in reaction order with respect to Mn catalyst from one to one-half at 10 mM could be due to a change from first to second order termination kinetics as the free radical population in the reaction zone increases. The inclusion of an inhibition step in the model resulted in a rate expression identical to the observed relationship for inhibition by thiosulfate, Eq. S-4.

A film theory model was solved on a computer in order to estimate the differences between bulk and interface (reaction zone) conditions during enhanced oxygen absorption. It was found that under FGD conditions significant lowering of pH and S(4) concentration in the reaction zone could occur. The cause of this increased sensitivity at FGD conditions is the low levels of S(4) which acts as both a reactant and, at the pH values of interest in this project, a buffer. Reaction at the interface can cause a significant decrease in the interfacial sulfite concentration which depletes its buffering ability and allows the interface to achieve pH values that are up to two units lower than the bulk pH of 5. At 10 mM the S(4) mass transfer limited enhancement factor would be about 33. The partial pressure of sulfur dioxide above the solution is predicted to increase because of this lower pH at the surface. A pH 5 and 10 mM sulfite solution would have a sulfur dioxide partial pressure of 20 ppm but at an enhancement factor or 15 it could rise almost up to levels that would be expected in flue gas from some coal-fired boilers (500 ppm).

Results and Discussion

The measured oxygen absorption rates for single catalysts, Fig. S-1, were correlated with the equations S-2 and S-3 to obtain the kinetic information in Table S-1. The slopes of the lines in Fig. S-1 equal one-half the catalyst reaction order so Mn shifts from first to 1/2 order at 10 mM, possibly due to a change in termination reactions at the higher reaction rates, while Co seems tending towards first order and Ni shows too little enhancement to determine a slope. Under the same conditions Fe catalyst showed apparent zero order kinetics at E=2.4 at pH 5 making it the most potent catalyst below 1 mM. The homogeneous oxidation rates in the reaction zone were on the order of 1 mM S(4)/l s.

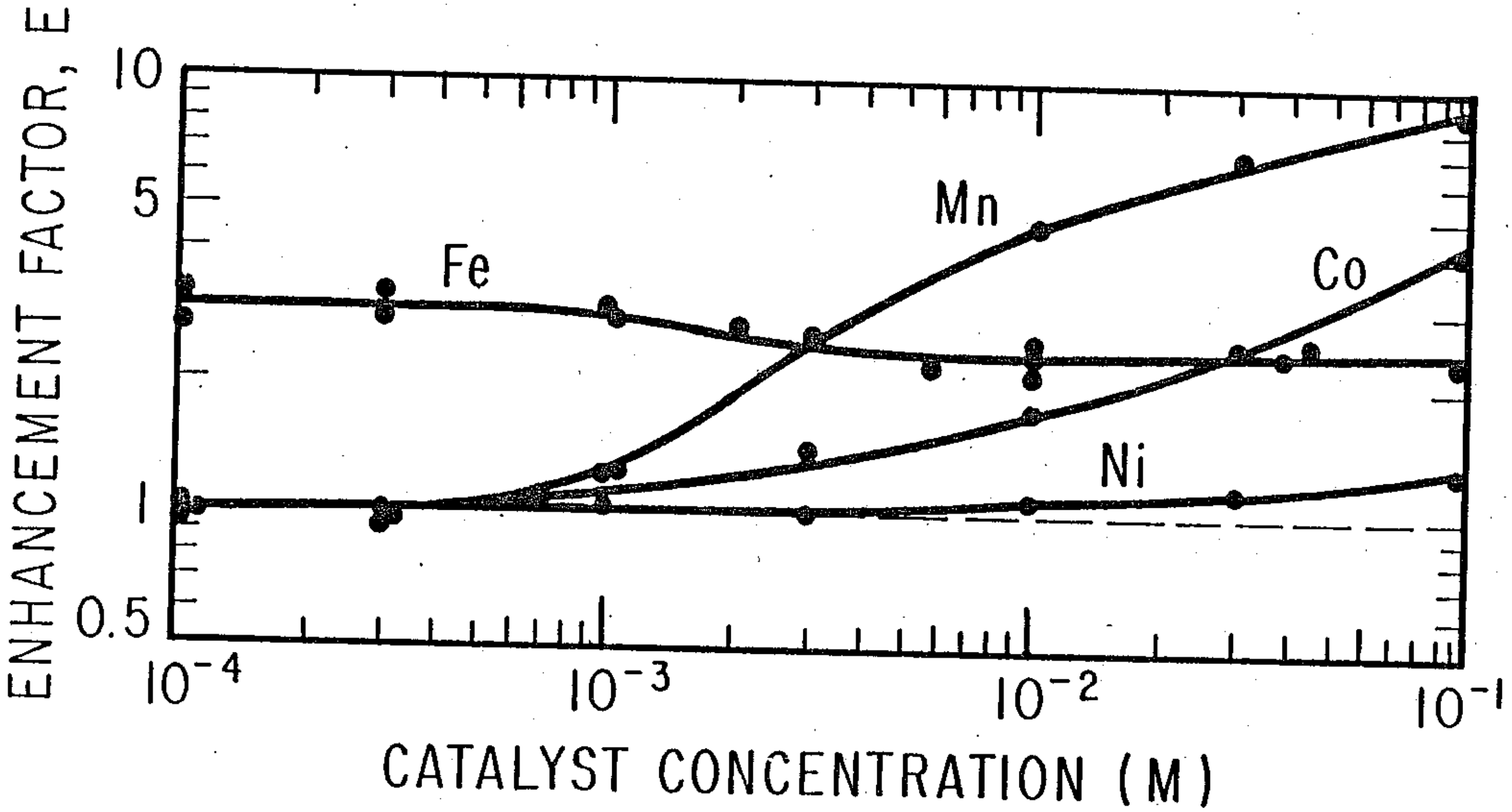

Figure S-1: Effect of Mn, Co, Fe and Ni catalyst concentration on the enhancement factor at 10 mM S(4) and pH 5

Table S-1

Comparison of catalytic activities during enhanced oxygen absorption into 10 mM S(4) and 300 mM S(6) at pH 5, $50^{\circ}C$ and 400 rpm agitation

k_1 = first order (in O_2) rate constant, s^{-1}

r_{S4} = average homogeneous oxidation rate in the reaction zone, gmols S(4)/liter sec.

mM catalyst		E	k_1	r_{S4}
5	Mn	2.5	9.5	0.0011
10	Mn	5.0	43	0.0050
50	Mn	7.5	99	0.0120
0.1	Fe	3.1	16	0.0019
0.5	Fe	3.1	16	0.0019
5	Fe	2.6	10	0.0012
10	Fe	2.4	8.6	0.0010
50	Fe	2.4	8.6	0.0010
5	Co	1.5	2.3	0.0003
10	Co	1.9	4.7	0.0005
50	Co	3.2	17	0.0020
10	Ni	1.1		
50	Ni	1.2		
10	Cr	2.7	11	0.0013
10	Cu	7.3	94	0.0110

Comparisons were made between r_{S4} values in Table S-1 and homogeneous reaction rates from published rate expressions extrapolated to the conditions of this project (Hoffmann and Jacob, 1982; Bengtsson, 1974, Martin 1983). The expressions were evaluated at 5 mM Mn or Co and 0.1 mM Fe (the lower level for iron was used since experiments indicate that the catalyst is solubility-limited above this point) and were found to give rate values higher than those reported here for Mn and Co but seemed to be of the right order of magnitude for Fe. Most of these expressions came from experiments performed at pH values comparable to those in this project but they were mostly at lower sulfite and catalyst concentration in order to obtain rates low enough to use homogeneous reactors. The agreement for Fe catalyst may be because the published rate expressions were exprapolated less for this case.

The distribution of catalyst valence states is at steady state since the catalyst ion which was reduced during initiation reoxidized by dissolved oxygen in the reaction zone or by other oxidizing species in solution. Experiments involving the addition of the catalysts to the solution in different valence states and literature data support the idea that it is the upper valence state of the metal ion that is the catalytic agent, acting by removing an electron from a S(4) ion to create a free radical chain reaction in the reaction zone.

The apparent zero-order kinetics of Fe catalyst were due to solubility limitations on a catalytically active ferric species. Hydrated Fe does not have a sufficient oxidizing potential (0.77 V) to remove an electron from sulfite (0.89 V) but FeOOH might (0.908 V) (Hoffmann and Jacob, 1982; Brimblecombe and Spedding, 1974). Fe scans at 0.001 to 0.1 mM (Fig. S-2) showed a change of reaction order from one to zero at some pH-dependent Fe concentration. These breakpoints were due to the catalytically active species reaching a solubility limit at 0.01 mM total Fe at pH 5. The solubility of FeOOH is much lower, about 10^{-9} mM and, if it is in fact the active species, its concentration reaches this point at 0.01 mM total Fe. These breakpoints shifted to higher concentrations at lower pH due to the increased solubility of the ferric species (Stumm and Morgan, 1981; Gayer and Woontner, 1956). The reaction rate with Fe catalyst was higher at higher pH because the catalyst regeneration reaction, ferrous oxidation to ferric, is base catalyzed (Tamura et al., 1976; Stumm and Lee, 1961). Red-brown Fe precipitates were visible at total Fe concentrations above 0.5 mM at pH 5. The amount of these solids were observed to increase with time and pH and were found to be catalytically inactive.

FGD systems operating under the conditions of this project with Fe catalysis would be expected to show enhancement factors that

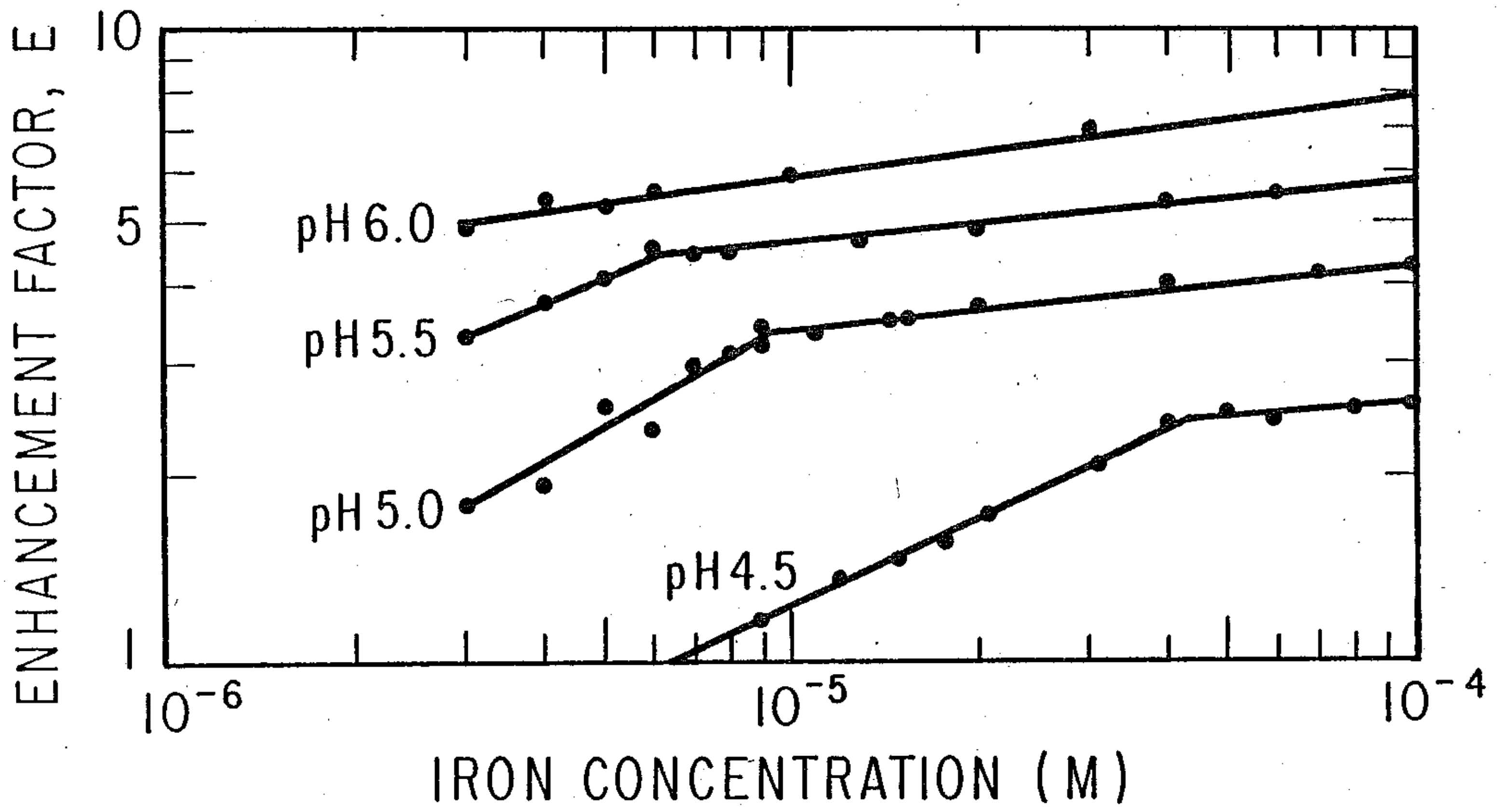

Figure S-2: Effect of low Fe concentration on the enhancement factor at 30 mM S(4) and various pH values are independent of pH. A decrease in pH retards the Fe-catalyzed oxidation reaction (Fig. S-2) but the increase in total dissolved S(4) concentration, together with the observed half-order dependency on S(4), results in equal offsetting effects.

Thiosulfate was found to inhibit the Mn and Fe catalyzed rate by acting as a free radical scavenger (Altwicker, 1977; Alyea and Backstrom, 1929; Backstrom, 1934). It was degraded only in the presence of sulfite oxidation in the time frame of a few hours and was consumed at a rate proportional to the remaining thiosulfate concentration raised to the three-halves power. Thiosulfate additions of 0.05 to 0.15 mM to Mn systems completely recovered to the uninhibited rate in 1 to 3 hours. There was no significant induction time following the addition of thiosulfate and the absorption rate recovered from the lowered value in a linear fashion. The absorption rate was inversely proportional to the square-root of the thiosulfate concentration (Fig. S-3) and this rate form was also successfully modelled by the generalized radical mechanism. At 30 mM Mn, 10 mM S(4) and pH 5:

$$E = \frac{6.17}{(1 + 46.8[S_2O_3^{-2}, \text{ mM}])^{1/2}} \qquad \text{(S-4)}$$

Thiosulfate required between one and two orders of magnitude

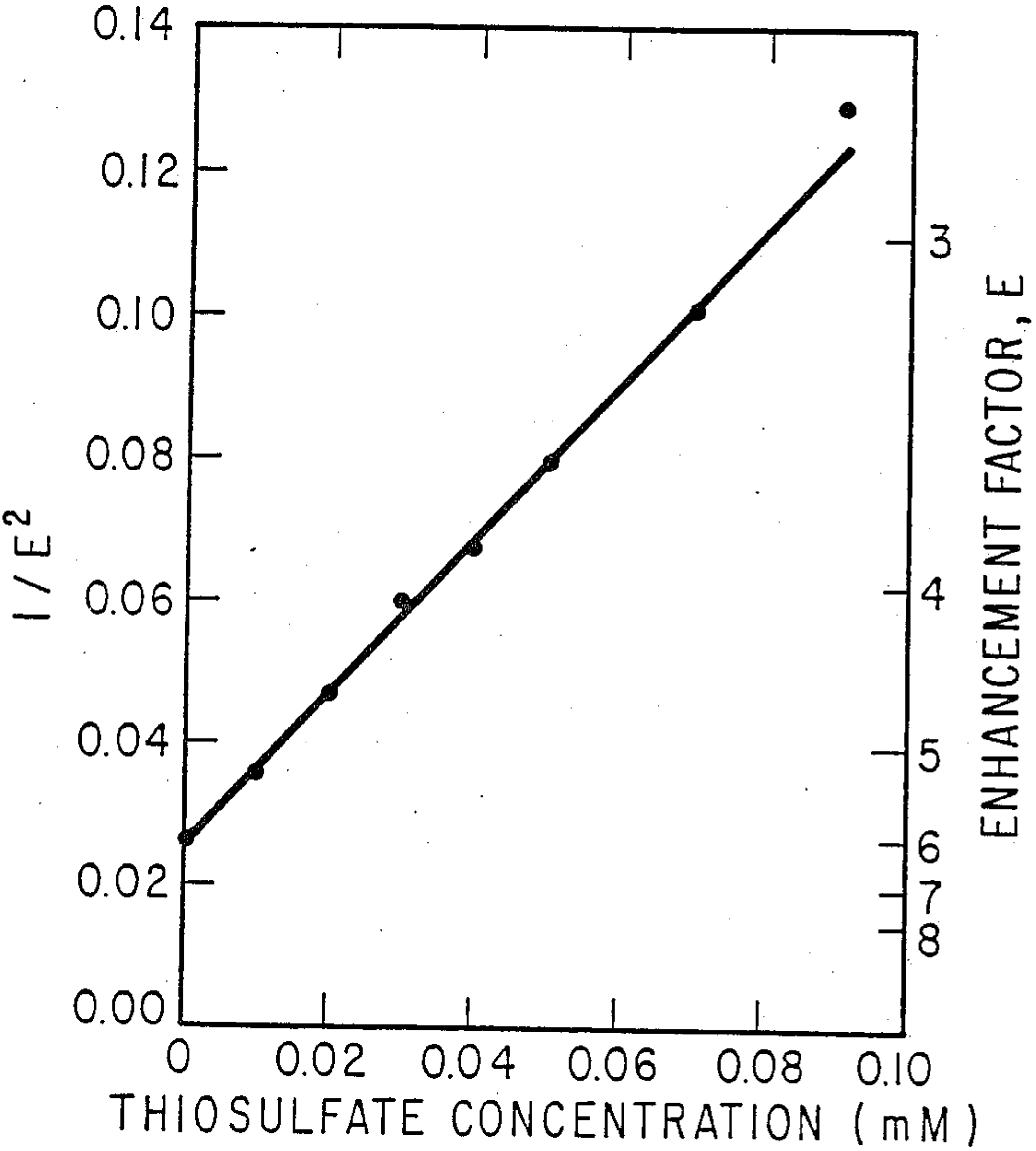

Figure S-3: Decrease of enhancement due to the addition of thiosulfate at 30 mM Mn, 10 mM S(4) and pH 5 more concentration to have the same percentage of retardation on Fe catalyzed systems than on those with Mn. Also, each thiosulfate ion prevented the oxidation of about 40 sulfite ions with Mn but prevented only about three with Fe. Therefore, the radicals that react with thiosulfate must be generated more rapidly by Fe catalyst than by Mn.

EDTA (ethylenediamine-tetraacetic acid) retarded the reaction by chelating metal ions thereby sterically hindering their catalytic action (Lim et al., 1982; Schwarzenbach, 1957). The Fe-EDTA complex seemed to be totally inactive. With 5 mM Fe giving obvious formation of a precipitate, an equivalent amount of EDTA was required. Therefore, EDTA would not be an effective inhibitor in systems with an excess of iron salt solids.

The rate of oxygen absorption into sulfite/catalyst solutions under FGD conditions was measured as a function of the agitation rate (Fig. S-4) in order to estimate the liquid-phase mass transfer coefficient and the interfacial contact area via a method that has the advantage of not requiring detailed prior knowledge of the reaction kinetics. The bottom curve is the physical absorption line since 0.1 mM Mn is sufficient to deplete the bulk-phase oxygen but not enough to cause enhancement (Fig. S-1). The upper absorption rate curves were made with enough catalyst to cause enhancement at

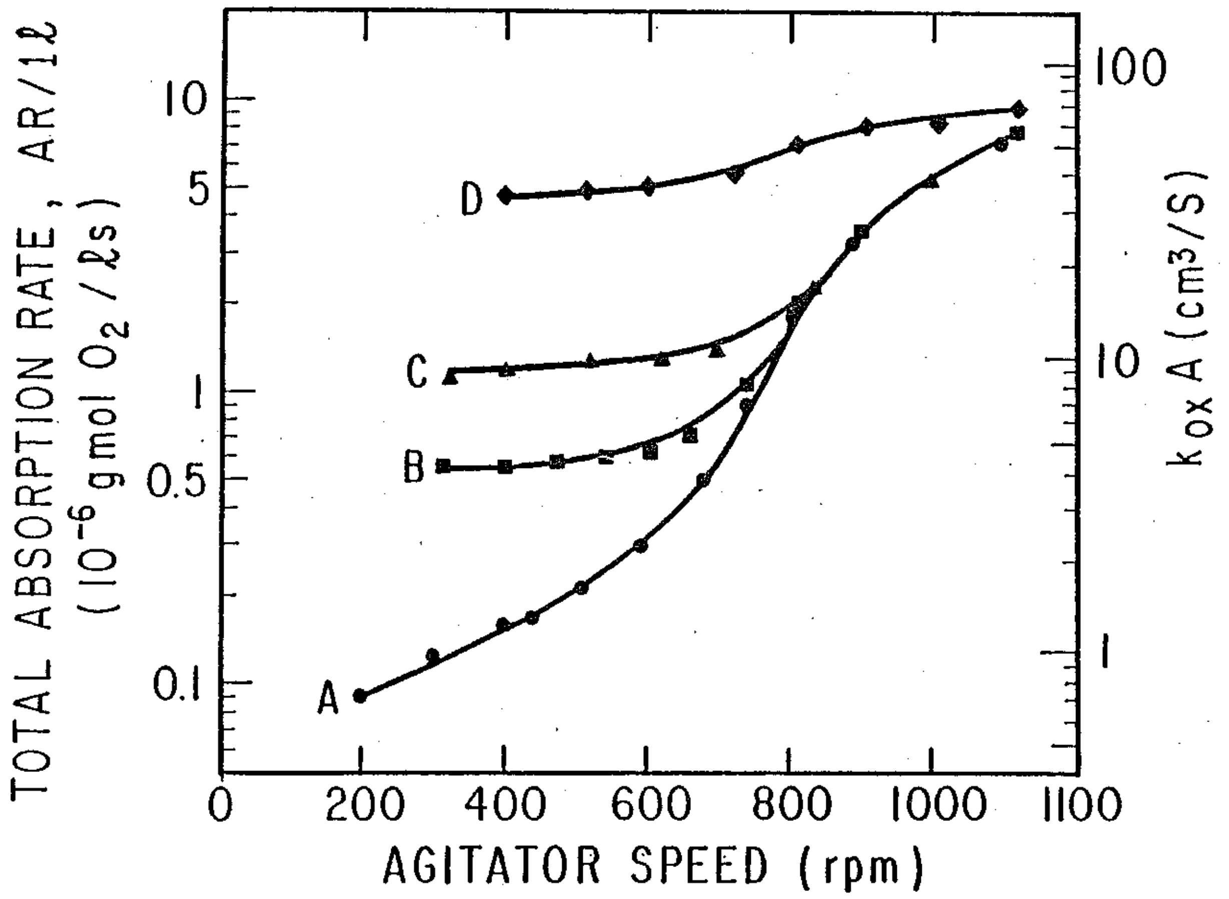

Figure S-4: Effect of agitator speed on the total oxygen absorption rate, Mn and Mn-Fe synergistic catalysts at pH 5 low agitation rates but E falls to unity when a catalyst's line converges with the physical absorption line. The calculated values of k_{ox} and A were found to be much too large and small, respectively, at high agitation intensities perhaps due to a slowing down of the local reaction rate. This effect has been observed by other investigators and is hypothesized to occur because the average length of time that fluid elements spend at the surface is shorter than the induction time of the free radical reaction in the elements so the average rate is less than that which would be observed at steady state.

The phenomena of catalytic synergism was studied by measuring the rate with two catalysts present in the solution simultaneously (Martin, 1983; Barrie and Georgii, 1976; Altwicker and Nass, 1983). Strong positive interactions were found for the Mn-Fe couple and strong negative interactions for the Mn-Cu pair. Some combinations of Mn and Fe were strong enough to cause the rate to reach the S(4) mass transfer limit at E=33 so no kinetic information could be garnered about faster rates. A dimensionless "synergism coefficient" was defined as the ratio of the absorption rate observed with both catalysts present to the absorption rate which would be expected from surface renewal theory if the catalysts did not interact. The separate rates cannot be added in a linear fashion as homogeneous rates would be because of the effects of mass transfer considerations so a more involved approach is necessary. This synergism coefficient was found to go as high as 5 for Mn-Fe and as low as 0.1 for Mn-Cu.

Conclusions

(1) Fe, Mn, Co, Cr and Cu are potent catalysts under FGD conditions but their relative activities depend on the specific conditions. Significant enhancement factors could be possible in actual scrubbers at Mn and Fe concentrations typically observed. Fe alone could give enhancements of 2 to 5 depending on pH and S(4) concentration while Fe-Mn synergisms could result in enhancements as high as 10 to 30. FGD units operating under these conditions with Fe catalysis would exhibit enhancement factors that are independent of pH.

(2) The upper state of multivalent transition metal ions initiates the free radical reaction chain by removing an electron from a sulfite or bisulfite ion. The catalytic mechanisms of Fe and Mn are quite different. Fe generates free radicals at a faster rate. Therefore it comes as no surprise that organic acid degradation is less severe in the presence of Mn.

(3) Some catalytically active ferric ion is solubility-limited resulting in apparent zero order kinetics above 0.01 mM total Fe at pH 5. Precipitated Fe solids are inactive.

(4) 0.05 to 0.15 mM thiosulfate effectively inhibits the reaction catalyzed by Mn but has less effect on Fe systems. Oxidation in FGD systems can be effectively inhibited by thiosulfate, although it degrades rapidly, especially with Fe catalysis.

(5) EDTA inhibits Fe catalysis at equal or higher concentrations by chelating the ferrous and ferric ions into an inactive complex. EDTA would not by an effective catalyst in FGD systems since the enough EDTA would have to be added to complex all of the dissolved and precipitated iron.

(6) Significant reductions in pH and [S(4)] can occur in the interfacial reaction zone under FGD conditions due to the combination of high absorption fluxes and low bulk S(4) levels.

(7) Oxygen absorption from air into sulfite/catalyst solutions under FGD conditions as a method of mass transfer characterization can lead to overestimation of the liquid-phase coefficient and underestimation of contact area perhaps due to reduced reaction rates at higher agitation intensities. The enhancement factors that were measured in this project may not be directly applicable to a real scrubber because of changes in k_{ox} and variation of the heterogeneous reaction kinetics with agitation.

NOTATION

The numbers in parenthesis refer to equations containing the term.

Symbols

A = interfacial contact area, cm^2 (6.1)

a = gas-liquid contact area per unit volume, cm^{-1}

c_r = lumped kinetic constant, cm/s (6.3)

D_x = diffusivity of species X, cm^2/s

E = absorption rate enhancement over physical absorption = R/R_o (3.3)

K_{S4} = equilibrium constant for sulfite/bisulfite, $gmols/cm^3$ (4.8)

k_1 = first-order reaction rate constant in oxygen, s^{-1} (3.10)

k_m = m-th order reaction rate constant in oxygen (3.12)

k_r = generalized reaction rate constant (3.15)

k_x = liquid phase mass transfer coefficient for species X, cm/s (4.2)

Me = some metal, superscripts U and L refer to upper and lower valences

N_x= flux of species X to the interface, moles X/cm^{2}s (4.1)

R = oxygen absorption rate, gmols O_2/cm^{2}s (3.15)

R_A = absorption rate with catalyst A (7.2)

R_{AB} = absorption rate for catalysts A and B with no synergistic interactions (7.3)

R_{el} = absorption rate for an individual surface element (3.7)

R_{lim} = S(4) mass transfer limited absorption rate (4.5)

R_o = physical absorption rate = $k_{ox}[O_2]_i$ (3.2)

R_{obs} = observed absorption rate for mixed catalysts A and B with possible synergistic interactions (7.1)

r_{inh} = rate that free radicals are consumed by inhibitors, gmols radicals/cm^{3}s (5.15)

r_{init} = rate that free radicals are produced by the initiation reaction, gmols radicals/cm^{3}s (5.1)

r_{prop} = average free radical propagation rate in the reaction zone, gmoles radicals/cm^{3}s (5.2)

r_{S4} = average homegeneous sulfite oxidation rate in the reaction zone, gmoles S(4)/cm^{3}s (5.9)

r_{term} = rate that free radicals are consumed by termination reactions, gmols radicals/cm^{3}s (5.3, 5.4)

S = synergism coefficient (7.1)

s = fraction of the surface renewed per second, s^{-1} (3.8)

[S(4)] = total sulfite concentration, sulfite + bisulfite, gmols/cm^3

[S(6)] = total sulfate concentration,

sulfate + bisulfate, gmols/cm^3

W_A = a function of conditions other that the concentration of catalyst A, (7.2)

X = some species in solution

x = distance into the liquid from the interface, cm (3.5)

x_d = thickness of the interfacial stagnant layer, cm (3.4)

x_r = thickness of the interfacial reaction zone, cm (5.9)

Subscripts

Subscripts are used to refer a symbol to a specific species or position

b = in the bulk solution (3.1)

BS4 = bisulfite (4.5)

BS6 = bisulfate (4.6)

el = refers to a fluid element (3.7)

i = at the gas-liquid interface (3.1)

inh = refers to an inhibition reaction (5.15)

init = refers to the initiation reaction (5.1)

prop = refers to the propagation reaction (5.2)

S4 = total sulfite

S6 = total sulfate

term = refers to the termination reaction (5.3)

US4 = sulfite (4.5)

US6 = sulfate (4.6)

x = refers to species X

Superscripts

L = lower valence state of a metal ion (5.1)

m = reaction order with respect to oxygen (3.12)

n = reaction order with respect to total sulfite (3.15)

p = reaction order with respect to catalyst (3.15)

U = upper valence state of a metal ion (5.1)

BIBLIOGRAPHY

Altwicker, E., "Sulfur Dioxide Absorption, Oxidation and Oxidation Inhibition," DeChema. Monogr., 343 (1976).

Altwicker, E., "The Role of Inhibitors in the Kinetics of Sulfite Oxidation," Trans. Inst. Chem. Eng., 55, 281 (1977).

Altwicker, E. and K. Nass, "Evidence for Enhanced Mass Transfer and Synergistic Catalysis of Aqueous Phase Sulfur Dioxide Oxidation by Mixtures of Mn and Fe," Atm. Env., 17, 187 (1983).

Alyea, H. and H. Backstrom, "The Inhibitive Action of Alcohols on the Oxidation of Sodium Sulfite," J. Am. Chem. Soc., 51, 90 (1929).

Backstrom, H., "The Chain Reaction Theory of Negative Catalysis," J. Am. Chem. Soc., 49, 1460 (1927).

Backstrom, H., "Der Kettenmechanisms bei der Autoxydation von Natriumsulfitlosungen," Z. Physik. Chem., 25B, 122 (1934).

Baes, C. and R. Mesmer, The Hydrolysis of Cations, John Wiley and Sons, New York (1976).

Bailar, J., H. Emeleus, R. Nyholm and A. Trotman-Dickenson, eds., Comprehensive Inorganic Chemistry, v. 3, Pergamon Press, Oxford, England (1973).

Barrie, L. and H. Georgii, "An Experimental Investigation of the Absorption of Sulfur Dioxide by Water Drops Containing Heavy Metal Ions," Atm. Env., 10, 743 (1976).

Barron, C. and H. O'Hern, "Reaction Kinetics of Sodium Sulfite Oxidation by the Rapid Mixing Method," Chem. Eng. Sci., 21, 397 (1966).

Bassett, H. and W. Parker, "The Oxidation of Sulfurous Acid," J. Chem. Soc., 1540 (1951).

Bengtsson, S., Topical Report on the Absorption and Oxidation of SO_2 in $CaCO_3$ and $Ca(OH)_2$ Suspensions, Ph.D. dissertation, Technical Univ. of Munich (1974).

Bengtsson, S., and I. Bjerle, "Catalytic Oxidation of Sulfite in Diluted Aqueous Solutions," Chem. Eng. Sci., 30, 1429 (1975).

Boozer, C. and G. Hammond, "Molecular Complex Formation in Free Radical Reactions," J. Am. Chem. Soc., 76, 3861 (1954).

Boozer, C., G. Hammond, C. Hamilton and J. Sen, "Air Oxidation of Hydrocarbons, III, Mechanism of Inhibitor Action in Benzene and Chlorobenzene Studies," J. Am. Chem. Soc., 77, 3238 (1955).

Borgwardt, R., "Effect of Forced Oxidation on Limestone/SO_x Scrubber Performance," EPA 600/7-78-058a, 205 (1978).

Braga, T. and R. Connick, "Kinetics of the Oxidation of Bisulfite Ion by Oxygen" in Flue Gas Desulfurization, ACS Symposium Series 188 (1982).

Brian, P., "Gas Absorption Accompanied by an Irreversible Reaction of General Order," AIChE J., 10, 5 (1964).

Brian, P. and M. Beaverstock, "Gas Absorption Accompanied by a Two-Step Chemical Reaction," Chem. Eng. Sci., 20, 47 (1965).

Brimblecombe, P. and D. Spedding, "The Catalytic Oxidation of Micromolar Aqueous Sulfur Dioxide," Atm. Env., 8, 937 (1974).

Brimblecombe, P. and D. Spedding, "The Reaction Order of the Metal

Ion Catalyzed Oxidation of Sulfur Dioxide in Aqueous Solution," Chemosphere, no. 1, 29 (1974).

Chan, P. and G. Rochelle, "Limestone Dissolution: Effects of pH, CO_2 and Buffers Modelled by Mass Transfer" in Flue Gas Desulfurization, ACS Symposium Series 188 (1982).

Chang, C. and G. Rochelle, "Mass Transfer Enhanced by Equilibrium Reactions," Ind. Eng. Chem. Fund., 21, 379 (1982).

Chen, T. and C. Barron, "Some Aspects of the Homogeneous Kinetics of Sulfite Oxidation," Ind. Eng. Chem. Fund., 11; 466 (1972).

Cotton, F. and G. Wilkinson, Advanced Inorganic Chemistry, an Advanced Text, Interscience Pubs., New York (1966).

Coughanowr, D. and F. Krause, "The Reaction of SO_2 and O_2 in Aqueous Solutions of $MnSO_4$," Ind. Eng. Chem. Fund., 4, 61 (1965).

Danckwerts, P., Gas-Liquid Reactions, McGraw-Hill, New York (1970).

Danckwerts, P., "Significance of Liquid Film Coefficients in Gas Absorption," Ind. Eng. Chem., 43, 1460 (1951).

Davies, J., A. Kilner and G. Ratcliff, "The Effect of Diffusivities and Surface Films on Rates of Gas Absorption," Chem. Eng. Sci., 19, 583 (1964).

DeWaal, K. and J. Okeson, "The Oxidation of Aqueous Sodium Sulfite Solutions," Chem. Eng. Sci., 21, 559 (1966).

Dogliotti, L. and E. Hayon, "Flash Photolysis of Persulfate Ions in Aqueous Solutions: Study of the Sulfate and Ozonide Radical Ions," J. Phy. Chem., 71, 2511 (1967).

Dogliotti, L. and E. Hayon, "Flash Photolysis Study of Sulfite, Thiocyanate and Thiosulfate Ions in Solution," J. Phy. Chem., 72, 1800 (1968).

Edwards, J., Peroxide Reaction Mechanisms, Interscience Pubs., New York (1962).

Eriksen, T., "pH Effects on the Pulse Radiolysis of Deoxygenated Aqueous Solutions of Sulfur Dioxide," J. Chem. Soc. Far.Trans., 70, 208 (1974).

Fuller, E. and R. Crist, "The Rate of Oxidation of Sulfite Ions by Oxygen," J. Am. Chem. Soc., 63, 1644 (1941).

Gayer, K. and L. Woontner, "The Solubility of Ferrous Hydroxide and Ferric Hydroxide in Acidic and Basic Media at 25°C," J. Phy. Chem., 60, 1569 (1956).

Gleason, R., "Improved Flue Gas Desulfurization Process with Oxidation," in Proceedings: The Second Pacific Chemical Engineering Congress--Denver (AIChE), Vol. 1, 371 (Aug. 1977).

Karraker, D., "The Kinetics of the Reaction Between Sulfurous Acid and Ferric Ion," J. Phy. Chem., 67, 871 (1963).

Hayon, E., A. Treinin and J. Wilf, "Electronic Spectra, Photochemistry and Autoxidation Mechanism of the Sulfite-Bisulfite-Pyrosulfite Systems: The $SO_2^{\bullet -}$, $SO_3^{\bullet -}$, $SO_4^{\bullet -}$ and $SO_5^{\bullet -}$ Radicals," J. Am. Chem. Soc., 94, 47 (1972).

Higbie, R., "The Rate of Absorption of a Pure Gas into a Still Liquid During Short Periods of Exposure," Trans. AIChE, 31, 365 (1935).

Hikita, H. and S. Asai, "Gas Absorption with (m,n)th Order Irreversible Chemical Reaction," Int. Chem. Eng., 4, 332 (1964)

Hoffmann, M. and D. Jacob, "Kinetics and Mechanisms of the Catalytic Oxidation of Dissolved Sulfur Dioxide in Aqueous Solution: An Application to Nightime Fog Water," in Acid Precipitation: SO_2, NO and NO_2 Oxidation Mechanisms, Ann Arbor Scientific Publishers, Ann Arbor, MI (1982).

Hudson, J., Sulfur Dioxide Oxidation in Scrubber Systems, EPA 600/7-80-083 (1980).

Huss, A., P. Lim, and C. Eckert, "On the "Uncatalyzed" Oxidation of Sulfur IV in Aqueous Solutions," J. Am. Chem. Soc., 100, 6252 (1978).

Huss, A., P. Lim and C. Eckert, "The Oxidation of Aqueous SO_2, Part I, Homogeneous Mn and Fe Catalysis at Low pH," J. Phy. Chem., 86, 4224 (1982).

Huss, A., P. Lim and C. Eckert, "The Oxidation of Aqueous SO_2, Part II, High Pressure Studies and Proposed Reaction Mechanisms," J. Phy. Chem., 86, 4229 (1982).

Huyser, E. ed., Methods in Free Radical Chemistry, v. 4, Marcel Dekker Pubs., New York (1973).

Jhaveri, A. and M. Sharma, "Absorption with Fast Chemical Reaction," Chem. Eng. Sci., 24, 189 (1969).

Johnstone, H., "Metallic Ions as Catalysts for the Removal of Sulfur Dioxide from Boiler Furnace Gasses," Ind. Eng. Chem., 23, 559 (1931).

Johnstone, H. and D. Coughanower, "Absorption of Sulfur Dioxide from Air," Ind. Eng. Chem., 50, 1169 (1958).

Kozinsky, A. and C. King, "The Influence of Diffusivity on Liquid Phase Mass Transfer to the Free Interface in a Stirred Vessel," AIChE J., 12, 109 (1966).

Kuo, C. and C. Huang, "Liquid Phase Mass Transfer with Complex Chemical Reaction," AIChE J., 16, 493 (1970).

Landolt, A. and H. Bornstein, Physikalisch-Chemisch Tabbellen, Bd. II-7, 259 (1960).

Leussing, O. and J.Kolthoff, "The Solubility Product of Ferrous Hydroxide and the Ionization of the Aquo-Ferrous Ion," JACS, 75, 2476 (1953).

Lim, P., A. Huss and C. Eckert, "The Oxidation of Aqueous SO_2, Part III, The Effects of Chelating Agents and Phenolic Antioxidants," J. Phy. Chem., 86, 4233 (1982).

Linek, V. and J. Mayrhoferova, "The Kinetics of Aqueous Sodium Sulfite Solutions," Chem. Eng. Sci., 25, 787 (1970).

Linek, V. and V. Vacek, "Chemical Engineering Use of Catalyzed Sulfite Oxidation Kinetics for the Determination of Mass Transfer Characteristics of Gas-Liquid Contactors," Chem. E. Sci., 36, 1747 (1981).

Martin, L., D. Damschen and H. Judeikis, Sulfur Dioxide Oxidation Reactions in Aqueous Solutions, EPA 600/7-81-085 (1981).

Martin, L., "Kinetic Studies of Sulfite Oxidation in Aqueous Solution," in SO_2, NO_2 and NO_3 Oxidation Mechanisms: Atmospheric Considerations, Ann Arbor Science, Ann Arbor, MI (1983).

Matheron, E. and O. Sandall, "Gas Absorption Accompanied by a Second-Order Chemical Reaction Modeled According to the Danckwerts Surface Renewal Theory," AIChE J., 24, 552 (1978).

Metha, V. and M. Sharma, "Mass Transfer in Mechanically Agitated Gas-Liquid Contactors," Chem. Eng. Sci., 26, 461 (1971).

Mishra, G. and R. Srivastava, "Homogeneous Kinetics of Potassium Sulfite Oxidation," Chem. Eng. Sci., 31, 969 (1976).

Mishra, G. and R. Srivastava, "Kinetics of Oxidation of Ammonium Sulfite by the Rapid Mixing Method," Chem. Eng. Sci., 30, 1387 (1975).

Nagata, S. Mixing: Principles and Applications, John Wiley and Sons, New York (1975).

Phillips, D. and M. Johnson, "Oxygen Transfer in Agitated Vessles," Ind. Eng. Chem., 51, 83 (1959).

Reid, R., J. Prausnitz and T. Sherwood, The Properties of Gases and Liquids, McGraw-Hill, New York (1977).

Reinders, W. and S. Vles, "Reaction Velocity of Oxygen with Solution of Some Inorganic Salts," Rex. Trav. Chem., 44, 16 (1925).

Reith, T. and W. Beek, "The Oxidation of Aqueous Sodium Sulfite

Solutions," Chem. Eng. Sci., 28, 1331 (1973).

Robinson, R. and R.Stokes, Electrolyte Solutions, 2nd ed., London (1965).

Rochelle, G., Process Synthesis and Innovation in Flue Gas Desulfurization, EPRI FP-463-SR (1977).

Rochelle, G., "Sulfur Dioxide Vapor Pressure and pH of Sodium Citrate Buffer Solutions with Dissolved Sulfur Dioxide," in Thermodynamics of Aqueous Systems with Industrial Applications, American Chemical Soc., Washington D.C., (1980).

Schultz, J. and E. Gaden, "Sulfite Oxidation as a Measure of Aeration Effectiveness," Ind. Eng. Chem., 48, 2209 (1956).

Schwarzenbach, G., Complexometric Titrations, Interscience Publishers, New York (1957).

Sherwood, T., P. Pigford and C. Wilke, Mass Transfer, McGraw-Hill, New York (1978).

Siddall, T. and W. Vosburgh, "A Spectrophotometric Study of the Hydrolysis of Iron(III) Ion," J. Am. Chem. Soc., 73, 4270 (1951).

Sideman, S., O. Hortacsu and J. Fulton, "Mass Transfer in Gas-Liquid Contacting Systems," Ind. Eng. Chem., 58, 32 (1966).

Sillen, L. and A. Martell, Stability Constants of Metal-Ion Complexes, The Chemical Society of London (1964).

Smith, R. and A. Martell, Critical Stability Constants, v. 4, Inorganic Complexes, Plenum Press, New York (1976).

Srivastava, R., A. McMillan and I. Harris, "The Kinetics of Oxidation of Sodium Sulfite," Can. J. Chem. Eng., 46, 181 (1968).

Stumm, W. and G. Lee, "Oxygenation of Ferrous Iron," Ind. Eng. Chem., 53, 143 (1961).

Stumm, W. and J. Morgan, Aquatic Chemistry, John Wiley and Sons, New York (1981).

Tamura, H., K. Goto and M. Nagayama, "Effect of Anions on the Oxygenation of Ferrous Ion in Neutral Solutions," Inorg. Nuc. Chem., 38, 113 (1976).

Taube, H., Electron Transfer Reactions of Complex Ions in Solution, Academic Press New York (1970).

Teramoto, M., K. Hashimoto and S. Nagata, "Effect of Mass Transfer on the Selectivity of (m,n)-(p,q) Order Consecutive Gas-Liquid Reactions," J. Chem. End. Jap., 6, 552 (1973).

Turney, T., Oxidation Mechanisms, Butterworth and Co., London (1965).

Twigg, G., "Liquid-Phase Oxidation by Molcular Oxygen," Chem. & Ind., Jan. 6, 1962, p. 4.

Uhl, V. and J. Grey, eds., Mixing: Theory and Practice, Academic Press, New York (1967).

Vivian, J. and C. King, "The Mechanism of Liquid Phase Resistance to Gas Absorption in a Packed Column," AIChE J., 10, 221 (1964).

Walling, C., Free Radicals in Solution, John Wiley & Sons, New York (1957).

Weisnicht, W., Forced Oxidation in Calcium Sulfite Slurries, Master's thesis, Univ. of Virginia (1978).

Wesselingh, J. and A.Van't Hoog, "Oxidation of Aqueous Sulfite Solutions: A Model Reaction for Measurements in Gas-Liquid Dispersions," Trans. AIChE, 48, 69 (1970).

Westerterp, K., L. van Dierendonck and A. Dekraaj, "Interfacial Areas in Gas-Liquid Contactors," Chem. Eng. Sci., 18, 157 (1963).

Winter, E. and H. Briscoe, "Oxygen Atom Transfer during the Oxidation of Aqueous Sodium Sulfite," J. Am. Chem. Soc., 73, 469 (1951).

Yui, N., Bull. Inst. Phy. Chem. Res. Tokyo, 19, 1229 (1940).

Zagorski, Z., K. Sehested and S. Nielsen, "Pulse Radiolysis of Aqueous Alkaline Sulfite Solutions," J. Phys. Chem, 75, 3510 (1971).

VITA

Richard Kevin Ulrich was born in Burnet, Texas on December 18, 1955, the son of Dan and Joy Ulrich. After graduating from Burnet High School in 1974 he entered The University of Texas at Austin, majoring in Chemical Engineering. During the summers he worked for Amoco Production, Ethyl Research and Exxon Research before graduating with his B.S. degree in December 1978. The next month he entered the graduate school of the University of Illinois at Urbana and graduated with an M.S. in Chemical Engineering in May 1981. His research in Illinois was on electrochemical corrosion and was supervised by Dr. Richard Alkire. He entered the graduate school at The University of Texas at Austin in June 1981 and worked on simultaneous free radical reaction and mass transfer for Dr. Gary Rochelle, receiving his Ph.D. in Sepember 1983. Following graduation he accepted a position at Texas Instruments in Dallas in their semiconductor materials research facility.

Permanent Address: 707 Lewis Dr.
Burnet, Texas 78611
(512)756-8464

This dissertation was typed by the author.

The figures were drawn by Jimmy Holmes.